The HIV-1 protein Nef disrupts T cell receptor signalling and thymic function.

Cassandra Marie Thomson

Faculty of Medicine, McGill University, Montreal

A thesis submitted to McGill University in partial fulfillment of the requirements of the degree of Masters of Science

ABSTRACT

The HIV-1 Nef protein is a virulence factor and major determinant of pathogenicity of the virus. Nef impairs T cell function by uncoupling TcR signaling from antigen stimulation and by down regulating CD4 on the cell surface. In Nef infected thymocytes, the activity of intracellular T signaling molecule Lck is increased in basal conditions and attenuated with stimulation. This phenomenon contributes to partial T cell activation allowing viral replication meanwhile preventing full activation of the cell in order to prevent cell death. In addition, Nef infection results in intracellular accumulation of Lck and delocalization from its regular compartments. In the first part of this study we use biochemical techniques and confocal microscopy to study other proteins that are involved in the tightly regulated Lck localization and activity in a normal thymocytes to attempt to understand the pathway in the context of Nef infection. We find that the delocalization of Lck disrupts the regulatory feedback loop of the protein and subsequently interferes with the activation of downstream mediators. TcR signaling and Lck are also important for thymic selection and progression from CD4+CD8+ double positive to CD4+ and CD8+ single positive thymocytes. In the second part of this study, we show that the loss of CD4+ thymocytes results in the loss of an incredibly important mediator of central tolerance, the transcription factor AIRE. We correlate this loss of AIRE to an impairment of maturation of thymic epithelial cells and a profound loss of expression of tissue restricted antigens necessary for inducing thymic tolerance. Such loss in the thymus is directly correlated to autoimmunity in mouse models and human studies. This study proposes a novel mechanism for autoimmunity frequently observed in patients with HIV/AIDS.

RESUMÉ

La protéine Nef du VIH-1 joue un rôle important dans la pathogenèse du virus en modulant les voies de signalisation du récepteur de la lymphocyte T et en baissant l'expression du corécepteur CD4 à la membrane. Ainsi, dans une cellule infectée par Nef, l'activation de la molécule Lck est augmentée avant la stimulation de la cellule et diminuée après stimulation par rapport une cellule normale. Cette activation partiale fait que le virus peut répliquer en évitant l'apoptose. De plus, Nef mène à une accumulation intracellulaire de la protéine Lck ce qui la délocalise de ses compartiments habituels. Dans la première partie de cette étude, nous employons des essais biochimiques ainsi que la microscopie confocale afin d'étudier les protéines que sont impliquées dans la régulation précise de Lck pour que nous puissions comprendre sa signalisation sous le contrôle de Nef. Nous avons trouvé que la délocalisation de Lck perturbe la rétroaction régulatrice de la protéine ce qui interfére avec l'activation des messagers secondaires. La signalisation du lymphocyte T et de la protéine Lck sont importantes pour la séléction des thymocytes et la progression des cellules doubles positives CD4+ CD8+ aux cellules simples positives CD4+ ou CD8+. Dans la deuxième partie de ce mémoire, nous démontrons que la perte des thymocytes CD4+ mène à une perte d'une protéine essentielle à la tolérance centrale immunitaire, AIRE. Nous avons lié cette perte d'AIRE à une déficience des cellules épithéliales médullaires matures. Une telle perte est directement corrélée à l'autoimmunité dans les modèles de souris et les études chez l'homme. Notre étude suggère un nouveau mécanisme pour l'autoimmunité que l'on voit souvent chez les patients qui sont atteints du VIH-1.

TABLE OF CONTENTS

Figure List

ABBREVIATIONS:

ADAP: Adhesion and degranulation-promoting adapter protein
AIDS: Acquired immunodeficiency syndrome
AIRE: Autoimmune regulator
Cbl: Casitas B-lineage Lymphoma
Cbp: Csk-binding protein
CD4C: Human CD4 promoter
Csk: c-Src tyrosine kinase
DAPI: 4',6'-diamidino-2-phenylindole
DOCK: Dedicator of cytokenesis
DNA: Deoxyribonucleic acid
DN: Double negative
DP: Double positive
ELMO: Engulfment and cell motility gene
Env: Gene coding glycoprotein envelope
Env: Envelope protein
ERK: Extracellular signal-regulated kinase
FITC: Fluoresceine isothiocyanate
GADS: Grb2-related adaptor protein
Gag: Gene coding for group antigen surface
Gag: Proteins of matrix, capsid, nucleocapsid and p6
GEF: Guanine Exchange Factor
Hck: Hematopoeitc cellular kinase
HIV: Human immunodeficiency virus
Hpk1: hematopoietic progenitor kinase 1
IL-2: Interleukin 2
IS: Immunological synapse
ITAM: Immunoreceptor tyrosine-based activation motif
ITK: IL2-inducible T-cell kinase
IVKA: *in vitro* kinase assay
JNK: c-Jun N-terminal kinase
kDa: KiloDalton
LAT: Linker of Activated T cell
Lck: Lymphocyte-specific protein tyrosine kinase
MAPK: Mitogen-activated kinase
MHC: Major Histocompatibility Complex
cTEC: Cortical thymic epithelial cell
mTEC: Medullary thymic epithelial cell
NAK: Nef-activated kinase
NCK: Non-catalytic region of tyrosine kinase adaptor protein
Nef: Gene coding for negative factor
Nef: Negative factor protein
NF-κB: Nuclear Factor kappa B
PAK: p21-assocaited kinase
PI3K: Phosphatidyl inositol-3 kinase

PLC: Phospho-lipase C
Pol: Gene coding for reverse transcriptase, protease and integrase
Pol: Reverse transcriptase, protease and integrase proteins
Pro: Gene coding for protease
PTK: Protein tyrosine kinase
Rac: Ras-related C3 botulinum toxin substrate
RANK: Receptor Activator for Nuclear Factor kappa B
RANKL: Receptor Activator for Nuclear Factor kappa B Ligand
Rev: Gene coding for protein implication in mRNA nuclear transport
Rev: Protein implicated in mRNA nuclear transport
RNA: Ribonucleic Acid
SH: Src-homology
SLP-76: Src homology 2 (SH2) domain-containing leukocyte protein of 76 kDa
SFK: Src family tyrosine kinase
Tat: Gene coding for trans-activator of transcription
Tat: Trans-activator of transcription protein
TEC: Thymic epithelial cell
TCR: T cell Receptor
TKB: Tyrosine kinase binding (domain)
TRA- Tissue Restricted Antigen
UEA: Ulex europaeus agglutinin
Vif: Gene coding for virion infectivity factor
Vif: Virion infectivity factor protein
Vpr: Gene coding for Viral protein R
Vpr: Viral protein R
Vpu: Gene coding for viral protein U
Vpu: Viral protein U
Zap-70: Zeta associated protein of 70 kDa

ACKNOWLEDGEMENTS:

I would first like to thank my supervisor and mentor Dr. Paul Jolicoeur for taking a chance on me giving me the opportunity to work on not only one but two very interesting projects. Without his encouragement and critique with respect to my work and my scientific reasoning I wouldn't have been able to achieve what I am about to present in this thesis. Furthermore, his faith in me as a scientist toward the end of my studies has also allowed me to make significant advancements independently. Dr. Ciro Piccirillo, my co-supervisor has also provided tremendous moral and scientific support for which I am grateful.

I am also grateful for the presence and guidance of Dr. Zaher Hanna during my training. He has always been available when his expertise was needed and his enthusiasm and advice has certainly contributed to my work.

I must mention my former collegue Joël Guertin, whose elegant work was a foundation for part of this thesis, and who helped me quickly integrate in the lab upon my arrival. Dr. Pavel Chrobak also had a huge part in starting my second project, a very novel idea, which I have seen to completion.

Finally I would like to sincerely thank my family, particularly Mom, Ed and Cyril for their emotional and moral support during the difficult parts of my studies, and for always believing in me, I can honestly say that I wouldn't be here writing this thesis if it weren't for you.

INTRODUCTION

1. HIV and AIDS

An estimated 39.5 million people currently live with HIV-1 worldwide, and about 25 million have died and new infections and deaths are reported every year. There is currently no region of the world unaffected by this pandemic, however Sub-Saharan Africa remains the most affected region. This blood-borne virus is transmitted between humans via many methods of transmission including but not limited to sexual intercourse, injection drug use, mother-to-child transmission and contaminated blood supplies (Hayes and Weiss, 2006; Quinn and Overbaugh, 2005; Rowland-Jones, 2003).

Human immunodeficiency virus (HIV) is a lentivirus of the retrovirus family. It is classified according to its morphologic and morphogenic characteristics, such as an electron dense cylindrical inner nucleoid, large envelope glycoproteins and structural homologies (Nájera et al., 1987). The lentivirus family is named as such due to its pathological characteristic to cause slow infections. The lentivirus family includes the two known human types- HIV-1 and HIV-2 and other members which infect primates (simian immunodeficiency- SIV), cats (feline immunodeficiency virus- FIV) and cattle (bovine immunodeficiency virus- BIV) (Barré-Sinoussi, 1996).

As is the characteristic of all other retroviruses, the HIV structural components are assembled at the membrane of the cell it infects, in a process called budding. HIV also shares the characteristic that gives the name retrovirus which is that it encodes a reverse transcriptase to transcribe the RNA genome into a DNA provirus to become integrated into the host chromosomal DNA (Nájera et al., 1987).

1.1. HIV-1 Genome

Like other retroviruses, HIV virions contain a virus capsid, a nucleocapsid, diploid single stranded RNA, and viral enzymes including reverse transcriptase and integrase (Cann and Karn, 1989). The genetic information of the virus is stored on two copies of positive-sense RNA strands of the virus which is reverse-transcribed into proviral DNA by the viral enzyme reverse transcriptase (Barré-Sinoussi, 1996). This DNA copy of the retroviral genome is then integrated into the host genome by the viral enzyme integrase. Finally, the DNA serves as a template for the host cellular machinery to generate new viral RNA genomes and subgenomic messenger RNAs (mRNA).

The HIV genome contains nine reading frames shown in **Figure 1**. The three structural genes *Gag*, *Pol* and *Env* encode polyproteins that are proteolyzed to give a total of 9 proteins required by the virus. The structural proteins or the virion are coded by Gag (inner core): matrix, capsid, nucleocapsid and p6 and Env (surface proteins): gp120 and gp41. gp120 and gp 41 are the proteins which facilitate entry to the host cell by binding with CD4 (the main cellular receptor of all lentiviruses) and CXCR4 or CCR5 respectively (Barré-Sinoussi, 1996; Frankel and Young, 1998). The proteins coded for by *Pol* provide essential enzymatic functions of the virus lifecycle that are not provided by the host; these enzymes are reverse transcriptase which transcribes ssRNA to dsDNA, integrase which catalyzes integration of dsDNA into host DNA and protease which is needed for cleavage of newly synthesized polypeptides to yield mature proteins (Frankel and Young, 1998; Tavassoli, 2011). HIV also encodes six additional proteins resulting from multisplicing of the RNA. These proteins are often called accessory proteins (*Vif*,

Vpr, *Vpu*, *Rev*, *Tat* and *Nef*) which modify the local environment within infected cells to ensure viral persistence, replication, dissemination and transmission, three of which are found in the viral particle (Frankel and Young, 1998)

Rev is a characteristic of all primate lentiviruses. Although it is not a structural protein, without a functional Rev protein, the virus cannot produce *gag*, *pol* and *env* (Sakai et al., 1990). Rev is needed for export of unspliced viral mRNA species into the host cytoplasm, a necessary step in viral replication as without this interaction, the genes cannot be translated into all proteins (Dayton, 2004).

The accessory protein Tat, first identified as *transactivating* protein is present for transactivation, which increases the efficiency of HIV genomic transcription one hundred-fold. Its purpose is to enhance the activation of the long terminal repeat (LTR), *Tat* also contributes to cellular dysregulation by interacting with transcription factors NF-kB and NF-IL-6 (Herrmann and Rice, 1995; Li et al., 2010).

Finally, *Nef*, a virulence factor unique to primate lentiviruses, is considered critical to the pathogenesis of the HIV virus, and will be discussed in great detail in this work.

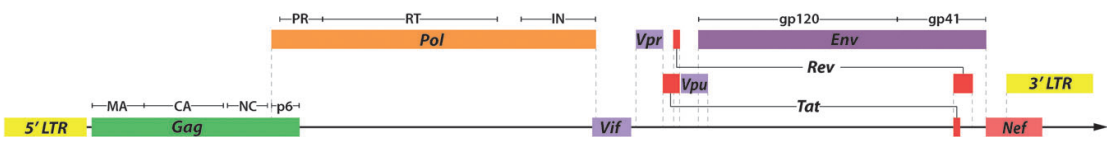

(Tavassoli, 2011)

Figure 1: HIV-1 Genome. Nine open reading frames code for fifteen different proteins including 6 structural, 3 enzymatic, and 6 accessory proteins.

1.2. HIV-1 Tropism

HIV was first isolated from CD4+ T cells however it was later discovered that HIV could infect other CD4+ cells such as dendritic cells or macrophages where the virus gains entry mediated through the viral gp120 protein and the CD4 molecule of the target cell. CD4 normally functions as a co-receptor (with the T cell receptor) to activate CD4+ T cells following interaction with antigen-presenting cells. Aside from CD4 as a crucial receptor for HIV, entry of the virus is dependant on a co-receptor, such as CXCR4 and CCR5 chemokine receptors, which are seven transmembrane spanning G-protein coupled receptors (Waters et al., 2008).

1.3. HIV-1 Life Cycle

Despite its modest genome size (less than 10kb) and its few genes, HIV-1 excels in taking advantage of cellular pathways while neutralizing and hiding from the different components of the immune system (Simon et al., 2006). Presently all forms of treatment of HIV-1 infection are targeted to interfere with one of the stages of the life cycle which are illustrated in **Figure 2**.

In the early steps, HIV-1 gains access to cells via endocytosis without causing immediate lethal damage but the entry process can stimulate intracellular signaling cascades which are thought to facilitate viral replication (Simon et al., 2006). Entry is an intricate, complex and multistep process involving viral envelope proteins gp120 and gp41 (coded by Env) and corresponding receptors on the host cell (CD4 and co-receptor). The binding of gp120 to CD4 initiates viral entry and causes gp120 to undergo dramatic changes in

conformation that brings a hydrophobic region in gp41 close to the host cells, resulting in its insertion into the host cell membrane. The outer lipid envelope of the virus is removed when the particle undergoes fusion with cytoplasmic vacuoles enabling the virus capsid to enter the cell (Cann and Karn, 1989; Tavassoli, 2011).

Once the virus enters the host cell, it aims to implant its genomic information into host cells, and must therefore copy its single-stranded RNA onto duplex DNA in a process called reverse transcription (RT). As the host lacks the cellular machinery to perform this function, the virus provides its own RT enzyme: reverse transcriptase. As the single strand DNA is synthesized, the complementary single strand RNA is degraded by the RNase H function of the enzyme (Kohlstaedt and Steitz, 1992). The DNA polymerase activity of HIV reverse transcriptase completes the synthesis of the double strand DNA copy of the viral genome.

Once the ss-RNA has been converted to ds-DNA, in can be integrated into the host genome with the assistance of the viral protein integrase. The ds viral DNA is contained within a pre-integration complex including integrase, matrix and accessory protein Vpr. The complex is transported to the nucleus via multiple nuclear localization signals. This initiates DNA strand transfer, which involves the insertion of processed viral cDNA ends into the host chromosomal DNA. Integrase catalyses the attack by the 3'-hydroxyl groups on a pair of phosphodiester bonds in the host's chromosomal DNA (Engelman et al., 1991). The host's DNA repair enzymes complete integration.

Transcription and translation of HIV genes and proteins are primarily achieved using the host cell machinery. However, the production of elongated transcripts is quite inefficient, therefore the viral protein Tat plays a key role in enhancing and rapidly up-regulating transcription (Cann and Karn, 1989). Moreover the complexity of the HIV genome with multiple overlapping genes calls for regulation by mRNA splicing. The viral mRNA is initially fully spliced by host splicing factors that retain and splice all intron containing pre-RNA. To produce differential splice transcripts, the viral protein Rev suppresses the host's nuclear retention mechanism to enable the translocation of intron-containing unspliced and partially spliced mRNA to the cytoplasm (Tavassoli, 2011).

Accumulation of structural proteins in the cell membrane permits the assembly of the virus particle. The viral protein Gag mediates the assembly and release of HIV from the host cell. Gag drives the spontaneous assembly or spherical virus-like particles and release of the virion. Although Gag enables the formation and assembly of viral spheres on membrane surfaces, components of the host endosomal sorting complex are essential for budding which involves separation of the nascent virion envelope from the cell membrane, releasing the viral particle (Demirov et al., 2002)

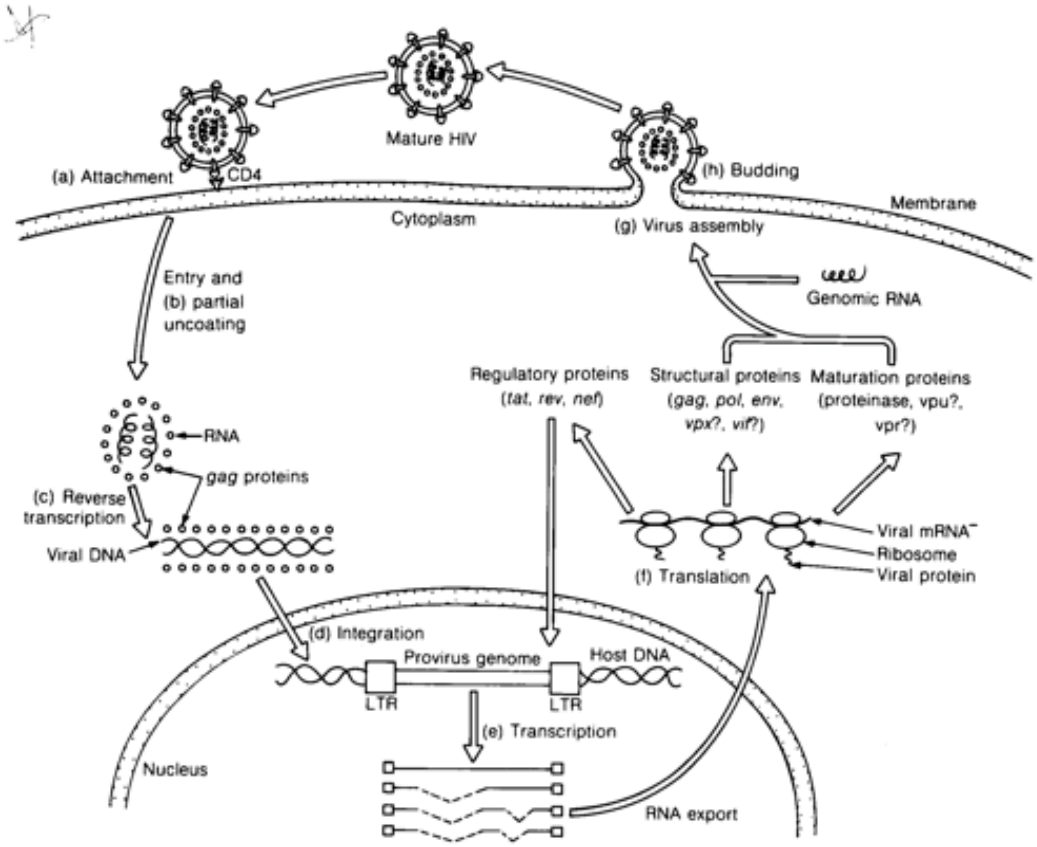

(Cann and Karn, 1989)

Figure 2: HIV-1 life cycle. a) attachment of virus to CD4 receptor b) entry and uncoating of the virion c) reverse transcription of viral RNA to proviral DNA d) integration of proviral DNA in host genome e) transcription and replication of proviral DNA by host cell machinery f) transcription of viral proteins g) assembly of virion and packaging of viral proteins h) budding and release of virions from the cell.

1.4. HIV-1 Infection

1.4.1. Primary Infection

During the first few weeks of infection, the patient often suffers from a flu-like illness and a rash, an illness termed acute HIV-1 infection syndrome (Klimas et al., 2008). During this phase of 6-12 weeks there is a massive burden of HIV that results in a steep loss of CD4+ T cells (Rowland-Jones, 2003).

1.4.2. Latency Phase

The subsequent steady-state level of plasma virus load is closely related to the ultimate clinical outcome. During this phase, the viral load is reduced and maintained at a low level and there is a partial recovery of CD4+ T cells viremia (Rowland-Jones, 2003). T-cell homeostasis is preserved in the early stages of infection. The duration of the latency phase depends on many variables including the overall health of the patient, co-infection, age, treatment and genetic factors (Klimas et al., 2008) but this generally asymptomatic phase typically lasts between 1-15 or more years. During this phase, viral replication occurs but viremia levels are generally low, and CD4+ T cell count declines at a very slow rate.

1.4.3. Late phase HIV-infection and progression to AIDS

A gradual destruction of the naïve and memory CD4+ T-lymphocyte populations is a hallmark of HIV-1 infection and there is believed to be a CD4+ T cell inflection point, which occurs when the population becomes too low to control the infection and viral replication dramatically increases. This phase generally lasts 2-3 years and ends with death. Once the CD4+ count falls below 500 cells/mm^3, the immune system is compromised and minor infections will frequently occur. However, as the CD4+ count falls below 200 cells/mm^3, the disease is considered to have progressed from HIV to AIDS as the patient becomes vulnerable to serious opportunistic infections and cancers of which they will typically die (Klimas et al., 2008). This is further illustrated in **Figure 3**.

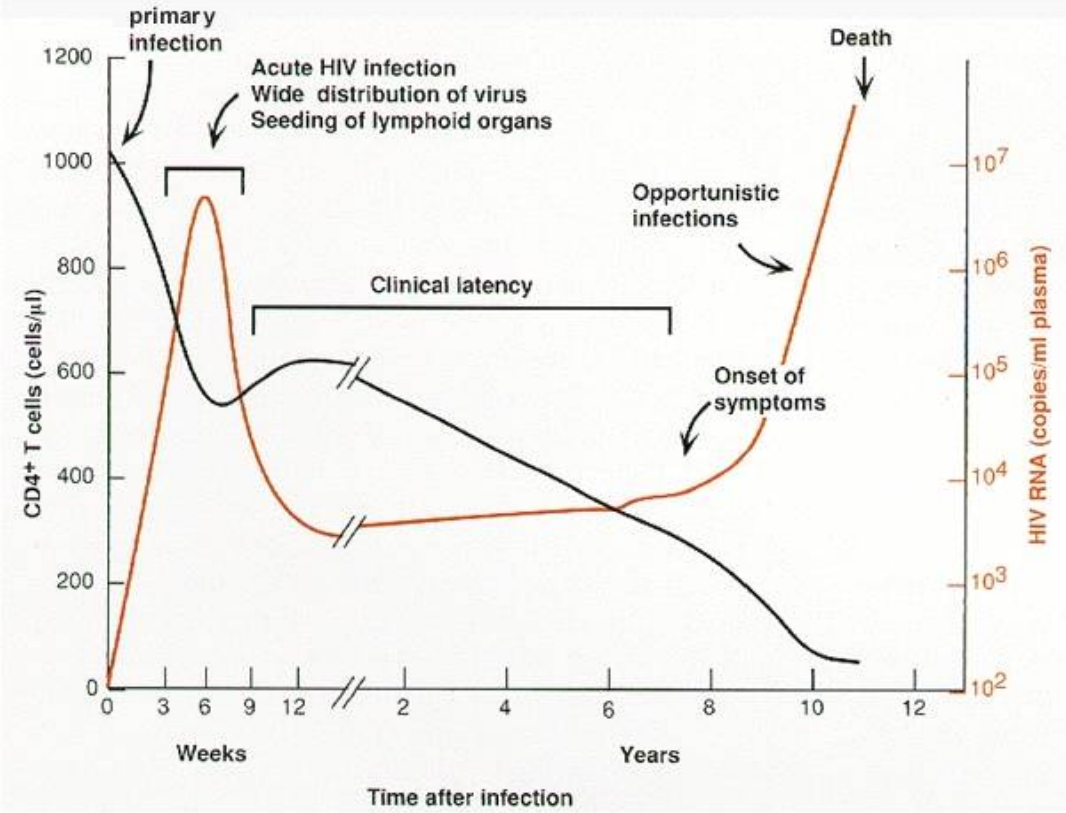

(Pantaleo et al., 1993)

Figure 3: Progression from primary HIV-1 infection to AIDS. The number of CD4+ T lymphocytes/ul (black) and the number of RNA copies per ml of plasma (gold) during the primary phase, latency phase and AIDS.

2. HIV-1 protein Nef

2.1. Nef, virulence factor

Nef is a known virulence factor which stands for "Negative Factor" as it manipulates host cellular machinery to allow infection, survival and replication of the virus. Macaques infected with the SIVmac239Δnef bearing a deletion in the Nef gene show only poor viral replication and do not develop disease. Moreover, in animals infected with an SIV strain

containing a premature stop codon or a 12bp deletion in the Nef gene, gene restoration correlates with disease progression (Kestler et al., 1991; Whatmore et al., 1995). Sequencing of the HIV genome of long-term non-progressors (HIV patients that do not develop AIDS in the absence of therapy) revealed the presence of discrete and stable deletions in the Nef gene in at least nine individuals (Deacon et al., 1995; Kirchhoff et al., 1995; Mariani et al., 1996). In addition, a blood donor and eight transfusion recipients of the Sydney Blood Bank Cohort (found to be infected with an *attenuated* strain of HIV-1 containing a deletion in the Nef gene) remained asymptomatic in the absence of therapy (Learmont et al., 1999). Finally a characterized transgenic mouse model shows that unique expression of Nef in CD4 positive cells of mice causes an AIDS-like disease in the absence of viral replication (Hanna et al., 1998a).

2.2. Structure of Nef

The accessory protein Nef is expressed by all primate lentiviruses: HIV-1, HIV-2, SIV, and is of great importance for their pathogenesis and expressed at high levels in the early stages in HIV infection. Determination of the structure of Nef has been facilitated by information derived from crystal structures of the core of HIV-1 Nef protein complexed with the third Src homology SH3 domain of tyrosine kinases Fyn and Hck (Arold et al., 1997; Lee et al., 1996) and NMR methods (Grzesiek et al., 1997). The molecular weight of Nef varies between 27-35kD and consists of 206 amino acids and an N-terminal myristoylation site to which the host cell membrane is associated (Grzesiek et al., 1997). The N- myristoylation of Nef is required for its association with cellular membranes and is critical for virtually all of its biological activities (Geyer et al., 2001; Matsubara et al., 2005). The core of Nef consists of a type II polyproline helix (aa70-77) which represents

the main binding site for Src family kinases; this domain is followed by two alpha helices (aa 81-120), a four-stranded anti-parallel beta-sheet (aa 121-186), and two additional alpha helices (aa187-203); residues 60-71 and 149-180 form flexible solvent-exposed loops (Grzesiek et al., 1997).

Like all myristoylated proteins, Nef starts with a Met-Gly sequence, but the initiating methionine is removed during translation and myristate is amide-linked to the glycine, the consensus sequence for the N-myristoyl transferase protein is MGxxx(S/T) with an additional preference for lysine or arginine at positions 7 and/or 8 (Resh, 1999). Membrane localization of Nef is a requirement for its role in the viral life cycle. Another post-translational modification of Nef results in its cleavage by HIV-1 protease between W57 and L58, separating it into anchor and core domains. The six residues at this point are highly conserved, however the functional relevance of this process is unclear (Geyer et al., 2001). Nef is also phosphorylated on serine and threonine residues, although the role of these modifications is also unclear (Yang and Gabuzda, 1999).

2.3. Biological functions of Nef

A large number of host cellular interaction partners for Nef have been discovered and binding sites for some of these proteins have been mapped to distinct locations within Nef. Regions of Nef have been mapped to functions in protein modification, signalling and trafficking. The widely accepted *in vivo* functions of Nef, namely support of viral replication in peripheral blood mononuclear cells (PBMC), the activation of the Pak kinase and down-regulation of CD4 and MHC class I molecules, contribute greatly to the progression of HIV infection.

2.3.1. Downregulation of CD4 co-receptor and MHC I

It is well reported that Nef down-regulates surface expression of both CD4 and major histocompatibility complex I (MHC I) (Geyer et al., 2001; Matsubara et al., 2005). The downregulation of CD4 results in impairment of the immunological synapse (Thoulouze et al., 2006) which prevents super infection that would kill the cell and counteracts interference with the viral envelope preventing sequestration of virions (Peter, 1998). The downregulation of major histocompatibility complex class I molecules contributes to the escape of HIV-1 infected cells from immunosurveillance and killing by immune cells as MHC class I is the basis of anti-viral immunity by presenting viral peptides to cytotoxic $CD8^+$ T lymphocytes (Geyer et al., 2001; Peter, 1998).

Nef-induced cell surface downregulation of CD4 is efficient in all CD4-expressing cells. On one hand, Nef binds to CD4, recognizing a dileucine-based signal in the membrane proximal region of the receptor cytoplasmic tail which binds to Nef around aa residues 57-59 (Grzesiek et al., 1996). This binding site is usually associated with a regulatory member of the Src kinase family, the T cell-specific protein tyrosine kinase $p56^{lck,}$ (Salghetti et al., 1995). The process additionally depends on the integrity of a di-Leu motif at position 164/165 of the C-terminal flexible loop of Nef; this di-Leu motif allows for the interaction with clathrin-associated adaptor protein (AP) complexes of the endocytic pathway, and has been shown to be essential for sorting of Nef into clathrin-coated pits and internalization of CD4 (Aiken et al., 1996; Grzesiek et al., 1996). The di-Leu motif must compete with $p56^{lck}$ for binding to CD4 as $p56^{lck}$ prevents CD4 from connecting with the APs thereby preventing endocytosis (Peter, 1998). Endocytosed CD4

molecules are then accumulated in the early endosomes and subsequently degraded in the lysosomes (Coutinho et al., 2005; Peter, 1998).

Nef-induced MHC I downregulation is less efficient than CD4 internalization and appears to employ different machinery. MHC I surface expression is fairly transient since the complex is constitutively endocytosed in the presence of viral protein, internalized more rapidly, routed to the trans Golgi network, and ultimately degraded (Schwartz et al., 1996). The downregulation of MHC class I surface expression is dependent on an intact SH3 domain binding motif (Greenberg et al., 1998). Amongst the mechanisms proposed is that Nef may bind directly to PACS-1/2, a sorting protein that controls endosome-to-Golgi trafficking, which was later mapped to an acidic cluster of four successive glutamic acids in Nef (62EEEE) (Geyer et al., 2001; Piguet et al., 2000). Mutations in this cluster are known to abolish MHC class I internalization (Peter, 1998). Blagoveshchenskaya et al., (2002) later confirmed that in fact PACS-1 and Nef combine to upregulate the ARF6 endocytic pathway by a PI3K-dependent process showing a mechanism for immune evasion.

While the MHC I downregulation mechanisms are numerous and clear, interaction of Nef with human thioesterase has been reported to influence Nef-mediated endocytosis of CD4 and MHC. This interaction has been mapped to a highly conserved and exposed cluster (FPD121) in the loop connecting the alpha helix4 and beta sheet 2 and the downregulation of both CD4 and MHC I are affected by mutation of these residues. Evidence suggests that the ability of Nef to form dimers is critical to its function (Liu et al., 2000).

2.3.2. Association with PAK and Actin Remodeling

Nef has been reported to associate with a serine/threonine kinase known as Nef-associated kinase (NAK) identified as a member of the p21-activated kinase (PAK) family. More recent data show that Nef specifically activates PAK2 but not PAK1 nor PAK3 and that a small fraction of PAK2 was transiently observed bound to Nef (Arora et al., 2000; Vincent et al., 2006). Vincent et al (2006) also found that PAK2 activation by Nef was not sufficient for full development of disease but may be required for induction of kidney and lung disease in Nef-expressing animal models.

It has been proposed that one of the main consequences of PAK activation by Nef is regulation of the actin cytoskeleton. Pak2 activation by Nef is involved in immunological synapse (IS) modulation by reducing signal transduction through actin remodelling and Lck recruitment to the IS (Van den Broeke et al., 2010). It is also proposed that Nef uses its association with PAK to induce a potent block on T-lymphocyte actin polymerization to impair chemotaxis of Nef-positive cells (Stolp et al., 2010). Nef was also reported to associate with guanine exchange factor (GEF) Vav (Fackler et al., 1999) but this finding is inconsistent with other work (Janardhan et al., 2004).

On the other hand, it has been shown that actin remodeling is partly achieved by modulation of Rac GTPases, Nef can bring Rac to the plasma membrane where it can be activated by forming an ELMO1/DOCK2-dependant complex with Rac while associating with the plasma membrane via its N-terminal myristoylation, uncoupling Rac activation from TcR activation, this event is subsequently disrupted via disruption of Nef N-myristoylation (Janardhan et al., 2004).

2.3.3. Increased Infectivity

Nef is capable of increasing the potential of HIV to infect cells via various mechanisms. One mechanism is via disruption of the actin cytoskeleton in the target cell, eliminating this particular barrier to infection (Campbell et al., 2004). Nef has also been shown to increase the efficiency of other accessory proteins, for example by downregulating an unidentified protein that serves to block the function of Env, thereby increasing the productivity of the virus (Pizzato et al., 2008). Data also shows that the presence of Nef results in an increase in the RT enzyme efficiency leading to increased viral transcripts (Schwartz et al., 1995). This may be owed to the fact that Nef protects the viral core from post-fusion degradation, which occurs upon viral entry, allowing reverse transcription to proceed and not be inhibited (Foster and Garcia, 2008). Furthermore, there is also data showing that Nef increases virion infectivity by altering protein transport and by targeting viral budding to the lipid rafts of the plasma membrane where budding is more efficient (Zheng et al., 2001).

2.3.4. Signaling Interference

In essence, Nef functions to hijack the host cell via various mechanisms in order to promote the survival and replication of the virus. In T cells, Nef forms a signalling complex with the TCR, thereby activating a transcriptional program similar to that triggered upon exogenous stimulation (Simmons et al., 2001). Proteins that have been shown to directly interact with Nef include PI3K, Vav, DOCK2-ELMO and Pak2, as a result several downstream proteins are triggered, some of which are implicated in apoptosis (Lenassi et al., 2010). Additionally, Nef results in aggregation of Lck and TCR-zeta in lipid rafts (usually occurs only after stimulation), which also contributes to

activation of downstream mediators (Lenassi et al., 2010). By overriding the internal control for stimulation (engagement of TCR) Nef brings the cell to an activated state (Peter, 1998). These effects are further illustrated in **Figure 5**.

Nef is found in the serum of HIV-infected individuals, as it is secreted from infected cells. This is achieved by interferring with endocytic compartments such as multivesicular bodies (MVBs) and secretory lysosomes. As result of Nef-induced activation, there is increased bidirectional (exo- and endo-cytosis) membrane trafficking. At the same time that Nef alters and accelerates T cell endocytosis (of MHC and CD4 for example), there is a resulting increase in exocytosis which leads to the release of large clusters of vesicles from the cell containing Nef (Muratori et al., 2009). Nef also results in the increase of FasL expression, which can be secreted to other cells, resulting in apoptosis of bystander cells via the mechanism of activation-induced cell death (Lenassi et al., 2010; Muratori et al., 2009).

Finally, Nef has the ability to promote the release of calcium stores from the T cell via interactions with the IP3 receptor, in the absence of IP3, which is catalyzed by PLCγ1. The result of calcium release in the absence of TCR engagement is that the transcription factor NFAT becomes activated downstream of the calcium signaling pathway, promoting gene expression and release of IL-2; the increased gene expression and IL-2 release in absence of external stimulation of the T cell is thought to be a synergistic effect with the ability of Nef to trigger Erk activity via association with the Nef-associated kinase (NAK) complex (Abraham and Fackler, 2012).

3. T cell Receptor Signalling of Thymocytes and Peripheral T cells

3.1. Activation of Lck

The Src family tyrosine kinases (SFKs) originally identified as proto-oncogene products are non-receptor tyrosine kinases that play pivotal roles in cell proliferation, survival, cell adhesion, cell morphology and motility (Yang et al., 2009). The main signaling molecules in T cells are the SFK lymphocyte-specific protein tyrosine kinases (Lck) and Fyn which participate in a variety of cellular processes: cytoskeletal assembly and organization, cell-cell contact, cell-matrix adhesion, induction of DNA synthesis, cell survival and cellular proliferation (Erpel and Courtneidge, 1995). The overall level of cellular protein tyrosine phosphorylation is a result of opposing actions of protein tyrosine kinases (PTKs) and protein phosphatases (PTPases). The regulation of Lck and Fyn is therefore regulated by the actions of PTK c-terminal Src kinase (Csk) and the PTP CD45 at C-terminal inhibitory tyrosine (Y505) (Palacios and Weiss, 2004). When phosphorylated by Csk, the C-terminal tyrosine binds intramolecularly to the SH2 domain which together with the SH3 domain interacting with a PPI alpha-helix packaged against the kinase domain, locks SFKs into an auto inhibited closed form (Nika et al., 2010). However recent work suggests a new model in which pY505-Lck is not solely inactive, but rather active if it is also phosphorylated on the Y394 motif (which represents 20% of Lck in unstimulated cells) demonstrating a dynamic regulation of Lck activity (Nika et al., 2010). Lck exists in four different phosphorylation forms, which govern its activation as described in **Figure 4**.

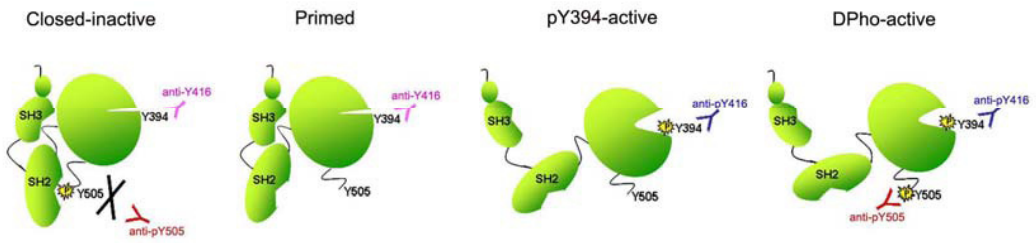

(Nika et al., 2010)

Figure 4: Four phosphorylation forms of Lck. Classically Lck is considered to be in its inactive form when phosphorylated on pY505 unless it is phosphorylated on both sites. When Lck is no longer phosphorylated on Y505 it must be autophosphorylated to become active, at this point when Y394 is phosphorylated

When activated, Lck can tyrosine-phosphorylate the immunoreceptor tyrosine-based activation motifs (ITAMs) found in the TcR complex (Mustelin and Taskén, 2003). The tyrosine-phosphorylated sites serve as a dock and bind SH2 domains of other signaling molecules with high affinity. The kinase ZAP-70 binds to Y315 and Y319 of the zeta-chains to maintain an active conformation (Au-Yeung et al., 2009). At this point, Y493 in the activation loop of ZAP-70 can be autophosphorylated or phosphorylated by Lck. Active ZAP70 is necessary for the phosphorylation of the two critical adaptor proteins: linker of activated T cells (LAT) and SH2 domain-containing leukocyte phospho-protein of 76 kD (SLP-76). Together, these two molecules create a platform for the required signaling proteins downstream of the TCR that direct transcriptional responses and induce cell proliferation (Schoenborn et al., 2011).

3.1.1. Regulation by Cbl ubiquitin ligase

The Cbl family of proteins consists of three homologues known as c-Cbl, Cbl-b and Cbl-3. Cbl-b and c-Cbl are expressed in hematopoietic cells whereas c-Cbl expression is high in thymocytes compared to Cbl-b, the highest levels of Cbl-b expression can be found in peripheral T cells (Naramura et al., 2002). All three forms share highly conserved regions in the N-terminus including the tyrosine kinase-binding (TKB) domain, the linker, and RING finger domains (Rao et al., 2002; Thien and Langdon, 2005). The TKB domain binds to activation-induced phosphotyrosine motifs and the linker helix and a RING finger domain mediate physical interaction with the E2 ubiquitin (Ub) conjugating enzymes of the Ub pathway (Thien and Langdon, 2001). Therefore, Cbl can function as an E3 ubiquitin ligase towards activated protein tyrosine kinases (PTK) targeting them for degradation. Notable targets of for c-Cbl-mediated ubiquitination are Lck, Vav, Fyn and ZAP-70 as well as the TCR/CD3-complex (Methi et al., 2008). The Cbl proteins are also a prominent susbtrate of PTKs and is phosphorylated following TCR engagement, specifically on Y700, Y731, Y774, residues which are efficiently phosphorylated by Fyn and less-efficiently phosphorylated by ZAP-70 and Lck (Methi et al., 2008; Thien et al., 2003). Phosphorylation of these sites provides a docking region for SH2 domains of target proteins (Thien et al., 2003). C-Cbl is a negative regulator of TCR signaling. In Cbl knockout mice, thymocytes have elevated levels of CD3, TCR, CD4 and Lck and enhanced signaling of Lck (Methi et al., 2008; Thien et al., 2003).

It has also been shown that c-Cbl sequesters Lck from the lipid rafts by associating to the protein via its SH3 domain. As c-Cbl is excluded from the lipid rafts, association with

Lck under basal conditions represents another mechanism of Lck regulation by Cbl, as localization of Lck and LAT to the rafts is needed for effective TCR signaling (Hawash et al., 2002). The localization of Lck to lipid rafts was diminished in c-Cbl overexpressing cells and enhanced in c-Cbl knockout T cells (Hawash et al., 2002).

Interestingly, studies have shown that HIV-Nef enhances c-Cbl phosphorylation in infected cells in an Lck-dependant manner, however the biological function of this phenomenon is not known (Yang and Henderson, 2005).

3.2. LAT- SLP-76 microclusters

LAT and SLP-76 are regarded as the crucial intermediates between proximal and distal TcR signaling. LAT is constitutively localized to the lipid rafts regions of the plasma membrane and embedded in the plasma membrane. Phosphorylation of LAT by ZAP-70 recruits SLP-76 to the plasma membrane and in proximity, SLP-76 also becomes phosphorylated by ZAP-70 (Zhang et al., 1998), as a result, the two adaptors nucleate a multimolecular complex that contains several signaling proteins, including phospholipase Cγ1 (PLCγ1), the guanine-nucleotide-exchange factor VAV, the adaptor non-catalytic region of tyrosine kinase (NCK), TEC-family kinase interleukin-2 inucible T-cell kinase (ITK), adhesion- and degranulation-promoting adaptor proteins (ADAP), LCK and hematopoeitc progenitor kinase 1 (HPK1) (Koretzky et al., 2006; Yokosuka et al., 2005).

As a molecular adaptor protein, the main mechanism of action of SLP-76 is its localization and proximity to the molecules that phosphorylate the protein and the

proteins that it scaffolds. In the absence of SLP-76, translocation of the proteins that it scaffolds to the plasma membrane is disrupted, such as is the case with VAV (Charvet et al., 2005). The facilitation of formation of an SLP-76 complex is dependent on phosphorylation of LAT at Tyr191 and the aide of an additional adaptor protein, GADS (Liu et al., 1999). SLP-76 contains three N-terminal tyrosine residues that are phosphorylated. ZAP-70 or Lck can phosphorylate Tyr145 which serves as a component of ITK-binding which subsequently targets PLCγ1 and is the most critical for TCR signaling (Koretzky et al., 2006; Sanzenbacher et al., 1999). Lck-phosphorylation of LAT and SLP-76 is debated, however, data show that Lck may indeed phosphorylate SLP-76 and LAT independently of ZAP-70 (Jiang and Cheng, 2007; Kabouridis et al., 2011; Sanzenbacher et al., 1999). Jiang and Cheng, 2007 showed that in the absence of ZAP70, Lck was able to phosphorylate the ITAM-like motifs of LAT at Y171/Y191. Moreover, Lck is more prevalent in non-lipid rafts contrary to LAT. However upon stimulation both proteins remain raft-associated (Schade and Levine, 2002). Finally Tyr112 and Tyr128 (of SLP76) are both thought to be required for binding of VAV and NCK and also contribute to PLCγ1 phosphorylation, a loss of either tyrosine site results in a loss of the VAV interaction (Koretzky et al., 2006; Sanzenbacher et al., 1999) and have not been shown to be phosphorylated by Lck. The signaling complexes along with the effects of Nef is further shown in **Figure 5**.

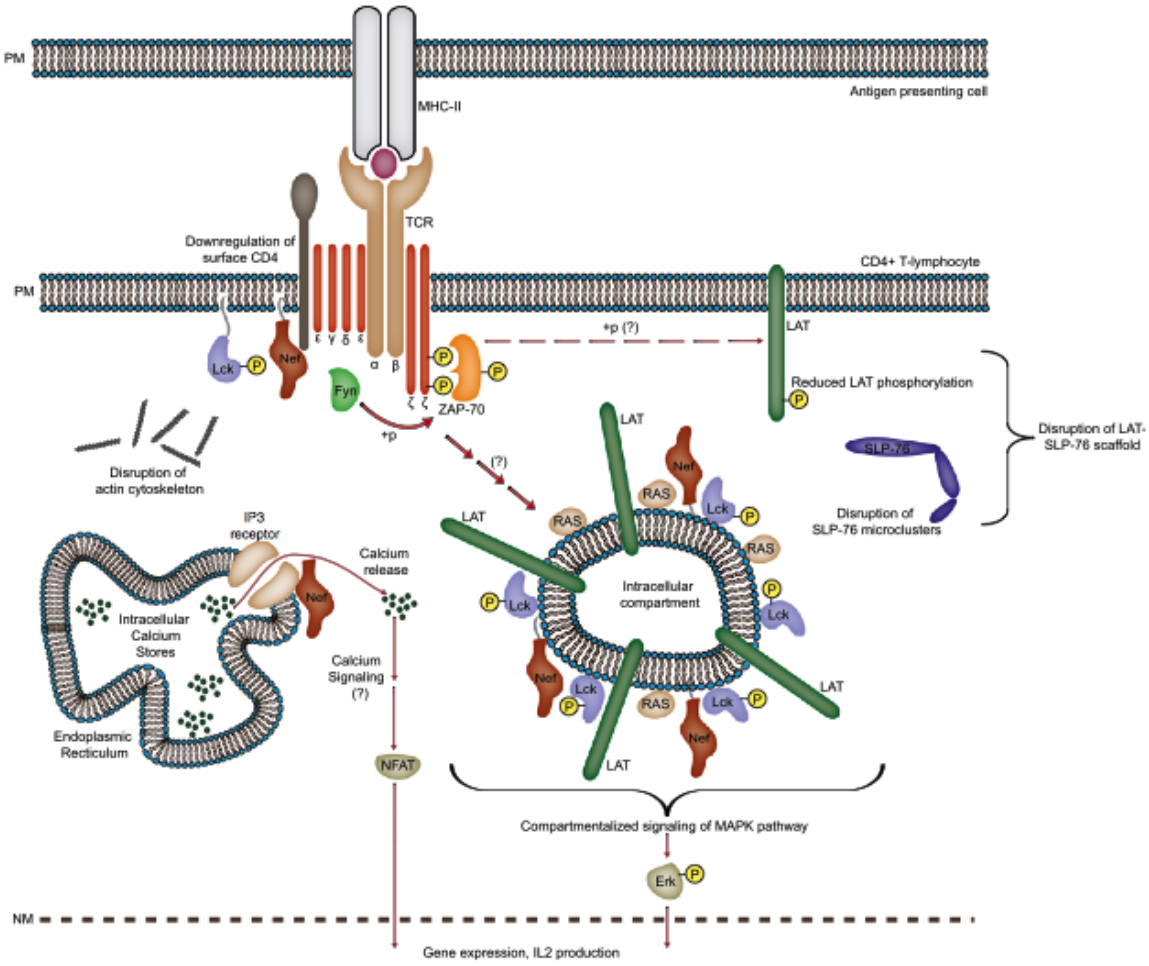

(Abraham, 2012)

Figure 5: Model of the effects of HIV-1 Nef on TCR signaling. Distal and proximal events of TcR signalling commencing with activation of Lck, activation of LAT and SLP-76 and subsequent downstream events.

3.3. PAK and RAC

Following TCR stimulation, VAV1 and NCK have been implicated in subsequent cytoskeleton rearrangement which serves in functions such as cell migration, adhesion, proliferation and survival (Dorrance et al., 2013). Vav, a guanine nucleotide exchange

factor, catalyses GDP/GTP exchange on Rac-1 rendering it active (Crespo et al., 1997). In this regard, activation of Rac-1 is associated with its recruitment to lipid rafts.

Rac proteins are members of the Rho GTPase family of proteins that have been shown to integrate multiple extracellular signals and play important regulatory roles of cytoskeleton rearrangement; Rac1 and Rac2 proteins have been shown to regulate distinct biological processes, but knockout models reveal overlapping functions (Cancelas et al., 2005). The best characterized Rac effector proteins are the p21-activated kinases (PAKs) which are a family of serine/threonine kinases characterized by two canonical N-terminal proline-rich motifs that mediate interactions with SH3-containing proteins, a p21 binding domain (PBD) which binds activated (GTP-bound) Rac, and a C-terminal domain. PAK is activated by Rac binding to the PBD relieving autoinhibition through a series of conformational changes (Dorrance et al., 2013). Activation of Rac therefore leads to actin polymerization, which is necessary for actin rearrangement, motility and cell adhesion. Furthermore, when PAK2 becomes activated, it mediates activation of Erk (extracellular-signal-regulated kinase), a serine/threonine kinase which activates one of the main transcription factors, AP-1 (activator protein-1) which contributes to gene expression and IL-2 production from the activated cell (Abraham and Fackler, 2012; Hough et al., 2012).

Activation of PLCγ1 via the phosphorylated Y132 of LAT and interaction with the SLP-76 complex leads to another important cascade in T cell signalling (Chuck et al., 2010). Upon activation, PLCγ1 hydrolyzes phosphatidylinositol 4,5, bisphosphate (PIP_2) to generate diacylglycerol (DAG) and inositiol 1,4,5-triphosphate (IP_3), IP_3 then binds to the IP_3 receptors on the endoplasmic reticulum (ER), inducing the flux of calcium from the

ER into the cytoplasm. The elevation of intracellular calcium leads to dephosphorylation and translocation of transcription factor NFAT into the nucleus (Jayaraman et al., 1996; Putney and Bird, 1993). NFAT (in synergism with AP-1) leads to gene expression and IL-2 production, a hallmark of activated T cells (Abraham and Fackler, 2012).

4. Thymic Education

T cells play a major role in guiding the immune system to specifically recognize a wide variety of foreign antigens and provide lasting immunological memory, all the while protecting against recognition of self-antigens resulting in autoimmunity (referred to as tolerance).

Developing thymocytes travel from the bone marrow to the thymus where they differentiate and mature. Stromal cells in the thymus provide chemokines, cytokines and cell surface molecules essential for the differentiation of thymocytes (Anderson et al., 2006).

The thymic microenvironment is an integrated network of epithelial reticular cells and nonepithelial stromal cells each characterized by typical structure, antigenic, and functional features (Zuklys et al., 2000). Notably, the organization of the thymic epithelium differs from most other epithelial organs in the body: rather than forming a sheet of cells positioned on a basement membrane, thymic epithelial cells (TECs) form a three dimensional meshwork (Zuklys et al., 2000). The typical architecture of the complex thymic stroma is critically dependent on intercellular communications- thymic

stromal cells need to be closely coached by developing thymocytes to provide the appropriate microenvironments for promoting and regulating further thymocyte development. Essentially, the lympho-stromal communication is a bilateral coordination, or crosstalk, between architechtural stromal cells and travelling thymocytes (van Ewijk et al., 1994). Depending on cell-cell interactions between developing thymocytes and stromal cells (thymic crosstalk), distinct microenivronments are created that allow all steps in T cell maturation to occur. It is well established that TECs guide developing thymocytes; conversely, the lack of inductive signals from developing T cells prevents the formation of the distinct cortical and medullary microenvironments (Takahama, 2006; Zuklys et al., 2000).

Central tolerance is established within the thymus by purging self-reactive thymocytes, and thus reducing the propensity for autoreactivity among mature T cells in the periphery. Thymic development involves a stringent repertoire selection in which only 1-3% of thymocytes succeed in survival and are exported from the thymus (Takahama, 2006). It is important to note that central tolerance is somewhat an imperfect process and necessitates additional mechanisms to maintain peripheral tolerance. However central tolerance in the thymus is nevertheless considered to play a crucial role in maintaining a healthy immune system (Metzger and Anderson, 2011).

The two main mechanisms of central tolerance are positive and negative selection. Positive selection is a process by which only fully functioning thymocytes may leave the thymus, and involves checkpoints in the thymus to ensure that thymocytes are functional before maturation proceeds (Shakib et al., 2009). Negative selection is a mechanism that

prevents autoimmunity. The thymus imposes self-tolerance on differentiating thymocytes, by purging self-reactive thymocytes, a function performed primarily by dendritic cells and TECs, which ectopically express a wide array of tissue-restricted antigens (TRAs), a representation of self that substantially expands the scope of central tolerance (negative selection) (Gray et al., 2007).

4.1. Thymic Epithelial Cells (TECs)

TECs are integral in the thymocyte maturation process and promoting central tolerance. As shown in **Figure 6**, after thymocytes first enter the thymus from the bone marrow they go through a series of developmental phases and T cell receptor (TCR) rearrangement as CD4-CD8- double negative DN thymocytes. The successful expression of the pre-TCR complex initiates the signals to develop into CD4+CD8+ double positive (DP) thymocytes, all of which takes place in the cortex of the thymus. DP thymocytes are then positively selected for their TCR recognition specificity with MHC complexes presented by cortical thymic epithelial cells (cTECs), known as positive selection (Takahama, 2006), and only thymocytes that succeed in recognition may move onto the medulla.

The process of single positive (SP) thymocyte maturation occurs in the medulla and is accompanied by further deletion of self-reactive thymocytes by negative selection. The maturation of SP thymocytes in the medulla also includes the production of suppressive FOXP3+ regulatory T cells which contribute to the maintenance of peripheral tolerance by suppressing auto-reactive T cells in the periphery that may have escaped the mechanisms of central tolerance by negative selection (Liston et al., 2003; Takahama, 2006). The crucial role of medullary thymic epithelial cells (mTECs) in central tolerance

is well accepted, ectopically expressing a vast range of tissue-restricted antigens (TRA) that mediate deletion of thymocytes which pose a danger to peripheral organs and tissues (Akiyama et al., 2008; Hikosaka et al., 2008; Irla et al., 2008; Kyewski and Klein, 2006; Zhu and Fu, 2008).

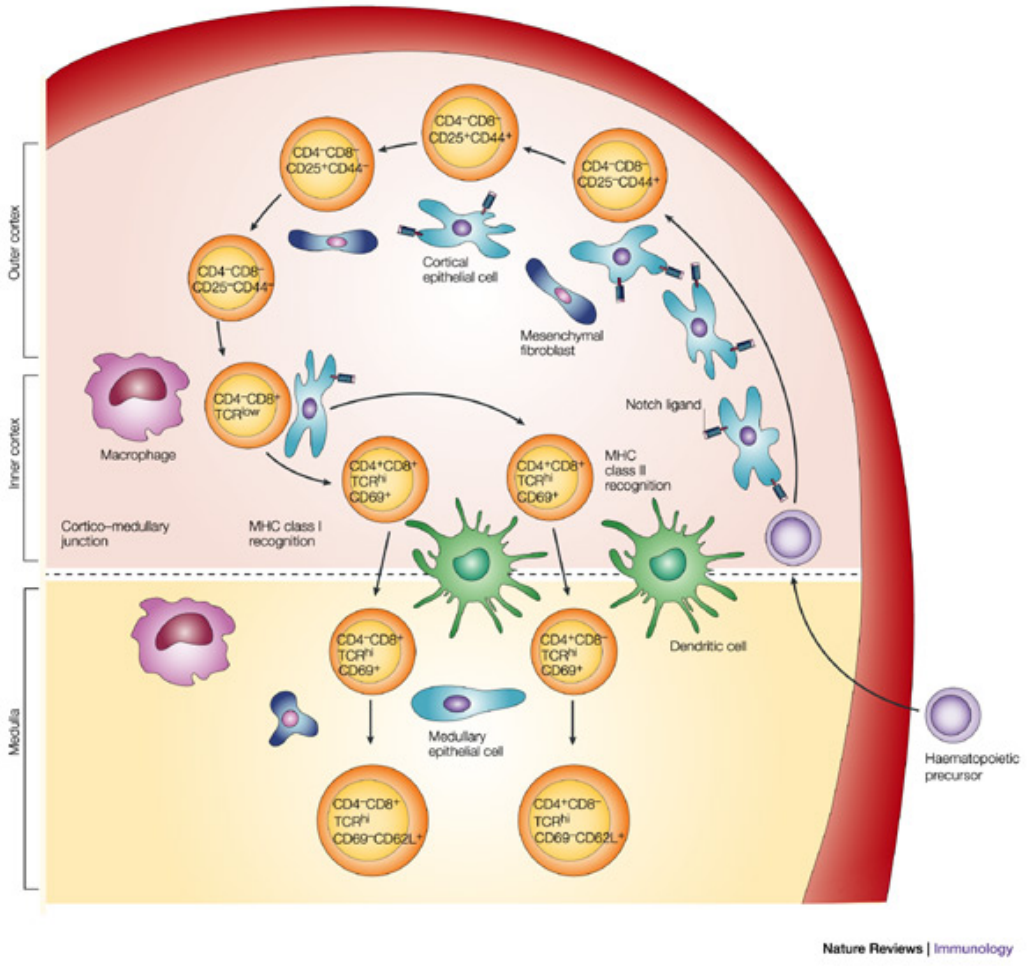

(Zúñiga-Pflücker, 2004)

Figure 6: T cell maturation and thymic epithelial cells. Subsets of thymocytes during maturation from hematopoeitic precursors to naive T lymphocytes.

4.1.1. AIRE

The thymic expression of many of these TRAs is dependent on a gene called autoimmune regulator (AIRE) (Gardner et al., 2008). It is clear that in the thymus, AIRE expression is restricted to mTECs, however it is disputed if AIRE is in fact present in secondary lymphoid tissue and contributes to peripheral tolerance (Gardner et al., 2008; Hubert et al., 2008).

AIRE is an important mediator of central tolerance that promotes the ubiquitous expression of organ-specific antigens in the mTECs and presentation of a number of proteins that are otherwise expressed only in the periphery. mTECs are associated with the negative selection of auto-reactive T cells. Self-reactive T lypmhocytes that recognize self-antigens are deleted to prevent attack of self-antigens in the periphery (Hubert et al., 2008; Schaller et al., 2008). Many tissue-restricted self-antigens (TRAs) are under AIRE-dependent transcriptional control in mature mTECs. AIRE-deficient medullary epithelial cells are less efficient presenters of antigen proteins and loss of the protein in mTECs is sufficient to cause autoimmunity (Gray et al., 2007; Matsumoto, 2011; Schaller et al., 2008; Seach et al., 2008).

Comprehensive self-antigen gene expression is compromised in humans and mice lacking the autoimmune regulator (AIRE), leading to autoimmunity that targets a range of organs and tissues (Gray et al., 2007). Autoimmune polyendrocrinopathy-candidiasis-ectodermal dystrophy (APECED) is an autosomal recessive disorder and is the only organ-specific human autoimmune disease described that affects multiple organs. This disease is caused by mutations in the AIRE gene in medullary epithelial cells, which is thought to be a

58kDa transcription factor and possibly E3 ubiquitin ligase (Gray et al., 2007; Hubert et al., 2008; Schaller et al., 2008). Debilitating autoimmunity as a result of self-reactive T cells is a condition experimentally observed in mice lacking AIRE protein (Metzger and Anderson, 2011). The multi-organ autoimmune pathology of individuals harbouring a mutation in the AIRE gene includes (but is not limited to): endocrine gland dysfunction, dysfunction of parathyroid and adrenal glands, hypoglycaemia, hypotension, lung disease and pulmonary hypertension (Gavanescu et al., 2008; Yano et al., 2008). These pathologies are largely humorally-mediated and B cells are required for development of autoinflammation as a result of AIRE loss (Gavanescu et al., 2008).

The expression of the 58KDa transcription factore AIRE is restricted to the thymic medulla compartment and specifically to mature (advanced differentiation state) mTECS defined as CD45- $MHCII^{hi}$ UEA-1+ $Ly51_{lo}$, K8+ and K5- (Hubert et al., 2008; Surh et al., 1992). AIRE encodes a predicted protein of 552 aa that contains structural features that anticipate a role in gene transcription. After gating on CD45- $MHCII^{hi}$ $Ly51_{lo}$ cells, which represent all mature mTEC, virtually all cells (88%) were shown to express AIRE (Hubert et al., 2008). AIRE+ cells represent 0.005% of a whole thymus yet are of great importance in thymic T cell education. (Hubert et al., 2008)

4.2. Thymic Stroma in HIV

Clinical studies of HIV-1 infected children and adults indicate that thymic function is impaired during infection with HIV-1. Examination of human thymic specimens have revealed morphological changes of the stromal architechture with loss of Hassal's

corpuscles (found in mTEC populations) (Ye et al., 2004). The thymus atrophies by the teenage years and its contribution to T-cell maintenance is significantly decreased. However, it is important to acknowledge that during HIV treatment, the thymus plays a role in immune reconstitution and several investigators have reported that HIV-induced thymic dysfunction could influence the rate of disease progression to AIDS (Clark et al., 1997; Kourtis et al., 1996; Ye et al., 2004).

4.2.1. Autoimmunity in HIV

An infectious trigger for immune activation is one of the postulated mechanisms in autoimmunity and derives from molecular mimicry. Multiple anti-retroviral drug therapy for patients with AIDS provides prolonged survival and immune restoration; a setting where autoimmune diseases develop (Haynes et al., 2000; Zandman-Goddard and Shoenfeld, 2002). The frequency of rheumatological syndromes in HIV patients varies from 1 to 60%. In addition to CD8+ T cell mediated autoimmunity, autoantibodies and anti-nuclear antibodies in HIV infection are frequently reported (Stratton et al., 2009). One study frequently found antibodies specific to cardiolipin and other phospholipids and the presence of auto-antibodies was significantly associated with lower CD4+ lymphocyte counts and increased mortality which implies a prognostic significance to this phenomenon in the context of HIV infection (Massabki et al., 1997).

Furthermore AIDS patients often present with renal pathologies, hallmark of autoimmune disorder systemic lupus erythematosus (SLE) such as renal disease, presence of antinuclear antibodies and manifestation of autoimmune IgG, IgA and IgM complexes

and B cell hyperstimulation (Kopelman and Zolla-Pazner, 1988; Malatzky-Goshen and Shoenfeld, 1989). In addition, T cell mediated autoimmune diabetes has been frequently reported in patients with no diabetes prior to HIV-infection (Takarabe, 2010). Autoimmunity in the form of T cell mediated psoriasis is also frequently reported in HIV-patients and tends to present during the later stages of HIV-infection (Fife, 2007).

While many mechanisms are proposed, immune restoration following treatment of HIV with possible altered immune regulation may lead to the emergence of autoimmune diseases (Zandman-Goddard and Shoenfeld, 2002, O'Leary, 2008)

5. CD4C/HIV^{Nef} Transgenic Mouse Model

In order to study the *in vivo* effects of the HIV-1 Nef accessory protein we employ a transgenic mouse model where Nef expression is driven by the human CD4C promoter fused to the mouse CD4 enhancer. As a result, Nef is expressed in CD4+CD8+ DP and CD4+ SP thymocytes, mature T lymphocytes and certain myeloid cells including macrophages and dendritic cells (Hanna et al., 1998a). These mice develop a very severe AIDS-like disease with several features remarkably similar to those reported in humans infected with HIV-1. These included thymic atrophy, loss of peripheral T-lymphocytes, loss of architecture of lymphoid organs and failure to thrive (Hanna et al., 1998a). This model was generated by the laboratory of Dr. Paul Jolicoeur at the *Institut de Recherches Cliniques de Montréal* (IRCM). This model has proven to be useful for the following discoveries: the depletion of DP thymocytes and impaired selection and lineage commitment of CD4+ SP thymocytes by Nef (Chrobak et al., 2011), the normal development and function of CD8+ T cells but impaired memory phenotype in Nef transgenic mice (Rahim et al, 2013), the activation of PAK2 by Nef which results in depletion of CD4+ T cells and downregulation of CD4 surface protein but is not sufficient to induce an AIDS-like disease (Vincent et al., 2006) and the indispensable role of Fas, FasL, ICE and TNFR-1 on the development of both T-cell loss and organ disease of Nef transgenic mice (Priceputu, 2005).

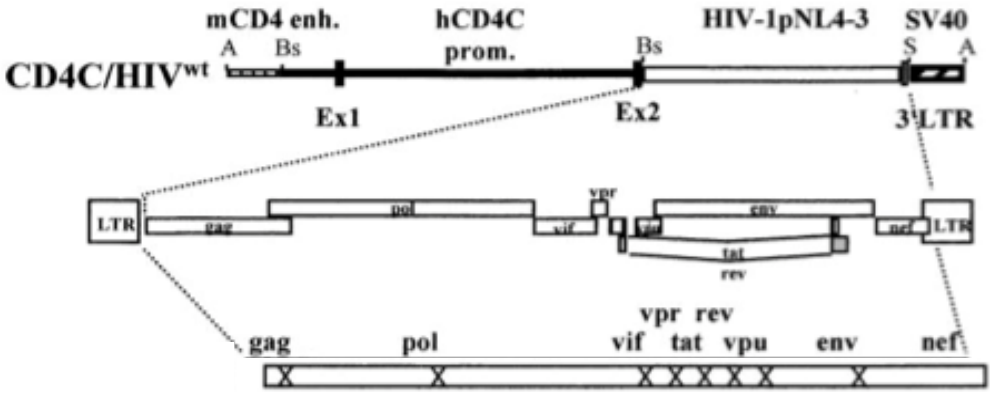

Figure 7: Structure of CD4C/HIV^{Nef} transgene. The mouse CD4 enhancer, human CD4 promoter and all the genes of HIV-1pNL4-3 and the polyadenylation sequence of the simian virus 40 (SV40) were ligated together. Ex1 an Ex2 are the two first non-transcribed exons of the human CD4 gene. The symbol x indicates that the reading frame of the gene is interrupted. All genes are interrupted except for Nef.

5.1. Alteration of T cell signaling at the immunological synapse

5.1.1. Rationalization

HIV-1 infection has a major impact on T cell signaling molecules. In Nef expressing thymocytes, the activity of intracellular T cell signaling molecule Lck is increased in basal conditions and attenuated with stimulation (Chrobak et al., 2010), contributing to partial T cell activation relieving the block of viral replication present in quiescent T cells all the while preventing host cell death induced by activation of the cell, another impediment to viral replication. Intracellular accumulation of Lck is simultaneous observed by in Nef affected cells (Haller et al., 2007), which is an important aspect relative to its activity. Several other proteins very tightly regulate the localization and activity of Lck in a normal cell, however the mechanism(s) of the phenomenon of un-coupled Lck activation or deregulation are very poorly understood.

5.1.2. Hypothesis

The level of Lck kinase activity depends on its phsophorylation status and it's localization. These functions of Lck are highly regulated by several proteins however Nef has not been implicated to have a direct effect on Lck. Therefore we hypothesized that Lck deregulation could be explained by an impairment in the alteration of Lck by regulatory proteins.

5.1.3. Objectives

In line with the elaborate and tight regulation of Lck activity, we decided to study the effect of Nef on other T cell signaling proteins in order to further depict the direct mechanism of Nef on immunological synapse signaling. In addition to proteins that directly regulate Lck activity, we studied downstream effects of Lck deregulation to further clarify the mechanism by which Nef can maintain uncoupled TcR signaling by which quiescent cells become semi-activated in the absence of TcR engagement and also do no respond to actual TcR engagement. A clearer picture of how Lck is deregulated by Nef and how downstream events are propogated in the context of Nef infection and dysfunctional Lck will provide crucial information on how to potentially override Nef-controlled T cell signaling.

5.2. Implication of Nef in AIRE activity and thymic epithelial cells

5.2.1. Rationalization

HIV-1 infection has a major impact of thymic structure and function. HIV-1 can infect thymoctyes leading to thymic abnormalities in humans where thymic atrophy is frequent and depletion of CD4+ SP and CD4+CD8+ DP thymoctyes has been reported (Joshi et al., 1985; Rosenzweig et al., 1993). Our lab previously reproduced this thymocyte

depletion in our Nef-expressing mouse model (Hanna et al., 1998b). These CD4+SP thymocytes provide essential survival signals that promote thymic medulla formation. The thymic medulla is essential for self-tolerance meanwhile during AIDS infection autoimmunity prevails. Promotion of self-tolerance by mTECs is highly dependant on the transcription factor AIRE which modulates the expression of tissue-restricted antigens (TRAs). The expression of AIRE is promoted by interactions of RANK on mTECS and RANK ligand on CD4+ T cells. Three independent *Immunity* studies from 2008 collectively demonstrate coordinating development of mTECs and essentiality of CD4+ SP and CD8+ SP for development of mTECs in a RANK dependant manner (Akiyama et al., 2008; Hikosaka et al., 2008; Irla et al., 2008; Zhu and Fu, 2008).

5.2.2. Hypothesis

Given the reciprocity in development of thymocytes and thymic epitheilial cells, we hypothesize that in Nef expressing thymi, there are significant and consequential changes to the thymic stroma and epithelial cells, including the downregulation of AIRE and depletion mTEC populations.

5.2.3. Objectives

Because of the critical role of AIRE in central tolerance and its unique expression in mTECs, the primary objective of this project was to demonstrate a significant impact of Nef expression on AIRE expression. We are especially interested in knowing if the impact of Nef expression is direct or indirect, i.e. a direct result of Nef expression or an indirect effect of Nef expression via CD4+ thymocyte depletion. Approaches will include studying changes in the absolute cell count of AIRE expressing cells (mTECs) and net changes of AIRE expression within the mTECs via single cell analysis. We will also

directly attempt to detect Nef in AIRE expressing population. Finally, to study indirect affects of Nef, we will attempt to rescue AIRE expression in transgenic mice where CD4+ thymocyte depletion is partially rescued.

6. Materials and Methods

6.1. Materials

Mice

CD4C/HIVNef transgenic mice where previously generated (Hanna et al., 1998a) and crossed onto a C3H non-Tg background (Harlan Laboratories, Indianapolis, IN). The LCK Y505G mice (line A16924) expressing the constitutive active form of Lck Y505F were obtained from Dr. P José Alberola-Ila (Oklahoma Medical Research Foundation, Oklahoma City, OK). Insert mDC4c, AIRE. The genotyping of transgenic mice was done by polymerase chain reaction (PCR) using oligonucleotides specific to different transgenes. Mice were maintained in an animal facility in sterile pathogen free conditions according to the guide established by the Canadian Council on Animal Care approved by the animal protection committee at the IRCM.

Antibodies and Reagents

Monoclonal antibodies α-CD3ε coupled to biotin, clone 145-2C11 and α-CD4 coupled to biotin, clone GK1.5 (BD Biosciences) and streptavidin (Zymed San Francisco, CA) were used for *in vitro* stimulation of thymocytes.

For **immunoprecipitation**: α-Lck 3A5 (Santa Cruz biotechnology, Santa Cruz, CA), α-CD3ζ (Santa Cruz biotechnology), α-Csk C-20 (Santa Cruz biotechnology), α-UNC119 L-17 (Santa Cruz biotechnology), α-p-Lck Y505 (Cell Signaling Technology, Beverly, MA), mouse monoclonal α-CD3ζ 6B10.2 (Santa Cruz biotechnology).

The following antibodies were used for **immunoblotting:** α-Lck clone 3A5 (Santa Cruz biotechnology), α-pSrc Y416 (Cell Signaling Technology, Beverly, MA), α-p-Lck Y505 (Cell Signaling Technology), rabbit polyclonal α-ZAP-70 sc-574 (Santa Cruz biotechnology), mouse monoclonal α-p-Y clone 4G10 (Upstate Biotechnology), α-LAT (Upstate Biotechnology), α-Cbl clone 7G10 (Millipore, Billerica, MA), α-Nef clone NF2-B2 (NIH AIDS Research and Reference Reagent Program). The antibody β-Actin (Sigma-Aldrich) was used as an internal control for protein loading. The secondary antibodies IgG α-rabbit (H+L) coupled to Alexa 680 and IgG α-mouse coupled to Alexa 800 were used and fluorescence was measured by Odyssery LI-COR.

The following antibodies were used for **immunofluorescence:** α-Lck clone 3A5 mouse monoclonal (Santa Cruz Biotechnology), rabbit polyclonal α-ZAP-70 sc-574 (Santa Cruz biotechnology), sheep polyclonal α-SLP-76 (Upstate Biotechnology, Lake Placid, NY), rabbit polyclonal α-LAT (Upstate Biotechnology), mouse monoclonal α-Rac-1 23A8 (Upstate Biotechnology), rabbit polyclonal α-Rac-2 C-11 (Santa Cruz). Secondary fluorescent conjugated antibodies were the following: IgG α-mouse (H+L) coupled to Alexa 555, IgG α-sheep coupled to Alexa 488 and IgG α-rabbit (H+L) to Alexa 633. Finally 4',6'-diamidino-2-phenylindole (DAPI) (Vector Laboratories, Inc. Burlingame, CA) was used to stain nuclei of thymocytes.

Antibodies used for **flow cytometry** were the following: monoclonal Rat α-CD45 Pacific Blue (Invitrogen, Camarilla, CA), monoclonal Ly-51 PE (BD Biosciences, Mississauga, ON), Ulex Europaeus Agglutinin 1 (UEA-1) Biotinylated (Vector Laboratories).

Primers

HIV-Nef Sense GCACGGCAAGAGGCGAGGG

HIV-Nef Antisense CTAATCGAATGGATCTGTCTCTG

AIRE- Sense GCAGTTGGGGATGGAATGCTACGC

AIRE- Antisense CCTGGGCTGGAGACGCTCTTTGAG

Hprt- Sense GTTGGATACAGGCCAGACTTTGTG

Hprt- Antisense GATTCAACTTGCGCTCATCTTAGGC

Insulin- Sense GCCCTTAGTGACCAGCTATAATC

Insulin- Antisense GGACTTGGGTGTGTAGAAGAAG

SAP1- Sense GTCTTCCTTGTCTCCTGGTATTG

SAP1- Antisense CCTGAGTTTCAGAGCCAGTATTT

6.2. Methods

6.2.1. Alteration of T cell signaling at the immunological synapse

Stimulation of thymocytes *in vitro*

As described in Chrobak et al., (2010), thymocytes were placed in an eppendorf tube at a concentration of $50x10^6$ cells/mL in RPMI media and 5% fetal bovine serum. Cells were then incubated on ice with biotinylated antibodies α-CD3ε and α-CD4 at a concentration of 10ug/mL for 10 minutes. After incubation, thymocytes were centrifuged at 2500 rpm for 5 minutes at 4°C. Stimulation was achieved by resuspending thymocytes in RPMI media and 5% fetal bovine serum with a concentration of 20ug/mL of pre-heated streptavidin and incubating for 5 minutes at 37°C. Following incubation, thymocytes

were placed on ice for 5 minutes to stop stimulation, and then centrifuged at 2500 rpm for 5 minutes at 4°C.

Cell Lysis and Protein Quantification

Following stimulation or not, thymocytes were lysed for 15 minutes on ice in lysis buffer (50mM Tris-HCl pH7.8, 150mM NaCl, 1% triton, 2mM EDTA) containing 4mM sodium orthovanadate (Na_3VO_4), 10mM sodium fluoride (NaF0, 1mM phenylmethylsulfonil (PMSF) and a cocktail of protease inhibitors. Lysates were cleared of cellular debris by centrifuging at 12 000 rpm for 10 minutes. 5ul of each lystate was reserved for protein quantification by micro-BSA method (Pierce, Rockford, IL).

Immunoprecipation

Following cellular lysis, approximately 500-1000ug of protein lysates (from 30-60 X 10^6 thymocytes) were incubated with the immunoprecipitating antibody for 2 hours with rotation at 4°C. Following incubation, the lysate and antibody mixture was incubated with 40ul of sepharose protein A or G (50% solution) pre-washed with lysis buffer for 1 hour with rotation at 4°C. Following incubation, the sepharose/antibody/target protein complex was pelleted by centrifuging at 1000 rpm for 10 seconds and washed 3 times with lysis buffer at 4°C.

In vitro kinase assay (IVKA)

Following immunoprecipitation, the sepharaose/antibody/target protein complex was washed with kinase extraction buffer (50mM Tris-HCl pH 7.8, 150mM NaCl, 0.5% triton, 10 mM $MgCl_2$, 2mM EDTA) at 4°C and subsequently washed twice with kinase

activation buffer (50mM Tris-HCl pH 7.8, 150mM NaCl, 0.5% triton, 10 mM $MgCl_2$). The supernatant was removed and 24ul of reaction mix (100ul KAB with 6ul of γ-^{32}P – 60 μCu total) was added to each reaction tube on ice. The kinase reaction was started by moving samples to room temperature for 6 minutes and stopped by putting samples back on ice. The precipitate was then washed with KEB. Following SDS-PAGE electrophoresis, proteins were transferred onto a membrane and radioactivity was visualized using Phosphoimager (Molecular Dynamics, Sunnyvale, CA) and quantified using ImageQuant (Molecular Dynamics).

SDS-PAGE electrophoresis

Following protein quantification by Pierce micro-BCA, 50ug of proteins were mixed with 4X electrophoresis buffer (62.5 mM Tris-HCl pH 6.8, 10% glycerol, 2% SDS, 5% β-mercaptoethanol and 0.00625% bromophenol blue) and heated to 100°C for 5 minutes. Prepared samples were then loaded onto a polyacrylamide gel. The separation gel contained 6-12% (w/v) acrylamide, 0.4M Tris-HCl pH8.8, 0.1% (v/v) SDS, 0.1% ammonium persulfate and 0.8ul/mL N,N,N',N-tetramethylenediamine (TEMED). The stacking gels contained 3.9% (w/v) acrylamide, 0.6M Tris-HCl pH6.8, 0.1% (v/v) SDS, 16% sucrose, 0.1% APS and 0.8ul/mL TEMED. Protein migration was performed at 100 volts until proteins reached the separation gels and then at 130 volts until the bromophenal blue had migrated out of the gel.

Western Blotting

Following SDS-PAGE electropheresis, proteins were transferred onto a polyvinyldene fluoride (PVDF) membrane with 0.45 um pores pre-wetted in methanol. The transfer was performed at 25 volts overnight in transfer buffer (10mM Tris, 96 mM glycine and 15% methanol). Following transfer, non-specific binding site of membranes were blocked with 5% bovine serum albumine (BSA) in TBS for a minimum of one hour. After blocking, membranes were incubated with the primary antibodies diluted in 5% BSA in TBS + 0.1% Tween for 2 hours at room temperature. Membranes were then washed three times in with 15mL of TBS + 0.1% Tween for 5 minutes with agitation. The secondary antibody was diluted in 5% BSA in TBS and incubated for one hour. Finally membranes were washed three times for five minutes with 15mL TBS + 0.1% Tween. Proteins were detected by fluorescent infrared scanner Odysssey LI-COR. Quantitation of protein signal was performed using Odyssey software and ratios were normalized to β-actin signal as a loading control.

Immunocytochemistry and confocal microscopy

Freshly isolated thymocytes were stimulated or not and resuspended in PBS at a concentration of $1x10^6$ cells/mL. The thymocytes were then fixed in 4% paraformaldehyde for 30 minutes at room temperature. After fixation, thymocytes were centrifuged for 5 minutes at 2500rpm and washed with PBS. Approximately 120,000 cells were put on slides by cytospoting technique using the Shandon Cytospin 2 at 300rpm for 5 minutes. The cells were permeabilized in a solution of PBS + 0.1% Triton for 5 minutes. The slides were washed with PBS for 5 minutes and a blocking solution (PBS + 5% BSA) was applied for one hour to block non-specific binding sites. The slides were

then incubated with the primary antibody diluted in a PBS + 1.25% BSA for a minimum of one hour. After incubation, slides were washed twice with PBS for 5 minutes and the slides were incubated with a secondary antibody diluted in PBS + 1.25% BSA. The slides were washed twice to remove excess antibody and 30ul of DAPI was applied to stain DNA (visualize the nucleus of the cell) for confocal microscopy. Acquisition of confocal microscopy was achieved using the LSM 700 confocal microscope (Zeiss) in coordination with ZEN imaging software (Zeiss). Analysis of confocal micrscopy images was performed on ZEN imaging software (Zeiss) and all quantification was done using Velocity 3D Image Analysis (Perkin Elmer).

6.2.2. Implication of Nef in AIRE activity and thymic epithelial cells

Extraction of stromal cells

Excised thymus was placed in a 35mm petri dish with a 0.25-mm mesh placed over top, a plunger from a 1ml syringe was used to press firmly on the tissue to force the fragments apart and allow the thymocytes to pass though. The thymocytes were discarded and the remaining tissue was recovered for extraction of stromal cells. The tissue from one thymus was placed in a polypropylene eppendorf tube with 400ul RPMI + 2μg DNAse + 0.5 mg Liberase Blendzyme (Roche). On ice, the tissue was cut into the smallest pieces possible with scissors at 4°C. The digestion was started by placing the tubes at 37°C, the tubes were left for 15 minutes, and stroma was forced through a 1mL Pasteur pipette every two minutes. The reaction was stopped by putting samples back at 4°C. This method is described by Williams et al., (2009).

Flow cytometry analysis and cell sorting

As published by Rahim et al., (2013), isolated thymocytes were incubated in blocking buffer (PBS+ 20% FCS) for 30 minutes at 4°C. After centrifugation, thymocyctes were resuspended in FACS buffer (PBS+ 2% FCS) and placed in a 96 well plate at $1x10^6$/100ul/well. Antibodies CD45 Pacific Blue, UEA-1 Biotin (+ Strepavidin APC) and Ly51 PE were added at a concentration of 1ug per 100ul and incubated at 4°C for 30 minutes. 7AAD was added during the last 15 minutes to detect DNA (dead cells). The cells were washed once before being transferred into FACS microtubes (Bio-Rad, 223-9391) containing and completed to 300ul. The acquisition was performed by the flow cytometer CyAN (Beckman Coulter, Brea, CA) et analysis software Summit (Dako, Markham, ON). When sorted cells need to be recovered, samples were sorted with a MoFlo cell sorter (Beckman Coulter).

RNA Extraction of total thymus

Excised thymi were divided into two lobes and snap-frozen in liquid nitrogen. One thymus lobe was homogenized in 1mL of Trizol (Invitrogen). 200ul of chloroform was added to the trizol reagent, shaken well and then centrifuged at 12,000rpm for 15 minutes at 4°C to separate phases, the aqueous phase was recovered and the non-aqueous phase discarded. The RNA was precipitated by adding 500ul of isopropyl alcohol to samples and incubating for 10 minutes at room temperature and then centrifuging at 12,000 rpm for 10 minutes at 4°C. After discarding the supernatant, the RNA pellet was washed with 1mL of 75% ethanol and centrifuged for 5 minutes at 4°C. The ethanol was removed and the RNA was resuspended in water and quantified using nanodrop (Thermo Scientific).

RNA Extraction of sorted samples

When RNA availability was low (ie. sorted small populations of less than 50,000 cells), RNA was extracted using the RNeasy Plus Mirco Kit (Qiagen, Hildon, Germany) to maximize the RNA yield, the extraction was performed according to manufacturer instructions and eluted in 14ul of water, of which 7ul was used for the reverse transcription, yielding a typical RNA concentration of 3 ug/uL.

Reverse Transcription

Unless otherwise described, 3ng of RNA was used for the preparation of cDNA using the MLV- Reverse Transcriptase kit (Invitrogen). The resulting mixture was 20ul of cDNA.

Polymerase Chain Reaction

Amplification of PCR sequences were performed in a reaction of 20ul containing 2ul of cDNA, 0.2ul of rTaq polymerase (Invitrogen), 2ul of 10X PCR Buffer (Invitrogen), 0.22mM dNTPs, 0.25uM antisense primer (Invitrogen), 0.25uM sense primer (Invitrogen). Thermal cycles were as follows: 94ºC for 2 minutes followed by 24-34 cycles of 94 ºC for 45 seconds, 60 ºC for 45 seconds and 72 ºC for 1 minute and finally 72 º C for 7 minutes after the last cycle. Samples were electrophoresed on a 1.5% agarose gel in 1X TAE (40mM Tris acetate, 1mM EDTA, pH 8). DNA bands were revealed by ethidium bromide staining under an ultrafluorescent light. Quantification was achieved using Image Quant software (Molecular Dynamics).

Northern Blot

For each sample, 6ng of RNA was electrophoresed on a 1% agarose gel in 1X MOPS (0.02 M MOPS pH7, 5mM sodium acetate, 1mM EDTA) and 1.85% Formaldehyde. The RNA was transferred onto a membrane overnight by placing the gel on 20X SSC soaked 3M paper with a nitrocellulose membrane placed on top of the gel. After transfer, the membrane was incubated with pre-hybridization buffer (5X SSC, 1% SDS, 0.1% sodium pyrophosphate, 5X Denhart's solution (0.1% (w/v) each BAS, Ficoll 400, PVP), 200ug/ml sheared salmon sperm DNA) for 2 hours before applying the probe. The probe was prepared by denaturing at 100 ºC for 3 minutes mixing with 3ul with ^{32}P-α-dCTP, 30ul of buffer, and 1ul klenow (New England Biolabs, Ipswich, MA) and incubating for 2 hours. Afterwards 55ul 0.3M NaCl TE , 4ul of tRNA and 200ul 95% ethanol were added to precipitate the probe on dry ice for 20 minutes. The probe was pelleted and resuspended in 200ul NaCl TE and transferred onto the membranes with hybridization solution (pre-hybridization buffer overnight + 10% dextran sulphate) at 65 ºC. Following hybridization, membranes were washed at room temperature for 20 minutes with wash solution 1, at 65ºC for one hour with wash solution 2 (2X SSC, 1% SDS, 0.1% sodium pyrophosphate), and rinsed with wash solution 3. The membranes were dried and imaged with the phosphoimager (Molecular Dynamics) and quantified with ImageQuant (Molecular Dynamics).

Statistical Analysis

Statistical analyses were performed using Graph Pad Prism software where a Student's *t*-test was used to compare means of various treatments with a confidence interval of 95%. Data represent the mean of a minimum of three independent experiments and are presented as the mean ± the standard error of the mean. Significant differences are

indicated on figures as follows: *p<0.05, **p<0.01, ***p<0.001. Where 0.05<p<0.1, Δ indicates a favorable trend.

7. Results

7.1. Nef and TcR signaling

Delocalization of Lck by Nef results in disruption of the Csk feedback loop

The tyrosine phosphorylation site Y505 of Lck is classically considered to be inhibitory of the protein activity. It is phosphorylated by C-terminal kinase (CSK) under basal conditions, until the cell becomes activated and Csk dissocaiates from PAG and is released into the cytoplasm at which point the phosphatase CD45 dephosphorylates Y505 and Lck is activated. Previous data (unpublished) shows that the kinase activity is attenuated in CD4C/HIV-Nef mice and therefore we hypothesized that one mechanism is inactivation of the protein by phosphorylation of Y505. We found that overall in Nef containing mice there is higher protein levels of pY505-Lck (**Figure 8B**) and total Lck (not shown) relative to actin, which was used as a loading control. This shows that the total level of Lck protein in higher in Nef+ mice and there is either more translation or less degredation of the protein. We find that under basal conditions, there is a higher proportion of pY505-Lck in Nef+ thymocytes (**Figure 8C**) compared to Nef- samples, and that the ratio in Nef+ unstimulated thymocytes is similar to that of Nef- stimulated thymocytes. In addition there is an even more profound increase in the proportion of pY505-Lck in Nef+ stimulated samples suggesting that a large proportion of the Lck in Nef+ mice could be in the inactive form.

Nika et al., (2010) showed that there are four forms of the Lck protein of which exists a double phosphorylated form where pY394 combined with pY505 actually renders the protein active. To test if the increased proportion of pY505 seen in Nef+ thymocytes could be the double phosphorylated active form, we immunprecipited Lck with a pY505 antibody which can recognize the double phosphorylated form and measured by Western blotting the amount of pY394 detected on the immunoprecipitate thus capturing the totality of the double phosphorylated form in sample lysates. We show that when Nef- cells are stimulated, there is a significant almost 3-fold increase in the amount of double phosphorylated Lck detected (**Figure 9**), whereas in the Nef+ samples, stimulated or not, there is no difference as compared to basal Nef- samples.

Given that the phosphorylation of Y505 is controlled partially by Csk (in competition with CD45), we wanted to study Csk in the context of Nef infection. In order to study the activation of Csk, we immunoprecipitated the protein and performed a Western blot using a phospho-tyrosine-specific antibody. No phosphorylation of Csk is detected. Further analysis of the blots revealed that tyrosine-phosphorylated p51 was immunoprecipitated in the Csk complex in non-trangenic CD3/CD4 stimulated Csk-immunoprecipitates but the signal is lost in transgenic thymocytes (**Figure 10**).

We subsequently decided to study the activity of Csk and associated proteins by performing an *in vitro kinase assay* (IVKA). We found that the kinase activity of Csk was considerably decreased in thymocytes in both stimulated and non-stimulated conditions as determined by the densitometry of the substrate Lck/Fyn (p51). In addition, the kinase activity of Csk-associated proteins (Fyn or Lck) is significantly lost in Tg samples as is

seen by the reduction in intensity of bands p51 (Lck or Fyn) and their substrates p70 (ZAP70), p16/21 (CD3ζ) p90 (Cbp/PAG) (**Figure 11**).

The hypothesis that Nef could associate with Csk and cause the differences in Csk-associated activity seen in Nef+ thymocytes did not lead to detection of the two proteins bound by immunoprecipitation (**Figure 12**). We therefore could not pinpoint the exact moment of disruption of the Lck/Csk feedback loop. Another hypothesis of a potential mechanism of Lck delocalization is related in an Lck-trafficking protein, UNC119. Lck targeting to the plasma membrane is crucial for T cell activation upon stimulation, which is achieved by a function of UNC119 (Gorska et al., 2009). Therefore we hypothesized that direct Nef inhibition of UNC119 would explain the delocalization of Lck however we failed to detect any interactions (**Figure 13**).

Altered Lck may facilitate downstream TcR signaling in the absence of ZAP-70 activity in the presence of Nef

Despite the lack of ZAP-70 kinase activity, there is nevertheless an increase in activation of downstream mediators of TcR signaling such as Erk MAPK (Hanna et al., 1998b; Schrager et al., 2002). A recent study suggests that Erk is activated downstream of N-Ras in Nef infected thymocytes (Pan et al., 2012), however multiple studies show the activation of Pak2 by Nef directly (Krautkrämer et al., 2004; Vincent et al., 2006) and indirectly (Janardhan et al., 2004). Therefore we decided to study the localization of Rac- a GTPase responsible for Pak2 activation- in the context of Nef expression *in vivo* in order to further clarify the situation.

The difference in localization of Rac-1 between Nef- and Nef+ cells is shown in **Figure 14**. In normal non-stimulated Nef- cells, Rac-1 is clustered, and present at the plasma membrane as well as towards the interior of the cell which we refer to as 'accumulation'. In the case of most Nef+ unstimulated cells, all of the Rac-1 is at the plasma membrane with little to no protein observed in the interior of the cell. Analysis of 'accumulation' on an individual cell basis shows a significant decrease in Rac-1 accumulation upon stimulation of Nef- cells, a state in which Rac-1 moves towards the cell membrane and becomes activated (**Figure 14B**). This phenomenon was also observed in Nef+ cells prior to stimulation, and a significant change did not occur after stimulation of these cells indicating that Rac-1 in Nef- cells is already activated before *in vitro* stimulation. Similarly, between non-stimulated and stimulated Nef- and Nef +thymocytes, the area of Rac-1 was significantly decreased correlating with a change in arrangement of the protein (Rac-1 protein clumped together rather than dispersed) (**Figure 14C**). There were no significant differences observed in Rac-1 area between Nef- and Nef+ unstimulated samples, likely due to the degree of variation in the data. Finally, there was no difference between the mean fluorescence of Rac-1 in Nef- and Nef+ cells, stimulated or not (**Figure 14D**) indicating that there was no increase or decrease in the quantity of protein measured..

As previously mentioned, the roles of Rac-1 and Rac-2 are not entirely redundant but do have overlapping effects; therefore we wanted to study Rac-2 in the same context as Rac-1. **Figure 15A** shows the localization of Rac-2 in Nef- and Nef+ cells, the Rac-2 protein in the Nef+ relative to the Nef- thymocytes is much less dispursed and more congregated

at the plasma membrane. Quantification of accumulation as percent accumulated on cell-to-cell basis shows that the Rac-2 of Nef+ cells in a basal state is much less than in Nef- cells indicative of hyperstimulation (**Figure 15B**). There were no differences observed in mean area of Rac-2 between stimulated or not Nef- and Nef+ thymocyte indicating that Rac-2, even though less concentrated in the cytoplasm of the cell, was not any more or less aggregated between samples (**Figure 15C**). Finally, there were no differences observed in mean fluorescence or Rac-2 (**Figure 15D**).

Biochemical studies from the lab suggest that Rac-1 is underactivated in Tg mice (unpublished) despite its increased localization to the plasma membrane shown in this thesis. Activation of Rac is associated with it's recruitment to lipid rafts as it comes in close proximity of Vav, a guanine nucleotide exchange factor that catalyzes exchange on Rac-1 rendering it active (Crespo et al., 1997). Vav becomes active when it is recruited to the LAT/SLP-76 microcluster scaffold which is suggested to be disrupted by HIV-Nef (Abraham et al. 2012). It has also been suggested that Rac can be brought to the plasma membrane as part of a Nef complex (Janardhan et al., 2004) therefore we wanted to investigate whether Rac or other downstream mediators could be activated in the canonical TcR pathway of thymocytes during Nef infection. In the absence of ZAP-70 activity we wanted to know if LAT could be phosphorylated by Lck, if the LAT/SLP-76 microclusters were disrupted as previously suggested, and finally if Lck could phosphorylate SLP-76, allowing the canonical pathway to continue in the absence of ZAP-70 activity.

Our initial goal was to pursue the hypothesis that Lck directly phosphorylates LAT independent of ZAP-70 in Nef+ thymocytes. This was studied using kinase assay with an external substrate (GST-LAT) approach which turned out to be unfruitful, therefore we measured co-localization of LAT and Lck by immunflourescence.

Even in Nef- thymocytes, upon stimulation, Lck and LAT have a significantly stronger co-localization measured by volume and intensity of signal (**Figures 16B and C**) likely due to Lck moving into the lipid-raft domain upon stimulation, which makes it more accessible to phosphorylate LAT. However in Nef+ non-stimulated thymocytes, co-localization is already significantly increased with respect to Nef- non-stimulated thymocytes, which makes Lck available to phosphorylate LAT and activate downstream mediators before and after stimulation. After stimulation of Nef+ thymocytes, there is no significant increase in Lck/LAT co-localization with respect to Nef+ unstimulated thymocytes (**Figure 16B,C**).

Previous studies *in vitro* suggest that LAT and SLP-76 are no longer found in the same compartments of Nef-infected cells (Pan, 2011). If this data is accurate then even if LAT is phosphorylated by a kinase in Nef+ thymocytes, the Lck of SLP-76 recruitment will disrupt many important events. We studied the co-localization of LAT and SLP-76 by methods of immunocytochemistry (**Figure 17A**). Measurements of the volume (**Figure 17B**) and mean intensity (**Figure 17C**) of the co-localization between the two proteins show that there is no disruption of SLP-76/LAT microclusters in non-stimulated and stimulated conditions between wildtype and HIV-Nef mice.

Knowing that LAT/SLP-76 microclusters were not disrupted by Nef, we next sought to determine if Lck could then phosphorylate SLP-76 by studying their co-localization in immuncytochemistry. We do not report any differences of mean intensity of volume of the colocalization of Lck and SLP-76 amongst control and Nef+ thymocytes under basal and stimulated conditions (**Figure 18**).

7.2. Nef and AIRE

Consequences of CD4C/HIV-Nef on thymic epithelial cell populations and loss of AIRE expression

Given the dependency of AIRE expression on RANKL signals from CD4+ thymocytes ((Zhu and Fu, 2008), which are lost in the thymus in CD4C/HIV-Nef mice (Chrobak et al., 2010), we investigated levels of AIRE mRNA expression in these mice. The first approach was achieved by extracting RNA from total thymus and separating transcripts by electrophoresis. RNA was transferred onto a membrane and hybridized with a radioactive AIRE probe **(Figure 19A).** We found that the total AIRE mRNA was decreased in CD4C/HIV-Nef mice. In order to validate the RT-PCR data by another method we confirmed the result by reverse transcribing thymus RNA and amplifying small segments of AIRE and housekeeping gene HPRT by PCR **(Figure 19B).** The results consistently demonstrate that the expression of Nef in the thymus provokes a significant decrease in the expression of AIRE mRNA.

We decided to reproduce the partial loss of AIRE mRNA expression in another transgenic mouse founder expressing Nef. The second transgenic mouse used is the mCD4/HIV-Nef mouse in which Nef is driven by the mouse CD4 promoter and not the human as in

CD4C/HIV-Nef mice. The main difference between these mice is the differential expression of Nef, whereas human CD4 drives Nef expression in myeloid cells and mouse does not. Moreover this founder of mCD4/HIV-Nef line contains approximately double the Nef protein in the thymus with respect to CD4C/HIV-Nef however the severity of CD4+ T cell depletion is not different (Hanna et al., 2009). Similar to the loss in CD4C/HIV-Nef mice, the mCD4C/HIV-Nef mice experienced an even more profound loss of AIRE **(Figures 20A and B).**

Consequently, we wanted to investigate if this AIRE loss was due to a loss of cells expressing AIRE or a downregulation of the AIRE gene. As AIRE is expressed uniquely in a single population (mTECs) and at a high rate of approximately 90% of mTECs being AIRE+ (Hubert et al., 2008), this question could be answered through single cell analysis (flow cytometry). After gating on CD45- non-hematopoietic cells of the thymus, cells are separated into three populations (medullary, cortical, endothelial/fibroblasts) based on their staining for Ly51 and UEA-1. While we were expecting to see a decrease in mTECs we were very surprised to find that there was a signficiant increase (enrichment) in the total amount (extrapolated from percentage) of mTECs from thymi of CD4C/HIV-Nef mice (**Figure 21E)**. Also to our surprise, the cTEC populations where also found to be enriched (**Figure 21C**) whereas this population is completely independent of AIRE expression and we did not expect to see a change. Finally endothelial/fibroblast cell populations remained unchanged (data not shown).

To further understand the enrichment of TECS, we obtained an AIRE/GFP reporter mouse and bred it with our CD4C/HIV-Nef mouse. When crossed with the CD4C/HIV-

Nef mouse, we saw a decrease in the mean fluorescence intensity of AIRE (**Figure 22C**). Due to the large variability in the data it was not possible to detect a difference in AIRE+ cells (**Figure 22B**). Nevertheless we did observe a significant decrease in the number of cells expressing a high level of AIRE (**Figure 22A**).

AIRE loss and TEC phenotype is dependent on CD4 SP loss and can be rescued

After observing a loss of AIRE and an enrichment of mTECs, we wanted to know if these phenomenona were simply a result of CD4 loss in the thymus or if they could be directly attributed to Nef expression in these epithelial cell populations. HIV-1 has previously been shown to infect CD4+ epithelial cell populations (Horejsh et al., 2002). However CD4 protein has never been found in TECs. Using a CD4C/GFP reporter mouse as a tool we sought to determine if we could detect GFP in our TECs of interest. In order to exclude hematopoeitc cells that may not have stained for CD45 we gated on CD45- and side scatter high cells (**Figure 23A**) before analyzing the epithelial cell staining. As a result we found in tetracycline-controlled inducible CD4C/GFP mice that UEA-1 cells were positive for GFP with a complete right shift relative to CD45-/UEA-1- cells, UEA-1+ cells positive for GFP had a much lower mean fluorescence intensity (left-shift) than CD45+ cells.

To rule out a possible founder effect, we investigated the same question in a constitutive CD4C/GFP mouse. When gating on CD45-, side scatter high cells, we also found that GFP was expressed in cortical and mTECs at a lower mean fluorescence intensity than CD45+ hematopoietic cells but not in endothelial cells and fibroblasts (**Figure 23B**).

Based on the hypothesis that Nef directly affect TECs, one might expect to observe and enrichment or depletion of TECs with CD4 promoter activity in cells expressing Nef. To address this, we crossed the CD4C/GFP reporter mouse with CD4C/HIV-Nef to generate a mouse expressing both Nef and GFP under the same promoter. We hypothesized that there to be a difference in the number of cells positive for GFP in CD4C/HIV-Nef mice. Data revealed that roughly 70% of cTECs and 35% of mTECs are positive for GFP, a value that does not change in Nef expressing mice **(Figure 24A, C).**

Finally, we attempted to study the presence of Nef mRNA in the TECs. We performed a fluorescence-activated cell sort using the same cell surface markers and sorted CD45+ cells, mTECs, cTECS and endothelial cells/fibroblasts (**Figure 25A).** The cell yield was very low but enough to perform RNA extraction with appropriate reagents. The successful amplification of housekeeping gene HPRT with a clean blank (**Figure 25B**) confirms that RNA was successfully extracted. Successful Nef amplification of the same samples is confirmed by the strong band in the positive control and in CD45+ cells of CD4C/HIV-Nef mice (**Figure 25C**). There is no detectable Nef mRNA in the thymic epithelial sorted cell samples of the CD4C/HIV-Nef mice.

The loss of AIRE could be potentially explained by CD4+ thymocyte loss in CD4C/HIV-Nef mice due to dependency of mTECs on RANK from CD4+ thymocytes. Therefore, we hypothesized that AIRE mRNA loss in CD4C/HIV-Nef mice could be rescued by double transgenic mice that were able to rescue CD4+ SP thymocytes. In the case of the Tailles x CD4C/HIV-Nef double transgenic mouse, the lack of an intracellular tail of CD4 is able to rescue defects in thymocyte maturation at the double positive stage (in cortex) in

addition to a partial rescue of CD4+ thymocytes (Chrobak et al., 2010). However, the partial rescue phenotype did not result in a rescue of AIRE mRNA expression in Tailles x CD4C/HIV-Nef mice as determined by probe hybridization (**Figure 26B**) or gene amplification (**Figure 26C**) and average quantity mRNA detected in the double transgenics resembles that of CD4C/HIV-Nef samples.

On the contrary, there is a potential rescue in a second CD4+ thymocyte rescue model where dLGF mice expressing a consitutively active Lck molecule. When crossed, the dLGF x CD4C/HIV-Nef double transgenic results in a complete rescue in CD4+ thymocyte loss in CD4C/HIV-Nef. In addition, the double transgenic causes a significant increase in CD8+ thymocytes (enrichment) relative to WT and CD4C/HIV-Nef. The fact that TECs rely on signals from both CD4+ and CD8+ thymocytes combined with a full rescue makes the dLGF double transgenic mouse a stronger rescue model in attempt to rescue AIRE mRNA loss. We did not observe a significant change in AIRE expression between the double transgenic and WT mice (**Figure 26E**), although the average in the double transgenic is slightly lower due to one sample.

Finally, since we were able to rescue the loss of AIRE mRNA with a CD4 rescue model we wanted to confirm that we could rescue the resulting enrichment of TECs. Indeed in the dLGF x CD4C/HIV-Nef mice we do not see the same enrichment of TECs as in the CD4C/HIV-Nef mice (**Figure 27**).

CD4C/HIV-Nef induced AIRE loss impairs central tolerance and confers autoimmunity

Finally we wanted to investigate the real biological significance of the impaired maturation of TECs and subsequent loss of AIRE. Clinical outcomes of AIRE loss in humans include a loss of expression of tissue-restricted antigens (TRA) (Anderson et al., 2002), therefore we decided to measure two of the most common TRAs studied: insulin and SAP by RT-PCR. Gene amplification reveals that a 50% loss of AIRE (**Figure 28**) leads to an 80% loss of insulin expression in the thymus, which is rescued by the dLGF dTG (**Figure 29**). Additionally we observed a profound loss of salivary protein 1 (SAP1) also rescued by dLGF dTg, although the data are more variable (**Figure 29**).

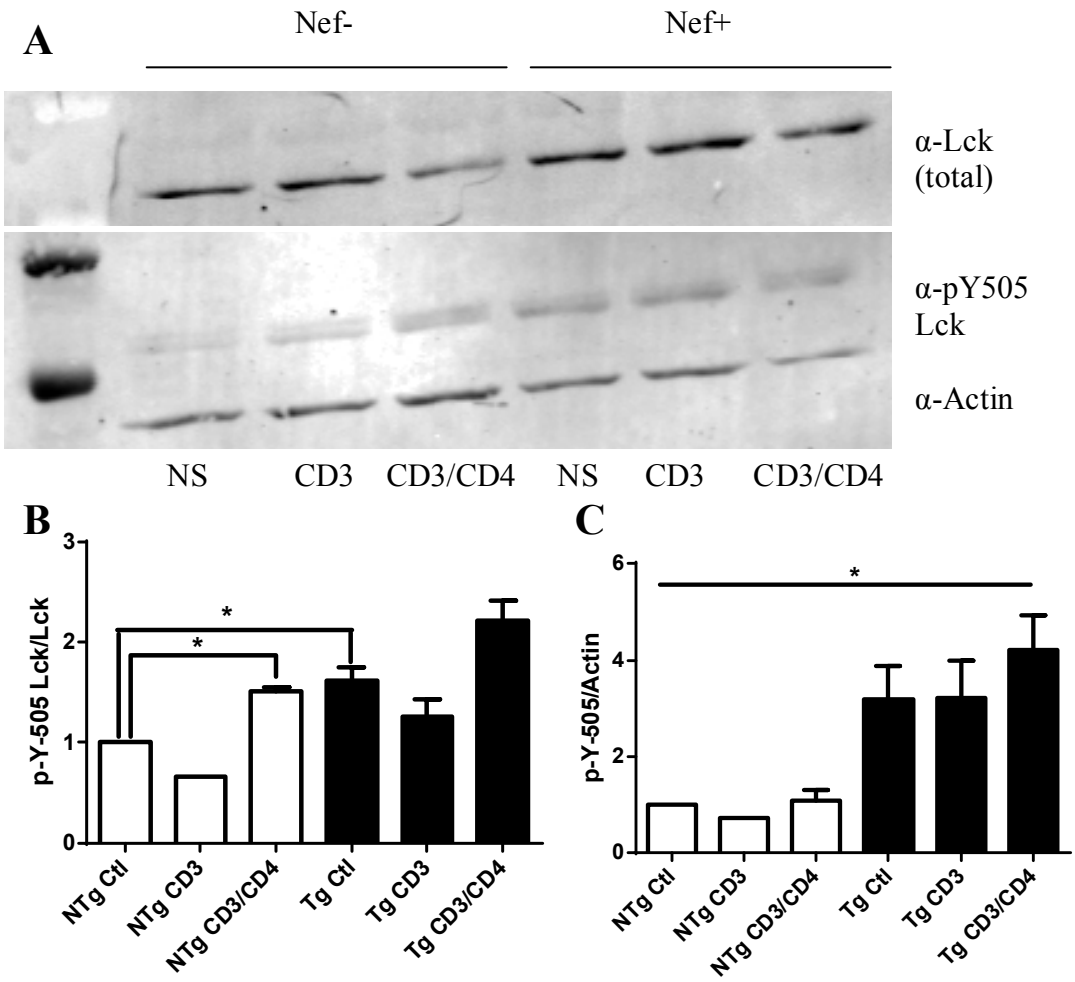

Figure 8: Hyperphosphorylation of Lck on tyrosine 505 in thymocytes of CD4C/HIV^{Nef} mice. Isolated Nef- and Nef+ thymocytes were stimulated (or not) with CD3 or CD3/CD4 for 5 minutes at 37°C. The inhibitory phosphorylation site (Lck Y505), total Lck and Actin (loading control) of total cell lysate were measured using an antibody against each form of the protein and quantified using Odyssey software. Data are representative of three independent experiments, * indicates $p<0.05$ as determined by a Student's *t*-test.

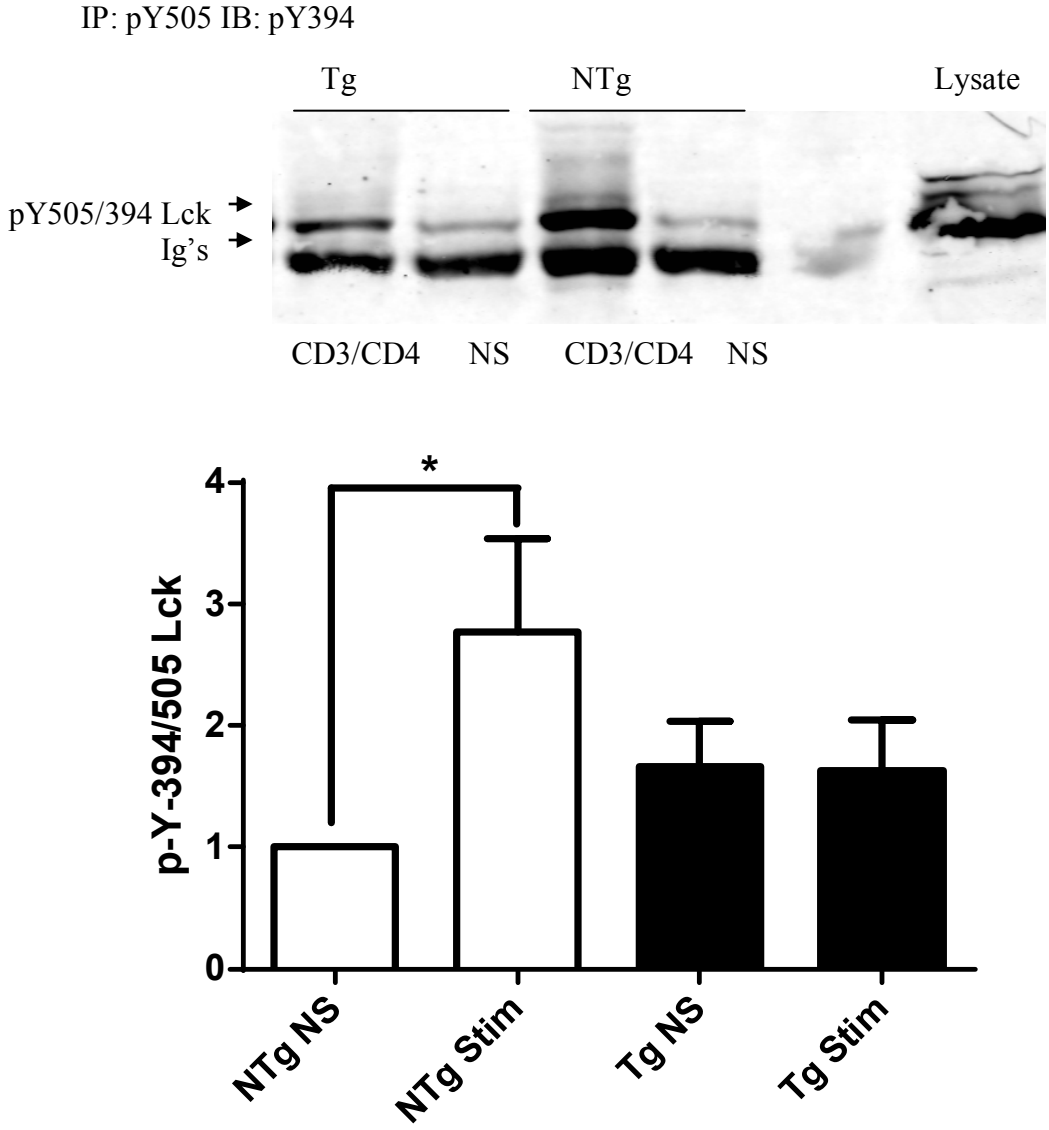

Figure 9: Nef results in a decrease in the activated form of pY505-Lck (double phosphorylated pY394) following CD3/CD4 stimulation in CD4C/HIV^{Nef} transgenic mice. Isolated thymocytes were stimulated or not for 5 minutes at 37°C and pY505 Lck were immunoprecipitated from total lysate. In order to detect the double phosphorylated form, pY394 Lck was immunoblotted on membranes and quantified using Odyssey software. Data are representative of four independent experiments. * indicates $p<0.05$ as determined by a Student's t-test.

IP: Csk IB: pY

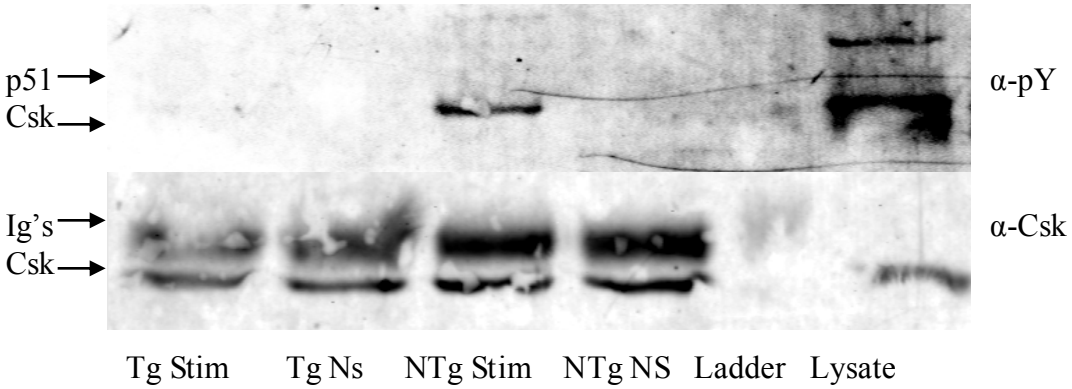

Figure 10: Alteration in the tyrosine phosphorylation of Csk in thymocytes of CD4C/HIV-Nef transgenic mice. Thymocytes isolated from Nef- and Nef+ mice were stimulated or not with CD3/CD4 for 5 minutes at 37°C. The lysate was subjected to immunoprecipitation of Csk, and tyrosine phosphorylation was detected using an antibody. The intensity of phosphorylated Csk (not-detected) and Csk-associated Lck were measured using Odyssey software. Data are representative of three independent experiments. * indicates $p<0.05$ as determined by a Student's t-test.

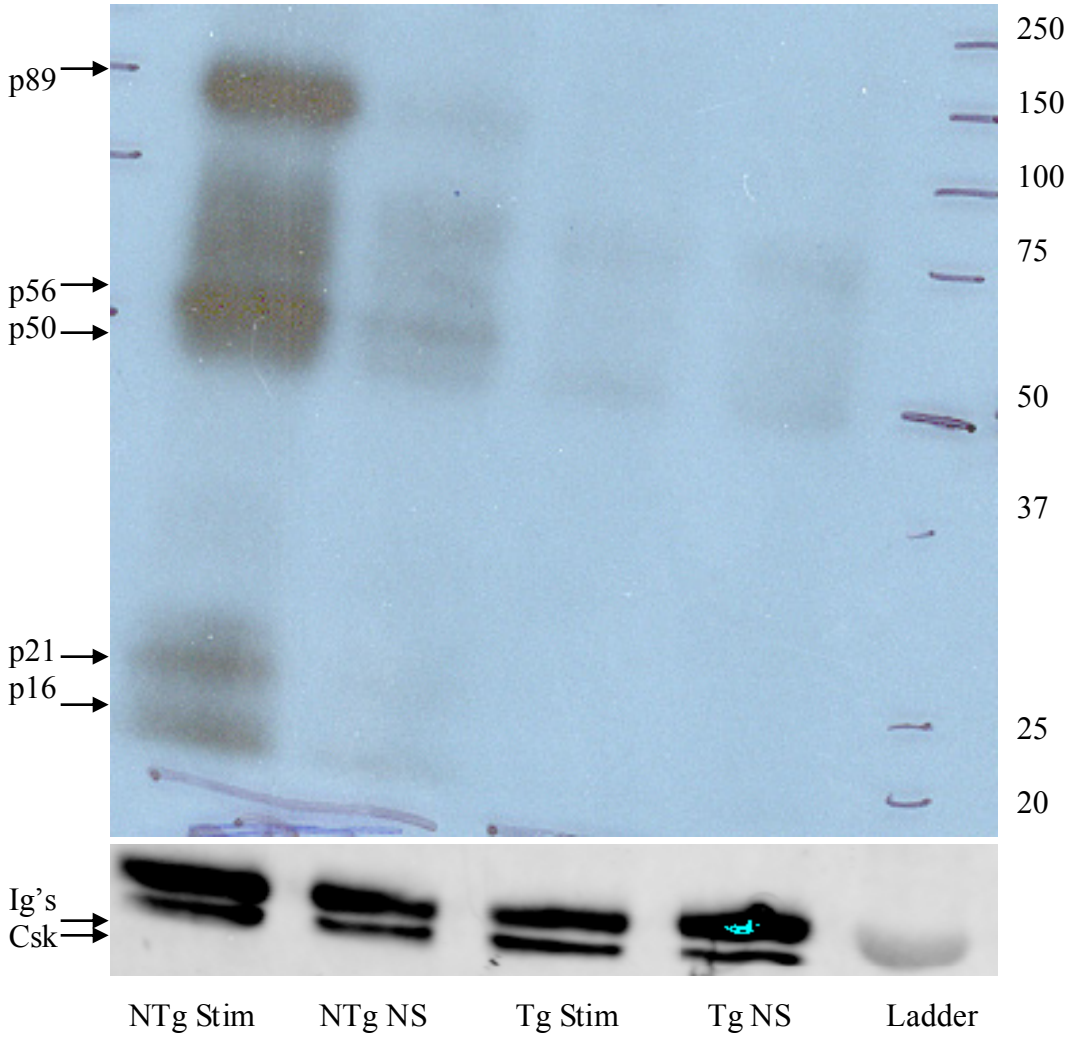

Figure 11: Alteration in the kinase activity of Csk in thymocytes of CD4C/HIV-Nef transgenic mice. Thymocytes isolated from Nef- and Nef+ mice were stimulated or not with CD3/CD4 for 5 minutes at 37°C. The lysate was subjected to immunoprecipitation of Csk, and an *in vitro* kinase assay was performed on the immunoprecipitates using ATP radioactively labeled with $\gamma^{32}P$. The analysis was performed over 2 independent experiments of 4 pooled mice for both Nef- and Nef+ thymocytes which gave similar results.

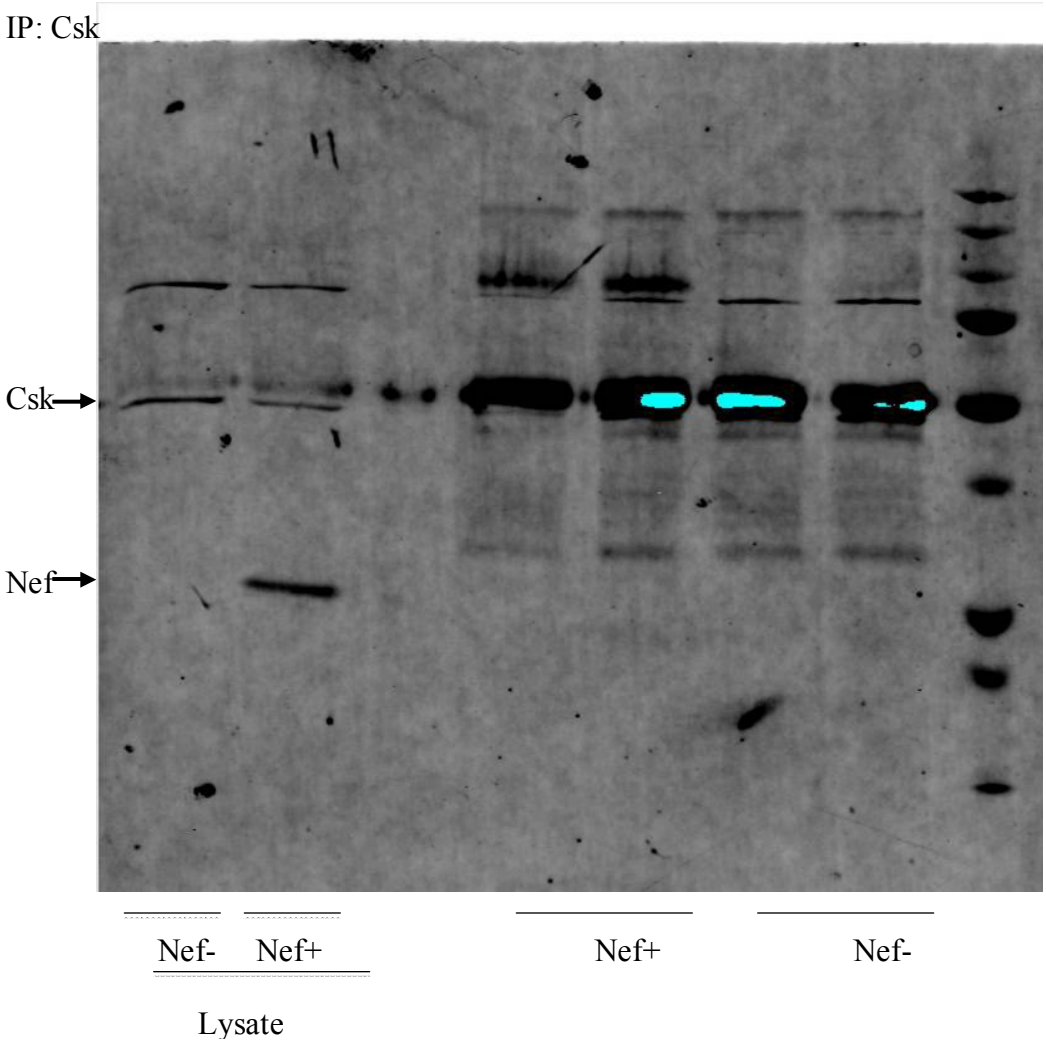

Figure 12: Csk/Nef protein interactions not detected by co-immunoprecipitation. Thymocytes isolated from Nef- and Nef+ mice were stimulated or not with CD3/CD4 for 5 minutes at 37°C. The lysate was subjected to immunoprecipitation of Csk, and Csk and Nef were both detected using an antibody, and non-immunoprecipated controls were loaded to very antibody staining. Proteins were revealed using Odyssey software. Image is representative of three independent experiments.

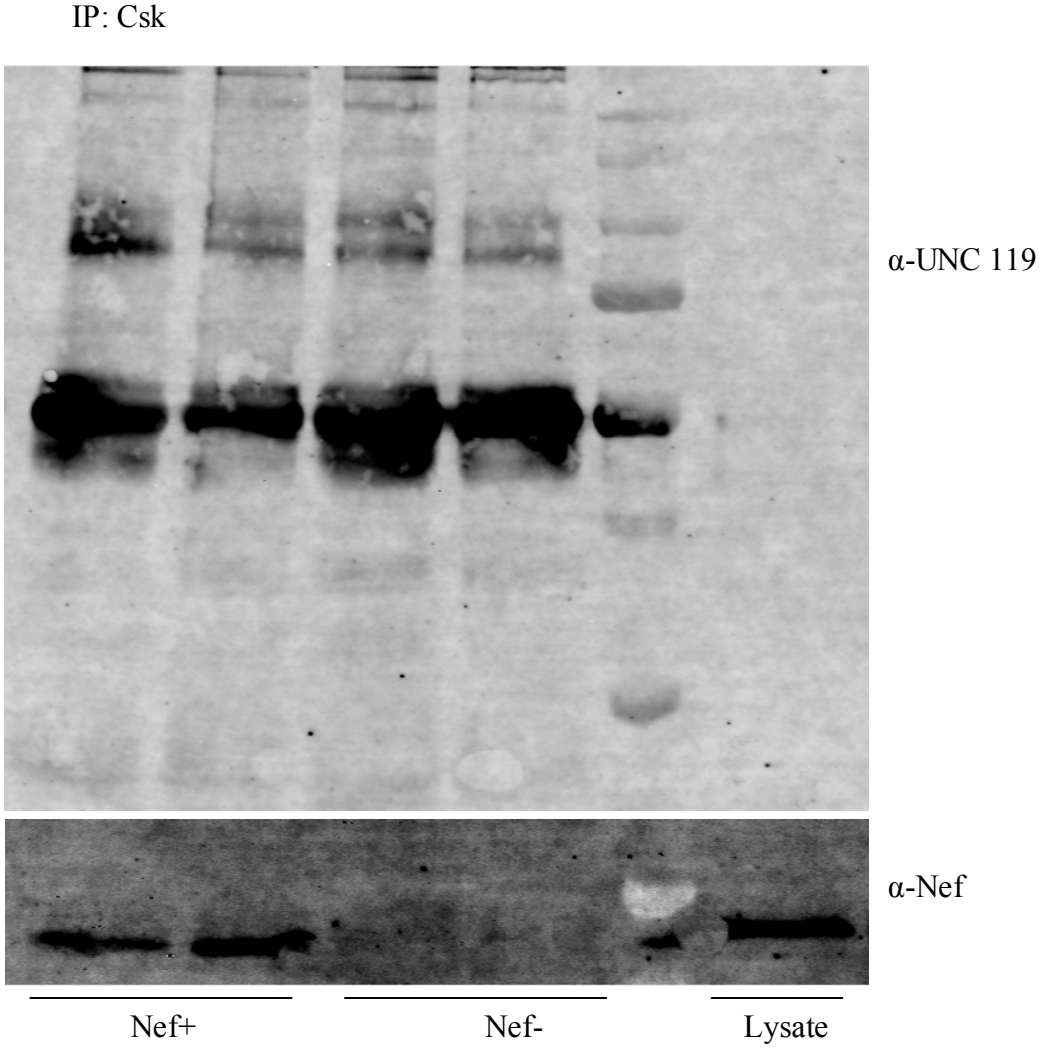

Figure 13: UNC119/Nef protein interactions not detected by co-immunoprecipitation.
Thymocytes isolated from Nef- and Nef+ mice were stimulated or not with CD3/CD4 for 5 minutes at 37°C. The lysate was subjected to immunoprecipitation with UNC119, and UNC119 and Nef were both detected using an antibody, and non-immunoprecipated controls were loaded to very antibody staining. Proteins were revealed using Odyssey software. Image is representative of three independent experiments.

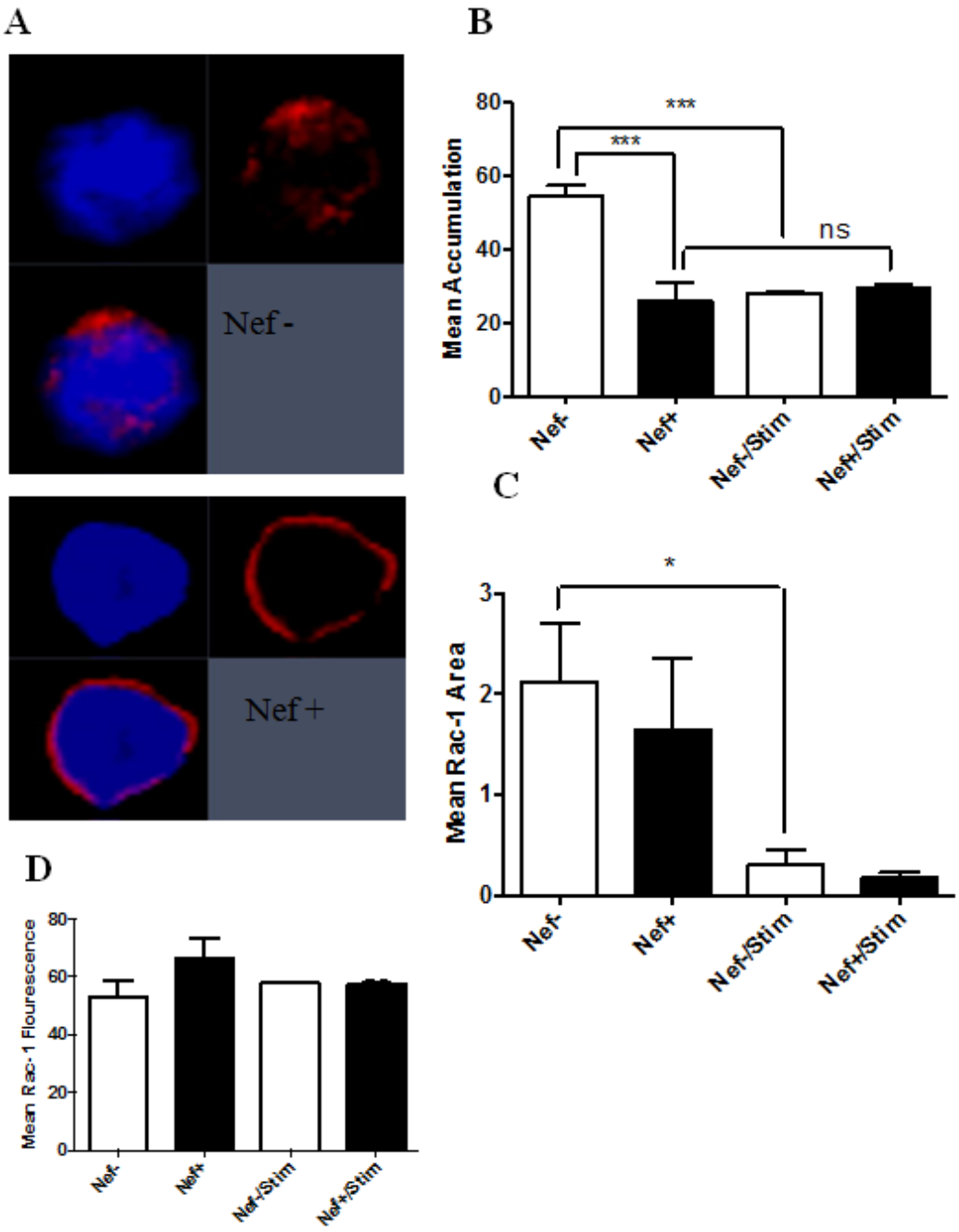

Figure 14: Rac-1 accumulation at the plasma membrane in unstimulated thymocytes is lost in CD4C/HIV-Nef mice.

Thymocytes isolated from Nef- and Nef+ ice were analyzed by immunofluorescence and confocal microscopy where they where cells were stained for Rac-1 (red) and DNA (blue) (Figure 6A), figures are representative of overall trend. The mean plasma membrane protein accumulation was quantified by individual cells analysis (n=50) over three distinct experiments. Results are represented as percent of cells demonstrating accumulation (Figure 6B), the mean area (Figure 6c) and the mean floursecnce (Figure 6D) of the staining. *$p<0.05$, ***$p<0.001$ as determined by a Student's t-test.

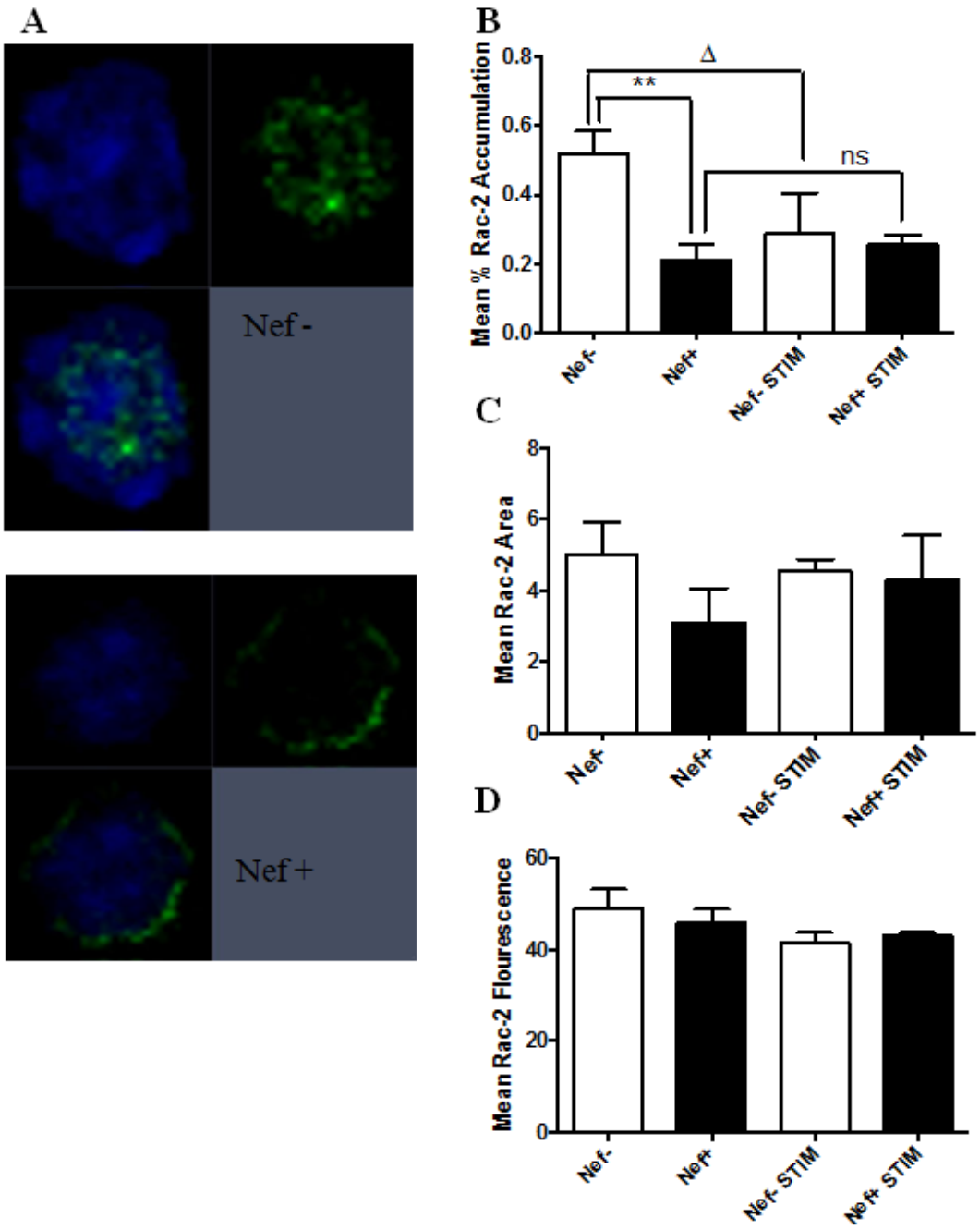

Figure 15: Rac-2 accumulation at the plasma membrane in unstimulated thymocytes is lost in CD4C/HIV-Nef mice.

Thymocytes isolated from Nef- and Nef+ mice were stimulated or not by CD3/CD4 and analyzed by immunofluorescence and confocal miscroscopy where they where cells were stained for Rac-2 (green) and DNA (blue) (**Figure 6A**). The mean plasma membrane protein accumulation was quantified by individual cells analysis (n=50) over three distinct experiments. Results are represented as percent of cells demonstrating accumulation (**Figure 6B**), the mean area (**Figure 6B**) and the mean fluorescence (**Figure 6D**) of the staining. $\Delta p<0.1$, $**p<0.01$, as determined by a Student's t-test.

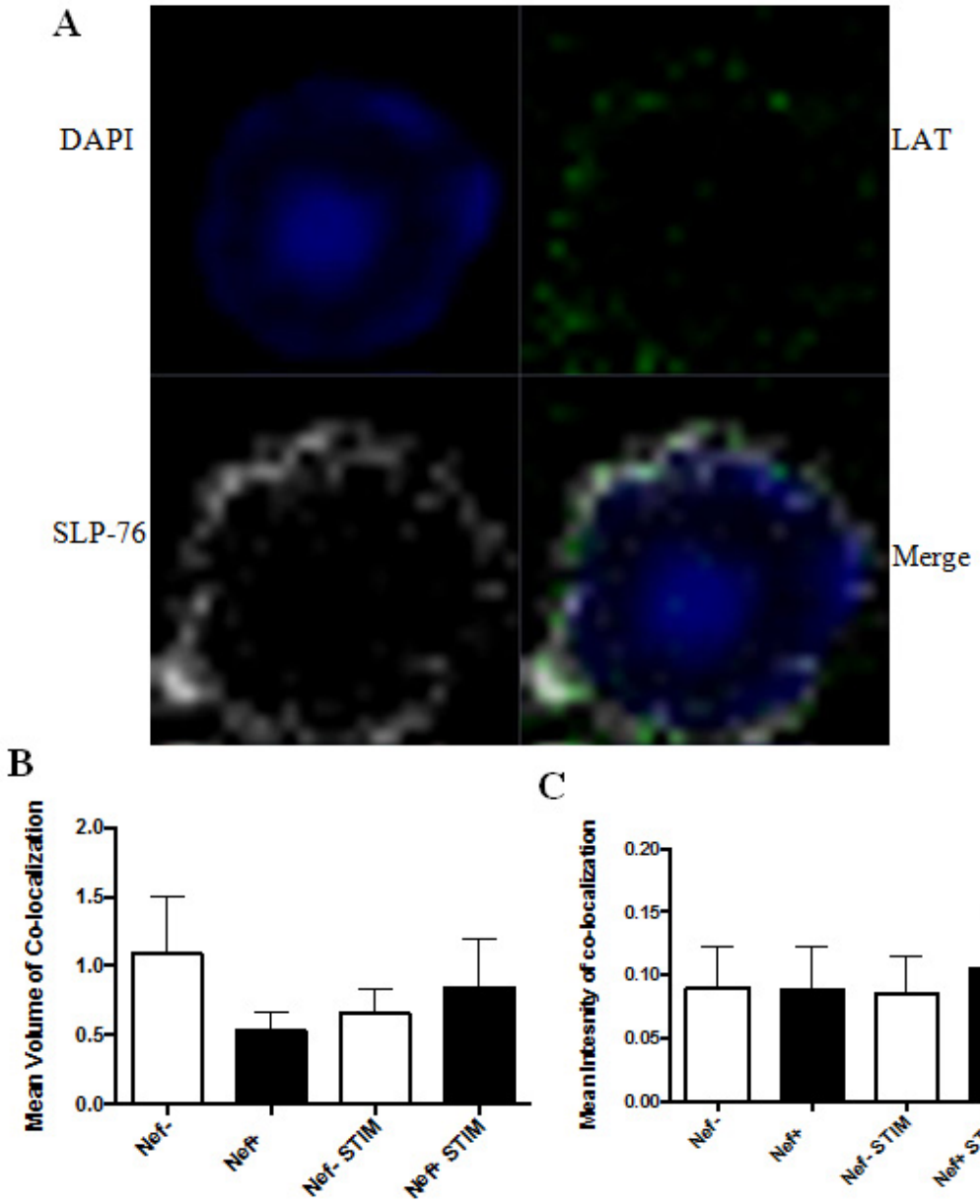

Figure 16: LAT and SLP-76 co-localization in unstimulated and stimulated thymocytes of CD4C/HIV-Nef thymocytes

Thymocytes isolated from Nef- and Nef+ mice were stimulated or not by CD3/CD4 and analyzed by immunofluorescence and confocal miscroscopy where they where cells were stained for LAT (green), SLP-76 (red) and DNA (blue) (**Figure 6A**). The mean intensity **(Figure 6B)** and volume **(Figure 6C)** of LAT/Lck co-staining is represented as mean ± standard error over three independent experiments.

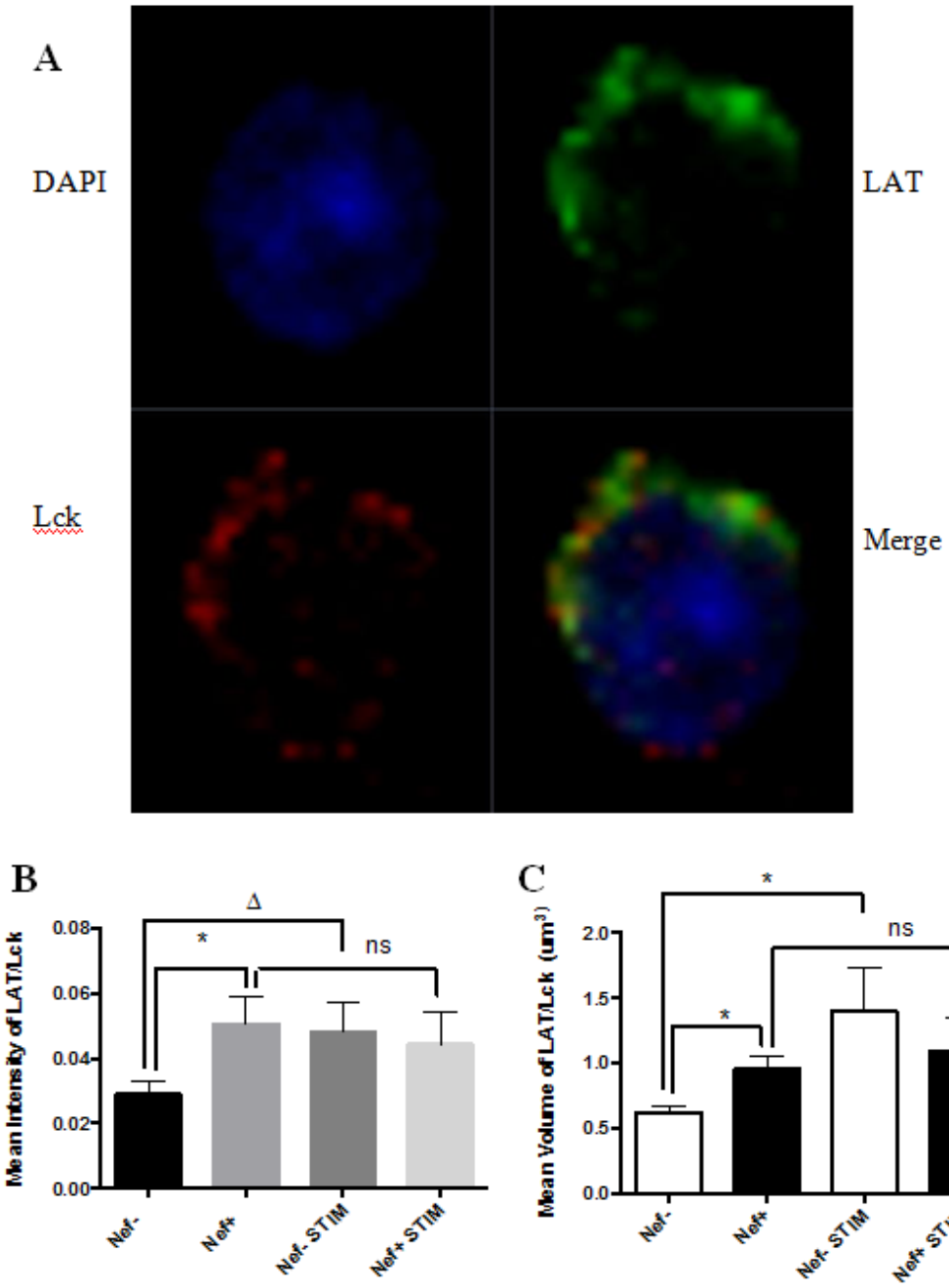

Figure 17: Increase in LAT and Lck co-localization in unstimulated thymocytes of CD4C/HIV-Nef thymocytes.
Thymocytes isolated from Nef- and Nef+ mice were stimulated or not by CD3/CD4 and analyzed by immunofluorescence and confocal miscroscopy where they where cells were stained for LAT (green), Lck (red) and DNA (blue) (**Figure 17A**). The mean intensity **(Figure 17B)** and volume **(Figure 17C)** of LAT/Lck co-staining is represented as mean ± standard error over three independent experiments. $\Delta p<0.1$, $*p<0.05$, as determined by a Student's *t*-test.

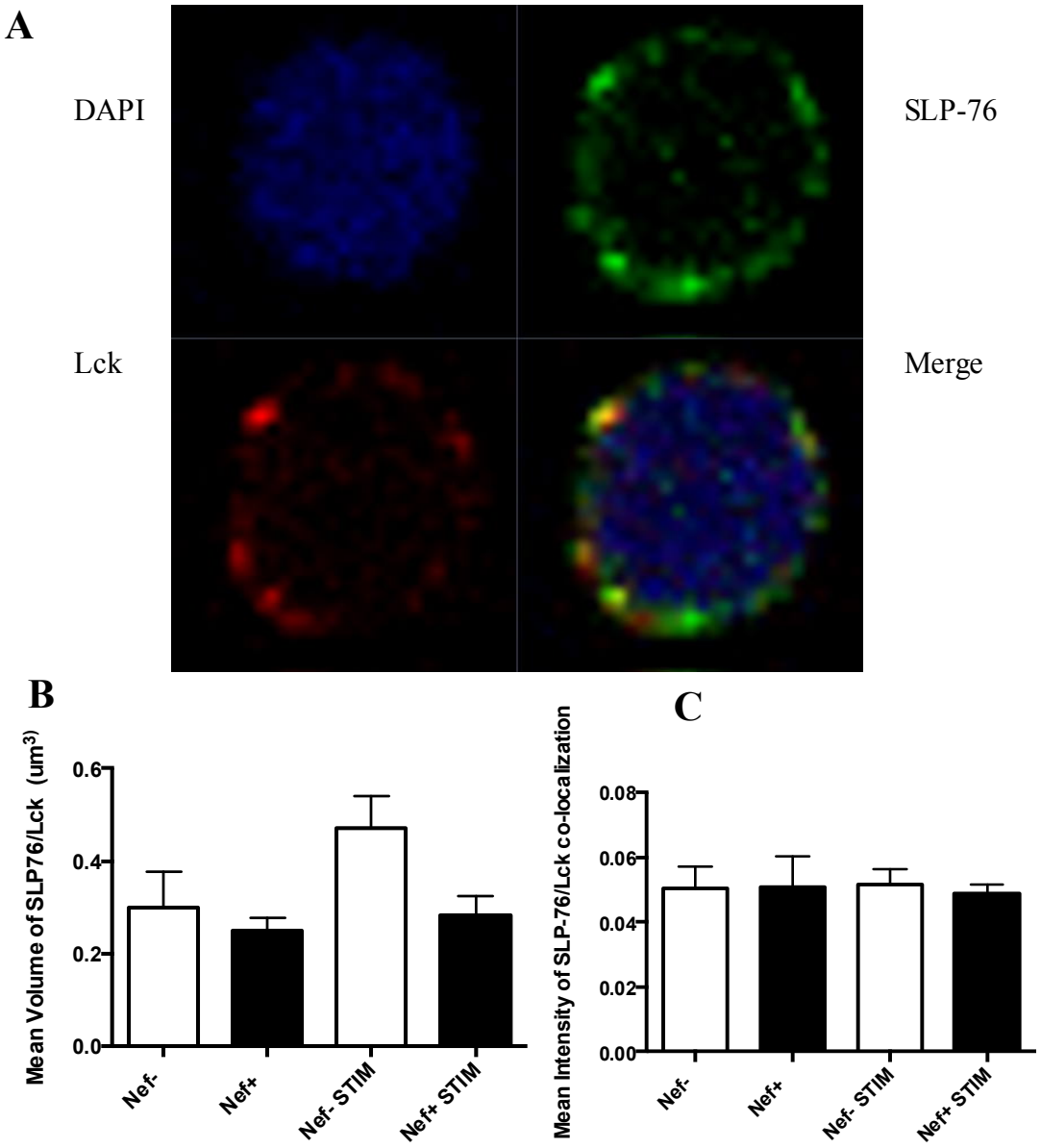

Figure 18: Lck and SLP-76 co-localization in unstimulated and stimulated thymocytes of CD4C/HIV-Nef thymocytes

Thymocytes isolated from Nef- and Nef+ mice were stimulated or not by CD3/CD4 and analyzed by immunofluorescence and confocal microscopy where the cells were stained for Lck (green), SLP-76 (red) and DNA (blue) (**Figure 18A**). The mean intensity **(Figure 18B)** and volume **(Figure 18C)** of Lck/SLP-76 co-staining is represented as mean ± standard error over three independent experiments.

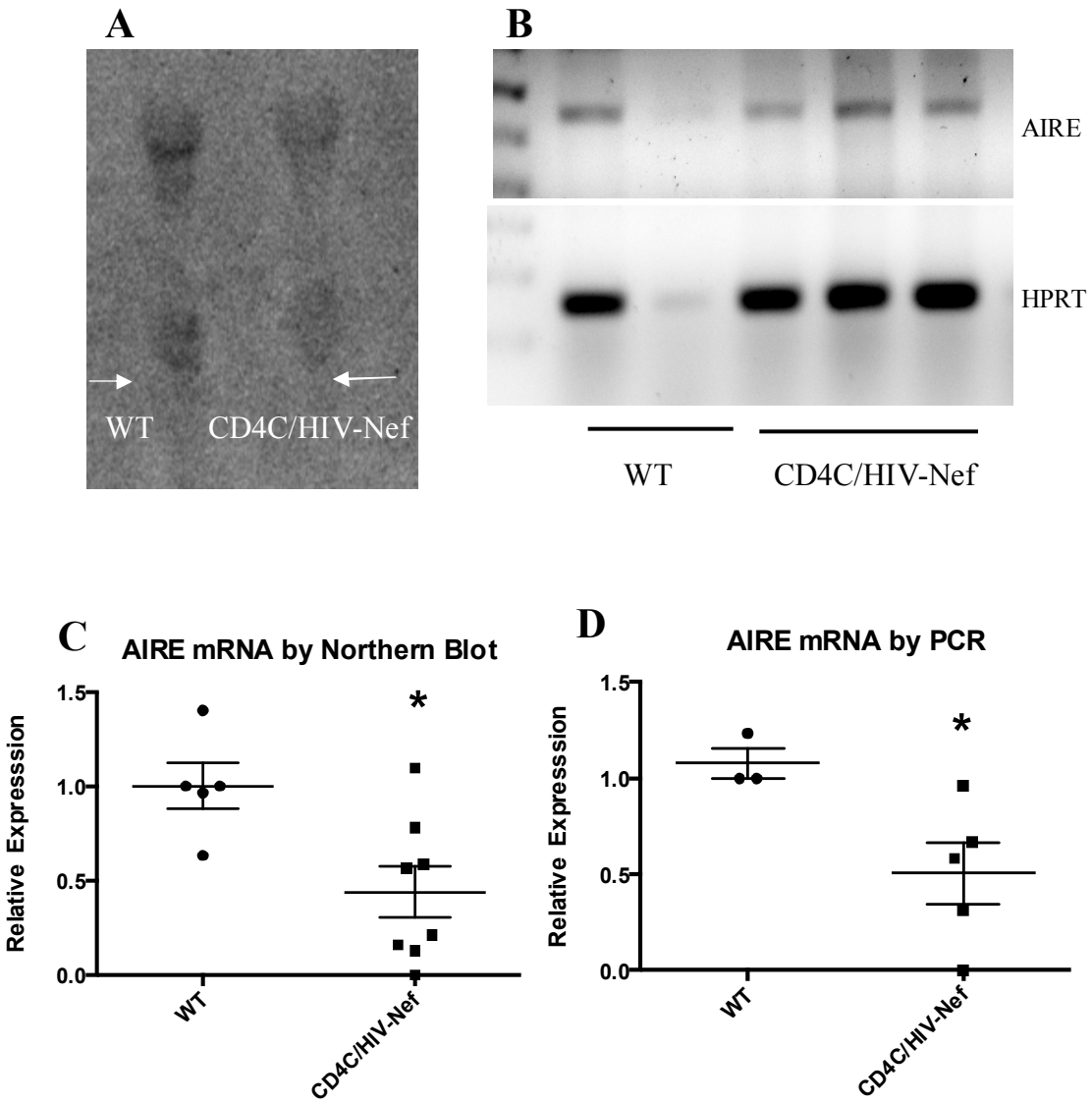

Figure 19: AIRE mRNA expression is decreased in CD4C/HIV Tg mice
Total thymus was isolated from WT and CD4C/HIV-Nef mice for RNA extraction. RNA was separated by electropheresis and probed with a radioactive AIRE probe sequence and imaged using a phosphoimager (A) or cDNA was generated and AIRE gene amplifaction was normalized to housekeeping gene HPRT (B). Quantification was achieved using ImageQuant software (C,D). Images are representative of all experiments and the data presented as mean ± standard error with each point representing a single mouse. Images are representative of trends. *$p<0.05$ as determined by an unpaired Student's t-test.

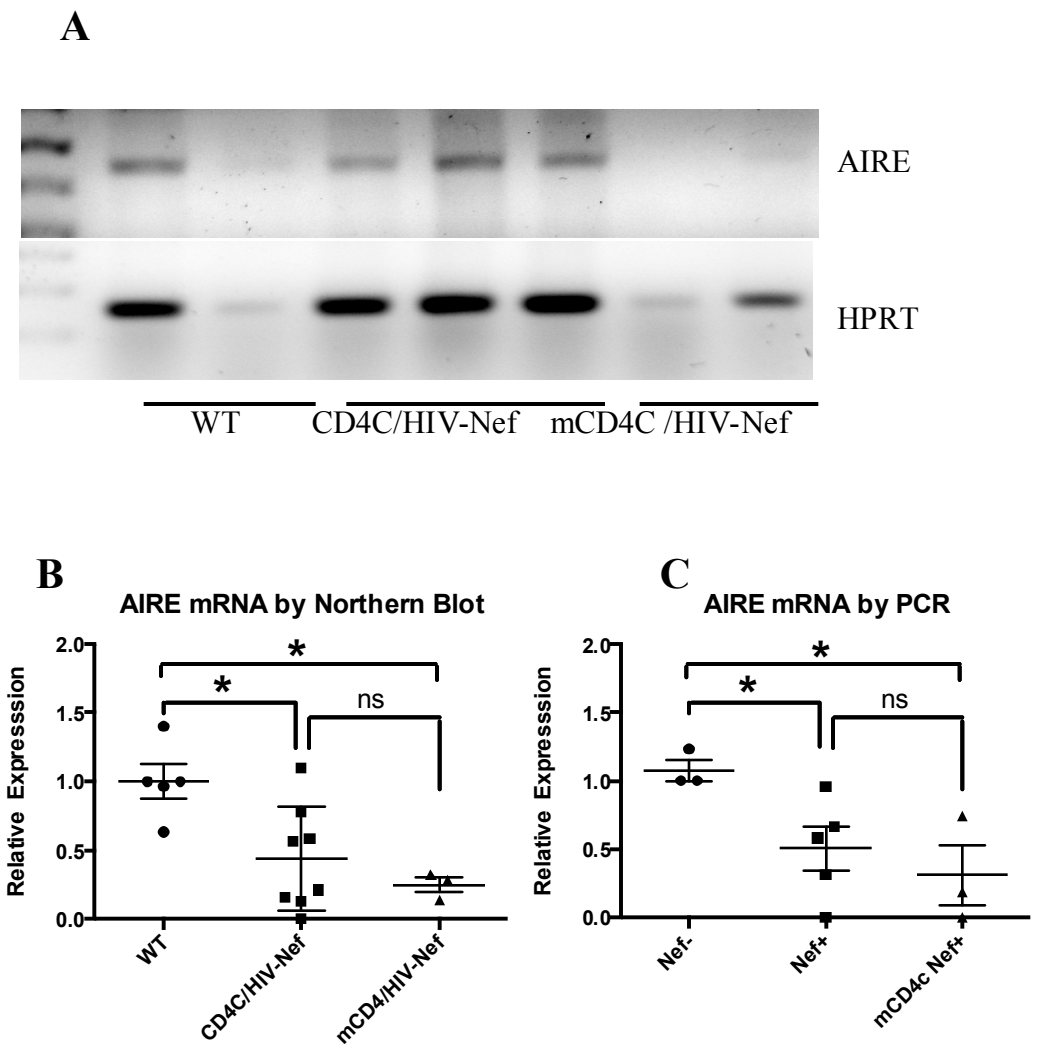

Figure 20: AIRE mRNA expression is more profoundly decreased in mCD4C/HIV Tg mice. Total thymus was isolated from WT, CD4C/HIV-Nef and mCD4C/HIV-Nef mice for RNA extraction. RNA was separated by electropheresis and probed with a radioactive AIRE probe sequence and imaged using a phosphoimager or cDNA was generated and AIRE gene amplifaction was normalized to housekeeping gene HPRT (A). Quantification was achieved using ImageQuant software (C,D). The data are presented as mean ± standard error with each point representing a single mouse. Images are representative of the trend. *$p<0.05$ as determined by an unpaired Student's t-test.

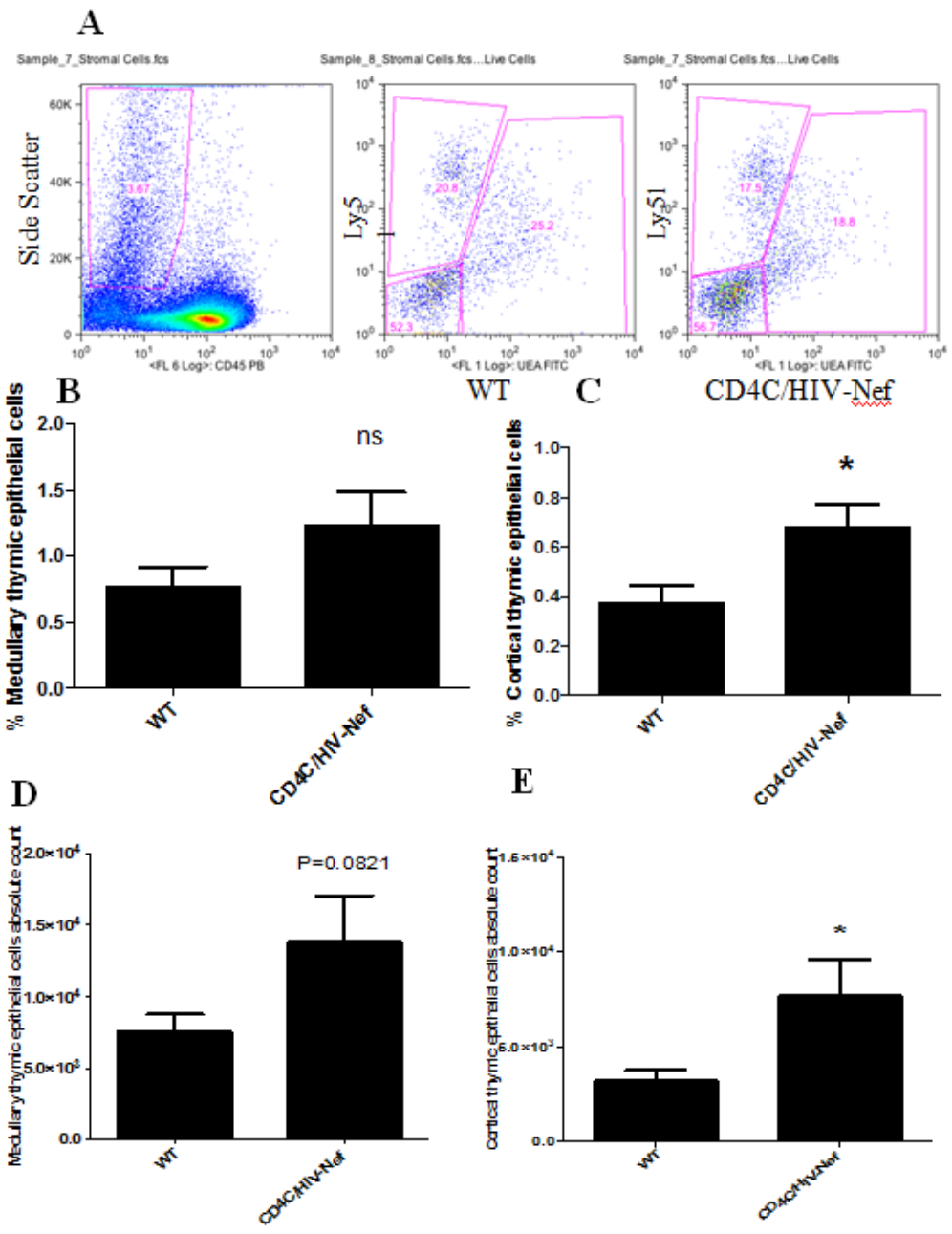

Figure 21: Enrichment of cTEC and mTEC populations of CD4C/HIV-Nef Tg mice. Staining of thymic epithelial cell preparation of WT and CD4C/HIV-Nef Tg mice. Cells gated as CD45- were sorted by staining for LY51 and UEA-1 (A). Data are presented as percent of total cells (B, D) and absolute number (C, E) of cortical and medullary thymic epithelial cells. The data are presented as mean ± standard error and represent three independent experiments. *$p<0.05$, $\Delta p<0.10$ as determined by an unpaired Student's t-test

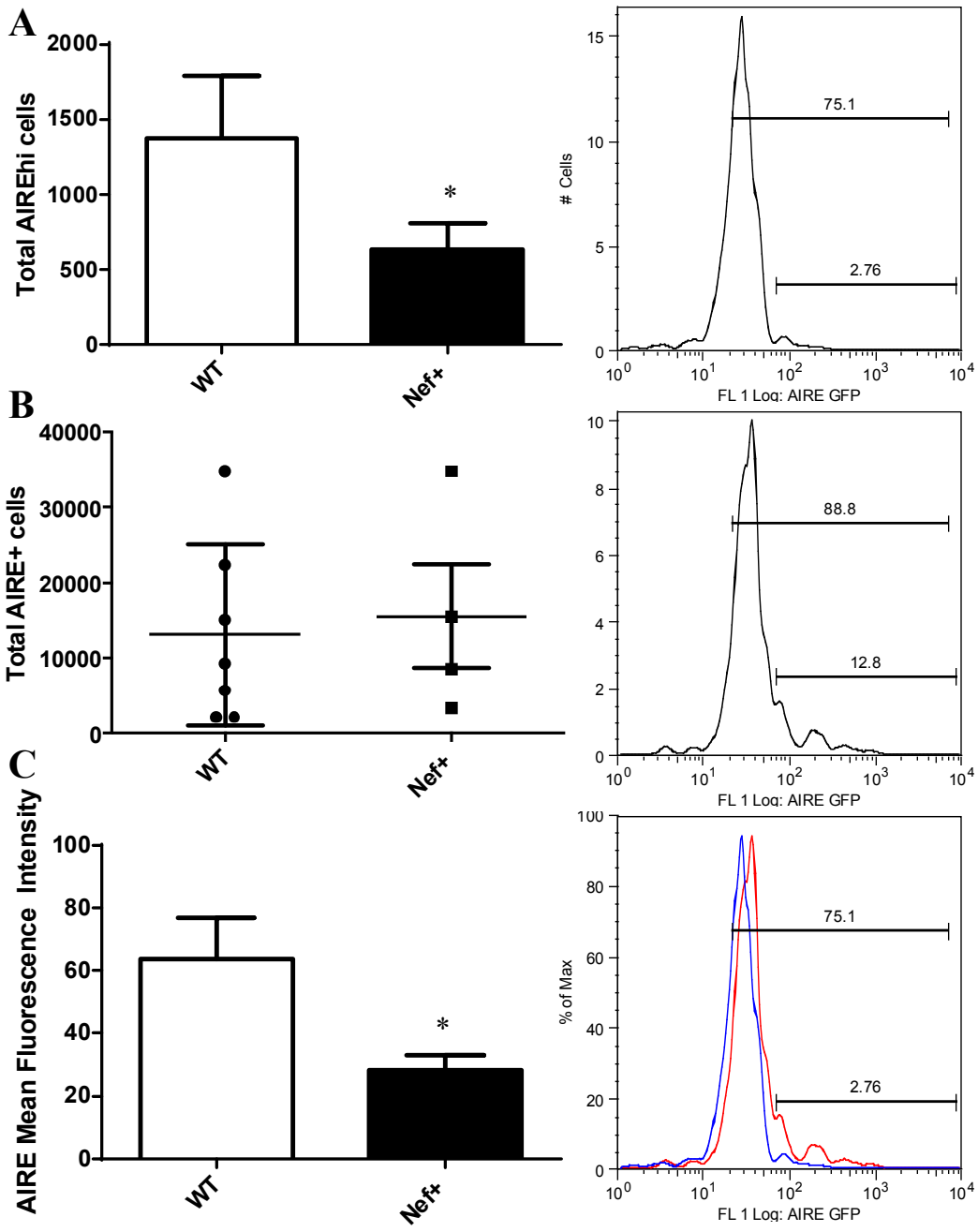

Figure 22: Shift in mean fluorescence intensity of AIRE-GFP in CD4C/HIV^{Nef} is correlated to a significant loss of AIREhi mTECS. MFI and cell count of AIRE+ and AIREhi TECs of WT and CD4C/HIV^{Nef} mice. Cells are gated as CD45-, Ly51lo and UEA-1+. In Figure 22C, the blue line (left) depicts CD4C/HIV-Nef and the red line (right) shows the WT. The data are presented as mean ± standard error and represent three independent experiments. *$p<0.05$, as determined by an unpaired Student's t-test.

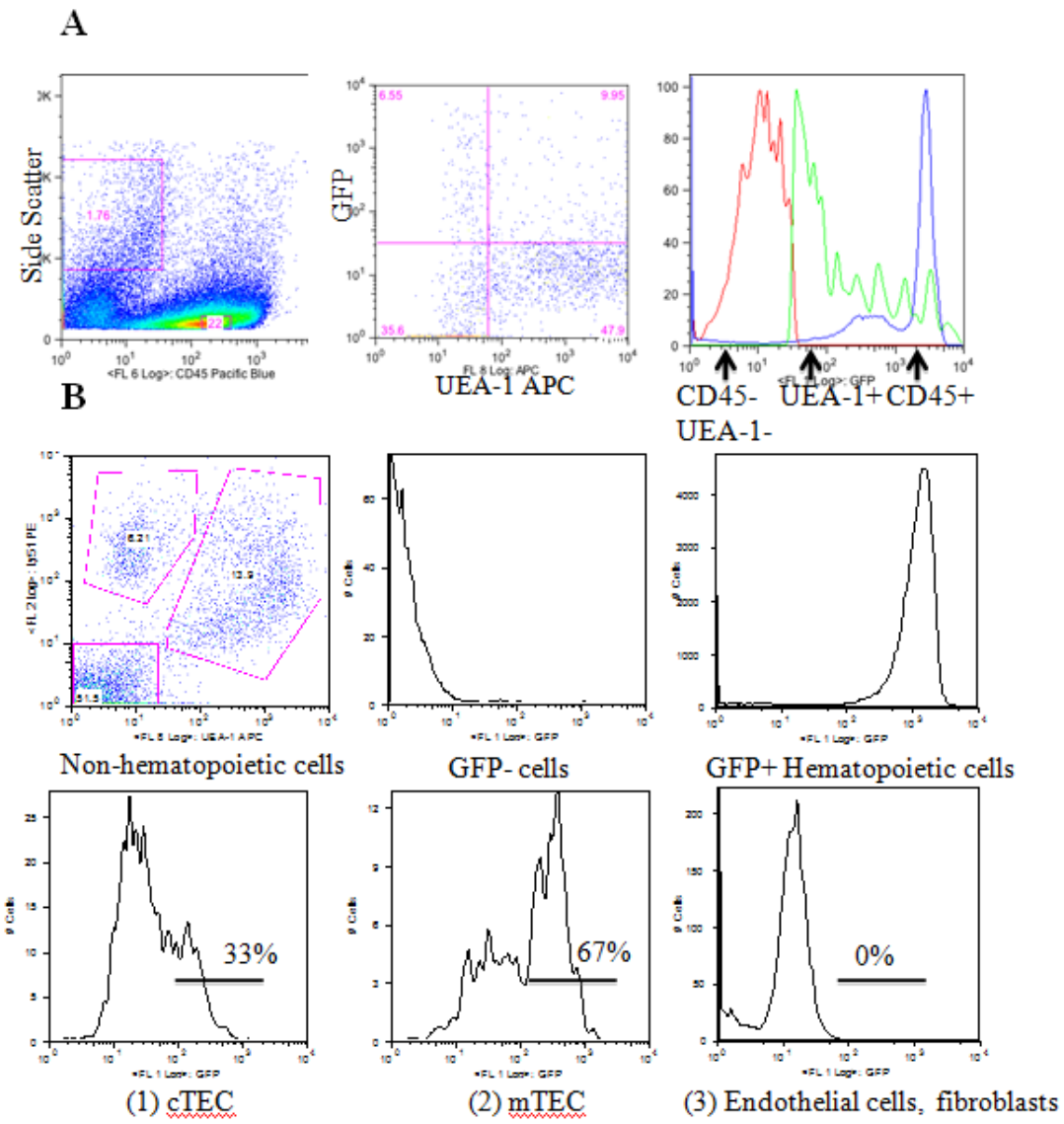

Figure 23: CD4C promotor activity in thymic epithelial cells in two distinct transgenic mouse founders: CD4C/GFP inducible mice and CD4C/GFP constitutive mice.

Staining of thymic epithelial cell preparation of WT and CD4C/GFP (A) inducible and CD4C/GFP (B) Tg mice. Cells gated as CD45- were sorted by staining for LY51 and UEA-1 and a histogram of GFP expression was generated. Data are representative of three independent experiments.

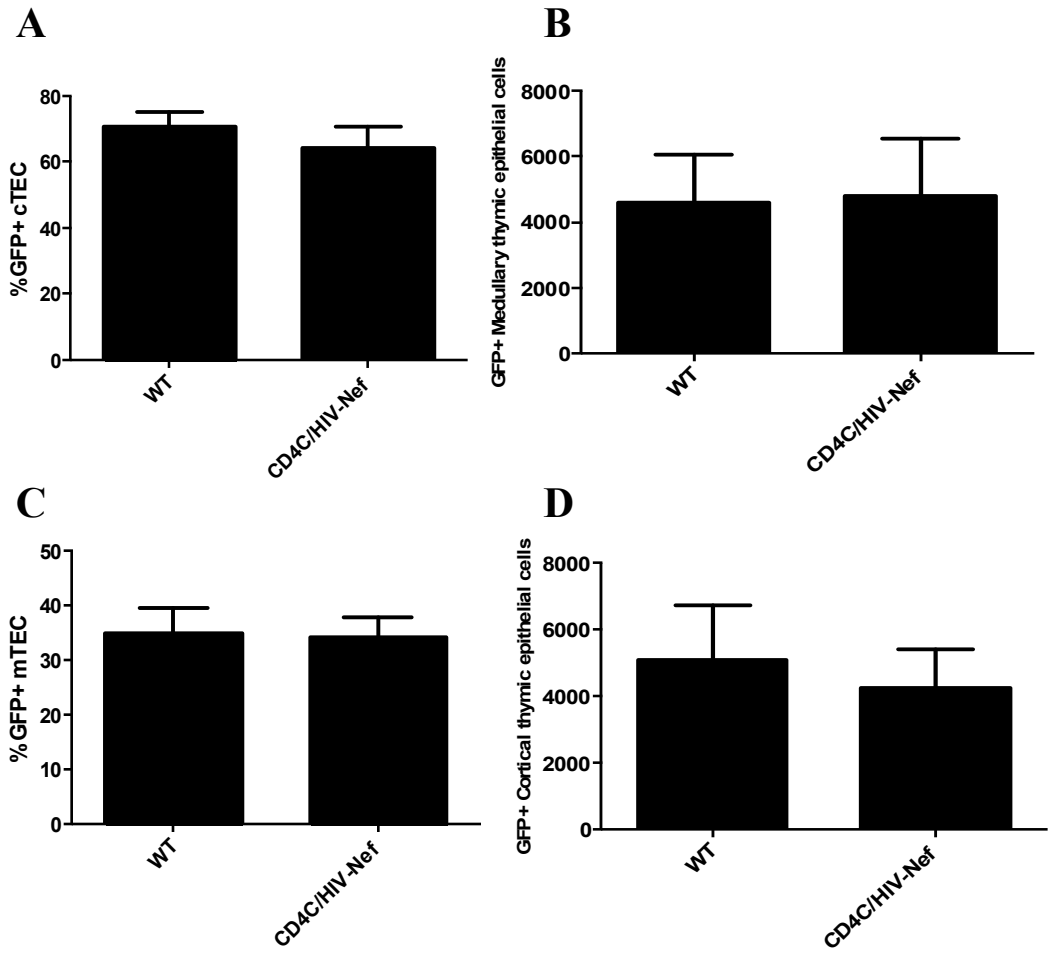

Figure 24: GFP+ thymic epithelial cells are not enriched nor depleted in CD4C/GFP x CD4C/HIV-Nef with respect to CD4C/GFP mice.
Proportion of GFP+ thymic epithleial cells of WT and CD4C/HIV-Nef Tg mice. Cells gated as CD5- were sorted by staining for Ly51 and UEA-1 and a histogram of GFP expression was generated. Data are presented as percentage (A, C) and absolute number (B, D) of cortical and mTECs expressing GFP. The data are presented as mean ± standard error and represent three independent experiments.

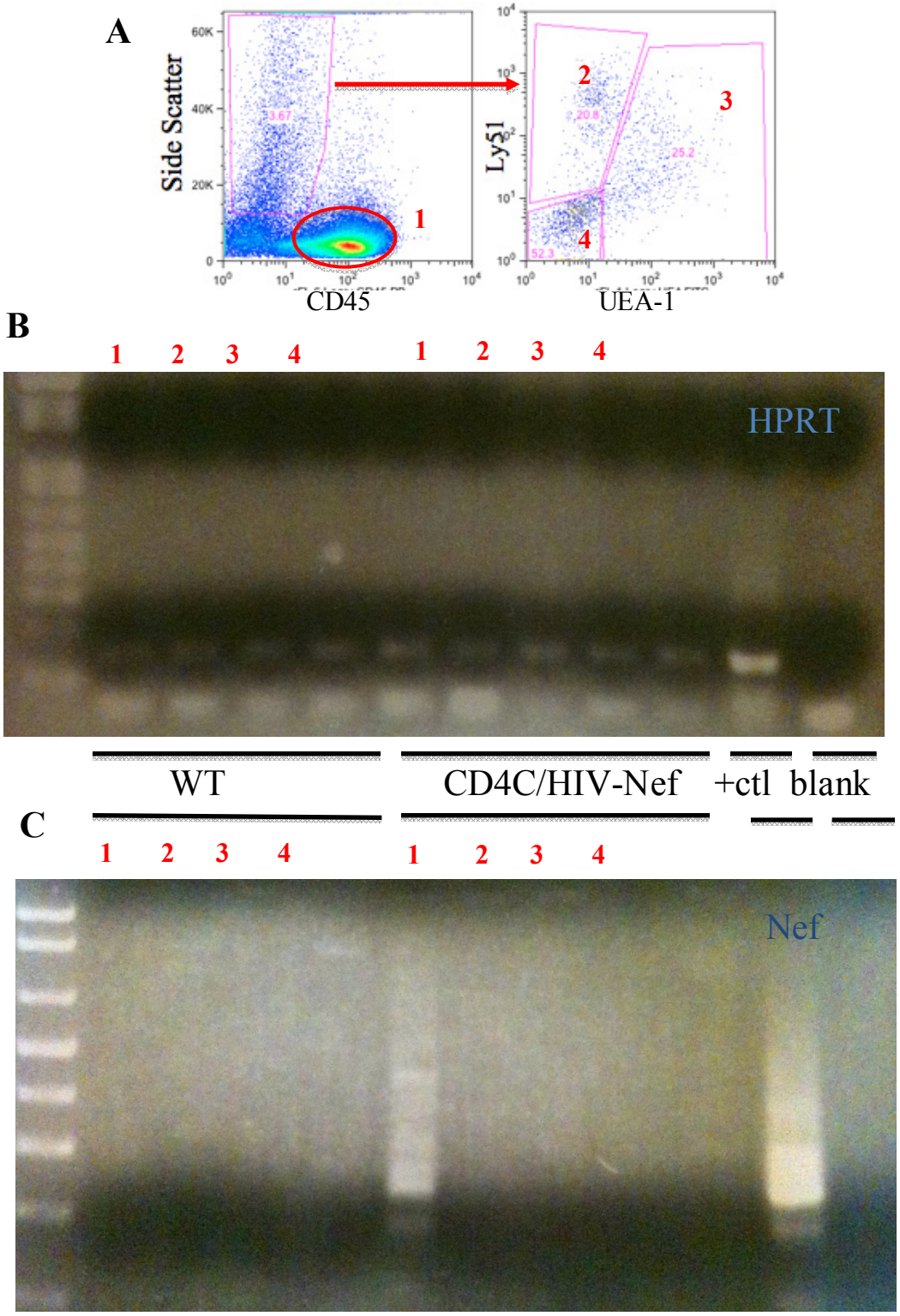

Figure 25: Nef mRNA expression in thymic epithelial cells
Expression of HPRT (A) and Nef (B) mRNA from a thymic subsets. Thymus was digested and cells were sorted by CD45- and CD45+, CD45- were further sorted according to Ly51 and UEA-1 staining. Sorted cells were recovered for mRNA extraction, reverse transcription and gene amplification.

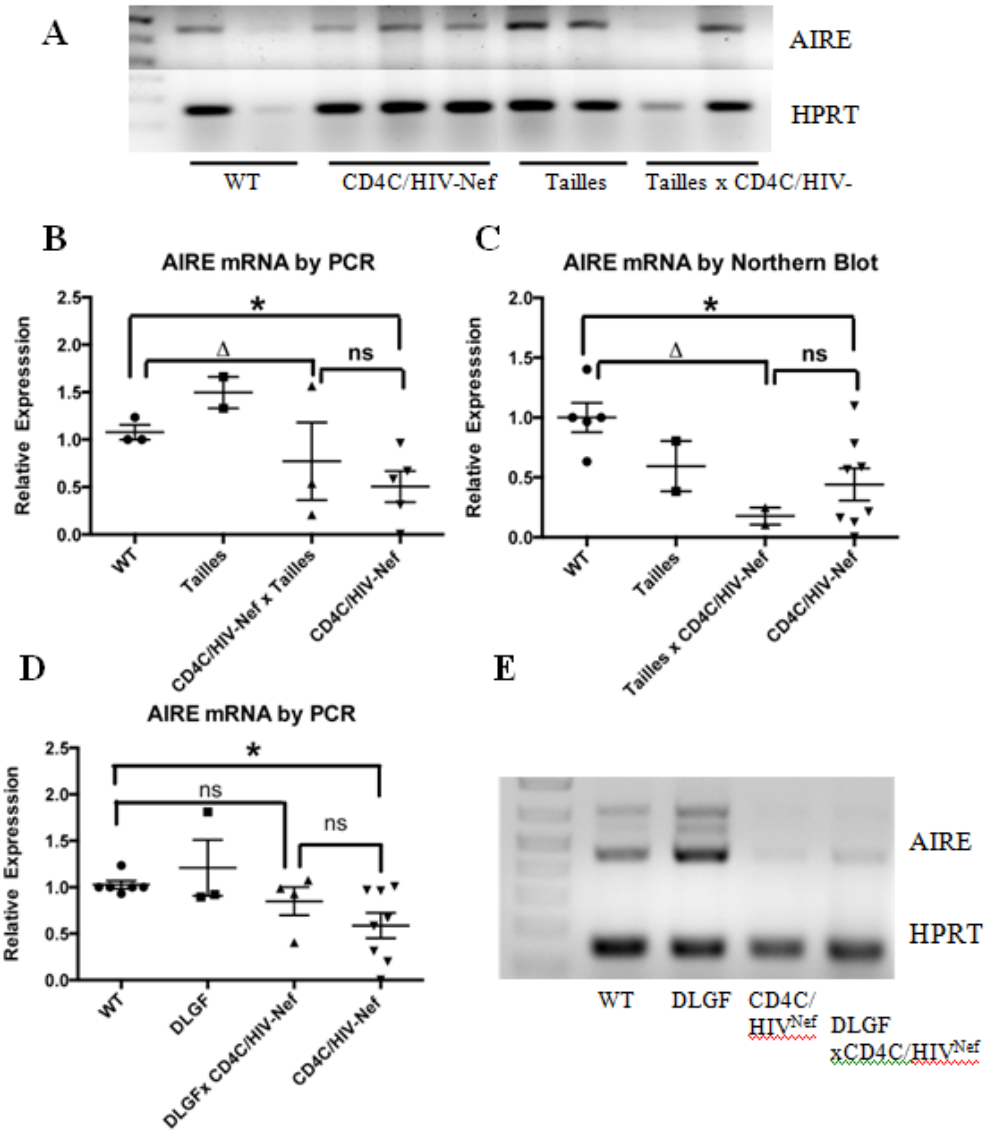

Figure 26: AIRE mRNA expression is not rescued by CD4 thymocyte rescue in CD4C/HIV-Nef x Tailles dTg and CD4C/HIV-Nef x dLGF dTg mice.
Total thymus was removed from WT, CD4C/HIV-Nef, Tailles, dLGF, Tailles/CD4C/HIV-Nef and dLGF/CD4C/HIV-Nef mice for RNA extraction. RNA was separated by electrophoresis and probed with a radioactive AIRE probe sequence and imaged using a phosphoimager or cDNA was generated and AIRE gene amplification was normalized to housekeeping gene HPRT (A, D). Quantification was achieved using ImageQuant software (B, C, E). The data are presented as mean ± standard error with each point representing a single mouse. *$p<0.05$, $\Delta p<0.10$ as determined by an unpaired Student's t-test

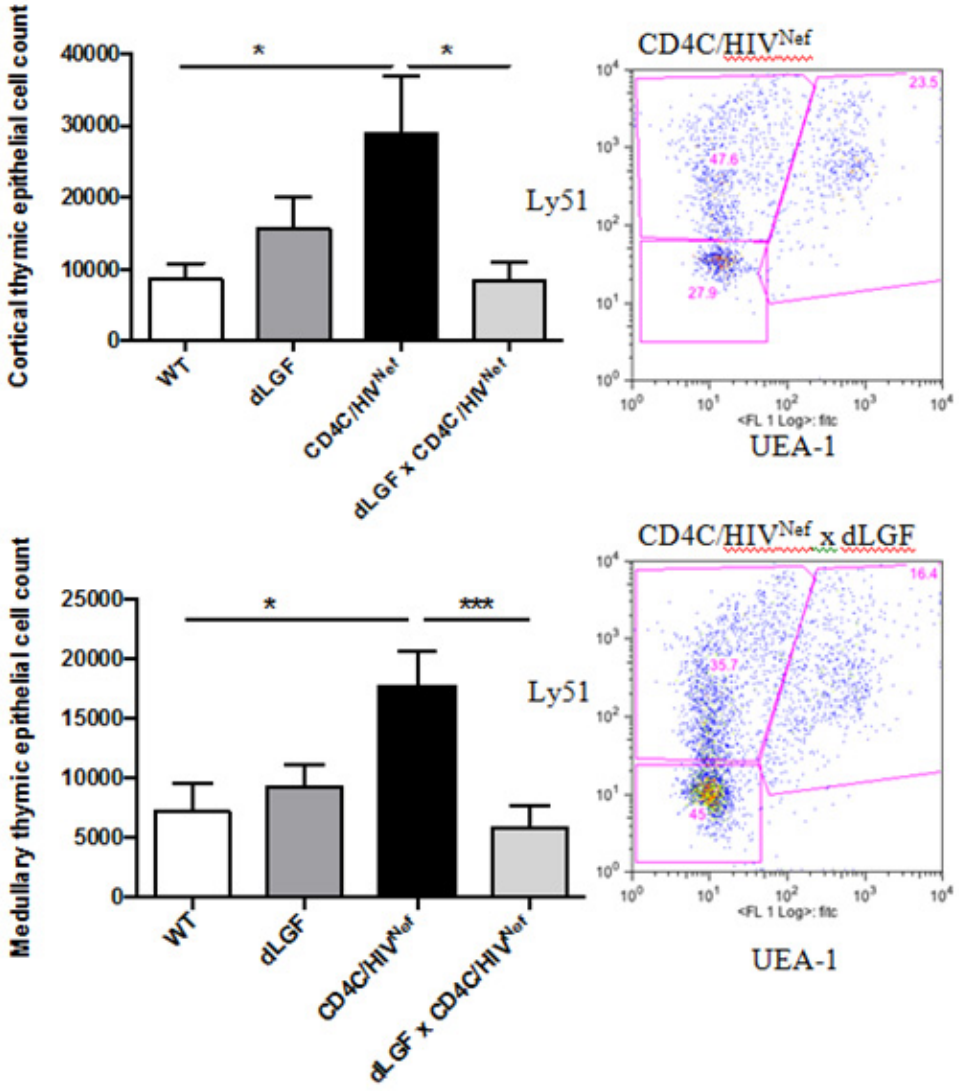

Figure 27: Enrichement of cTECs and mTECs is rescued by dLGF phenotype. Staining of thymic epithelial cell preparation of WT, CD4C/HIV^{Nef}, dLGF and dLGF x CD4C/HIV^{Nef} mice. Cells gated as CD45- were sorted by staining for LY51 and UEA-1. Data are presented absolute cell count of cortical and mTECs. The data are presented as mean ± standard error and represent three independent experiments. *p<0.05, ***p<0.001 as determined by an unpaired Student's t-test

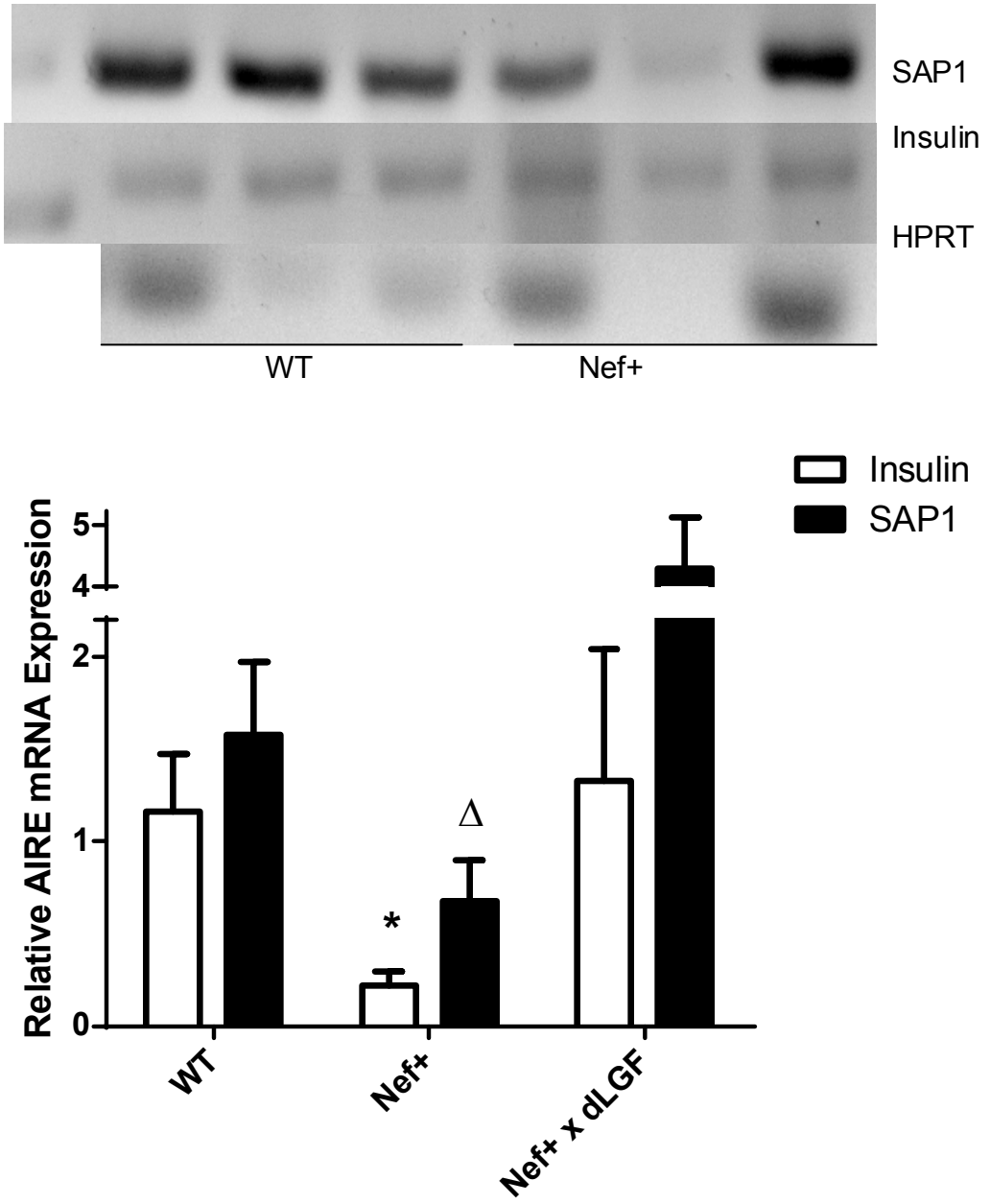

Figure 28: Loss of AIRE confers a loss of expression of tissue-restricted antigens in the thymus and is rescued by CD4. Total thymus was isolated from WT and CD4C/HIV-Nef for RNA extraction. cDNA was generated and Insulin and SAP1 gene amplification was normalized to housekeeping gene HPRT (A). Quantification was achieved using ImageQuant software (C,D). The data are presented as mean ± standard error. Images are representative of the trend. *$p<0.05$, $\Delta p<0.10$ as determined by an unpaired Student's t-test.

8. **Discussion**

Delocalization of Lck by Nef results in disruption of the Csk feedback loop

In this study, we employ biochemical techniques to attempt to explain the delocalization of Lck by Nef previously outlined in thesis of (Guertin, 2011) and by (Haller et al., 2007). This part of the study investigates the various factors that regulate Lck activation and localization in normal thymocytes. However, due to the complexity of feedback loops to Lck, it becomes difficult to decipher phenomena resulting from Lck delocalization, or if Lck delocalization could be potentially explained by the phenomena, our data suggest the former, and this would be further confirmed by a couple of future experiments.

With respect to altered Lck activity, we show that an increased level of tyrosine phosphorylation in Nef+ non-stimulated and stimulated cells, similar to levels in Nef- stimulated cells (**Figure 8**), however the level of the double phosphorylated form is not matched (**Figure 9**), indicating that there is a higher proportion of pY505 closed form, or a lower ratio of the pY505 open form in Nef+ thymocytes (**see Figure 4**). C-terminal kinase (Csk) being the culprit of C-terminal (505) phosphorylation of Lck, we investigated its activation. Although tyrosine phosphorylation of Csk has been detected (Yasuda et al., 2002), it is more associated with serine/threonine phosphorylation (Torgersen et al., 2001; Yaqub et al., 2003) and it is above all regulated by its localization in the cell (Schoenborn et al., 2011; Torgersen et al., 2001; Yasuda et al., 2002). By immunoprecipitation, we do not detected tyrosine phsophorylation of Csk, but the association of Fyn kinase under Nef- stimulated conditions is lost in Nef+ thymocytes (**Figure 10**). Moreover, in an *in vitro kinase assay* (IVKA), we reveal phosphorylation of

Fyn by Csk and of CD3ζ (p16/21) and Cbp (p90), the major substrate of Fyn (Yasuda et al., 2002), all of which is lost in Nef+ thymocytes (**Figure 11**). We exclude the possibility of Lck as the kinase since Csk preferentially binds Fyn (Yasuda et al., 2002), and that the profile does not resemble that of an Lck IVKA (not shown).

We propose a mechanism whereby in Nef+ thymocytes, delocalization of Lck during TcR engagement prevents activation of Fyn, which normally phosphorylates Cbp in order to recruit Csk to the plasma membrane. This could possibly explain why the CD3ζ chains are not phosphorylated (not shown), and as a result ZAP-70 may not recruited, which is required for its activation ((Neumeister et al., 1995). This hypothesis was tested by co-immunoprecipitation of CD3 and ZAP70 however the data could not be confirmed (not shown). This also could be confirmed by studying the localization of Csk by immunocytochemistry with lipid raft markers, or a sucrose gradient that separating cell compartments followed by Western blotting.

Finally, in an attempt to understand the mechanism for the relocalization of Lck, we hypothesized that Nef could be binding to a critical Lck trafficking protein Unc 119 (Gorska 2009), however we fail to show any interactions (**Figure 13**). We also fail to detect interactions between Nef and Csk (**Figure 12**). Another possibility is that Cbl, an E3 Ubiquitin ligase, targets Lck for degredation more in Nef+ thymocytes. We tested this experimentally and found an increase in Lck and Cbl association by immunprecipitation, albeit the data were weak and could not be repeated (not shown**)**. As Cbl associates with Lck when its in its phosphorylated open confirmation (Tsygankov et al., 1996), the

increase associated of Lck and Cbl would be representative of the activation of Lck. The subsequent ubiquitination of the Lck protein would indicate its degradation however we were not successful in measuring this by immunoprecipitation (not shown).

Alteration of Lck localization prevents ZAP-70 activation but may facilitate downstream activation in place.

As mentioned, (Guertin, 2011) previously showed that a complete abrogation of ZAP-70 kinase activity in Nef+ thymocytes, which is required for downstream phosphorylation of LAT and SLP-76, connecting signaling at the immunological synapse to the rest of the cell. A recent study shows that Lck signaling is compartmentalized and that Nef triggers Lck-dependent activation of Ras-Erk signaling (Pan et al., 2012), which is in coherence with the increased Erk stimulation observed in our model (Hanna et al., 1998b). As another mediator between Lck an Erk (Eblen et al., 2002), we investigated the activation of Rac (in a separate pathway from Ras) by co-localization experiments. The increased presence of Rac1/2 at the plasma membrane in Nef+ thymocytes is an indicator of its activation (**Figures 14 and 15**), as Rac must be recruited to the plasma membrane (Okada 2005, Koo 2007). However it is unclear if Rac is actually activated by Nef's apparent ability to bind to the GEF DOCK2-ELMO1 complex (Janardhan et al., 2004). Unlike ZAP-70, the kinase activity of Lck is not completely lost (Guertin, 2011), and therefore it is possible that Lck phosphorylates substrates of ZAP-70 in its absence (Jiang and Cheng 2007,(Kabouridis et al., 2011; Sanzenbacher et al., 1999).

Co-localization studies between Lck and LAT (**Figure 16**) show that (despite Lck being delocalized in Nef+ thymocytes) Lck is in proximity with LAT in the lipid rafts and could potentially phosphorylate certain residues, such that the micro-clusters of LAT/SLP-76

are not distrubed (**Figure 17**) as previously suggested by (Abraham et al., 2012). Finally, we wanted to know if in Nef+ thymocytes Lck would be found in higher proximity with SLP-76 than non-infected thymocytes, perhaps as a result of ZAP-70 kinase activity loss, however we were not able to detect a difference (**Figure 18**).

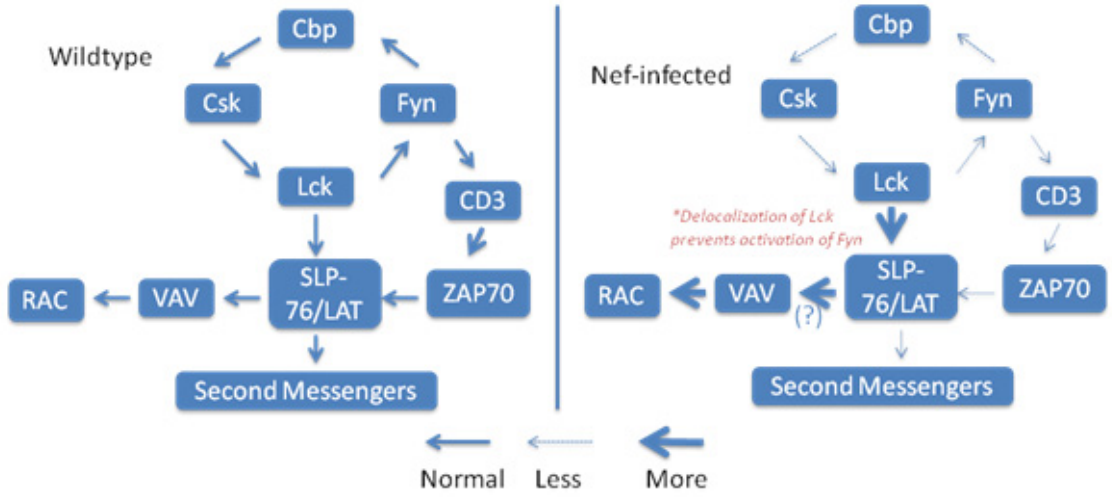

Figure 29: Schematic representation of proposed model. As Lck is delocalized in Nef-infected thymocytes, ZAP-70 is not activated which disrupts activation of many second messengers.

Future work

In order to properly target the alterated activation of the T cell during Nef infection, it is necessary to understand the full picture. We show the potential for cellular activation downstream of SLP-76 in Nef+ thymocytes, which disagrees with the notion that LAT and SLP-76 are disconnected (Abraham et al., 2012). Furthermore the GEF nessecary for Rac activation, Vav, is recruited to SLP-76 by phosphorylation of a tyrosine residue that Lck has been reported to be able to phosphorylate (sourcce). It is possible that Ras is actually responsible for the increased Erk activation as reported (Pan et al., 2012).

Although this team also reported Nef-mediated activation of Vav (Fackler et al., 1999), upstream of Rac. In order to understand if the recruitment of Rac to the plasma membrane actually results in its activation, and what other SLP-76-dependant mediators can be activated, phospho-specific biochemical studies should be performed, as each phospho-site of the SLP-76 protein (in addition to LAT) recruit unique proteins.

Consequences of CD4C/HIV-Nef on thymic epithelial cell populations and loss of AIRE expression

In the second half of this thesis, we show for the first time an effect of *in vivo* Nef infection on AIRE expression, an extremely crucial transcription factor involved in central tolerance. We have shown that the Nef-induced depletion of thymocytes and subsequent thymic atrophy leads to a disruption of TECs and a subsequent loss of AIRE. The loss of AIRE RNA in total thymus shown by northern blot analysis in addition to RT-PCR (**Figure 19**) and confirmed with a decreased MFI of AIRE expression by flow cytometry in thymic epithelial cells (**Figure 22**), is consistent with previous reports of loss of AIRE expression where normal thymic architecture is disturbed (Akiyama et al., 2005). We also confirm the loss of AIRE mRNA expression in an additional founder mouse model where Nef is driven under the mouse CD4 promoter instead of the human; these mice do not express Nef in macrophages, have twice the amount of Nef protein and a more profound loss of CD4 T cells however they do not develop nonlymphoid organ diseases (Hanna et al., 2009). We find a significant and severe loss of AIRE in the thymi of mCD4C/HIV-Nef mice, which is even more profound than in CD4C/HIV-Nef mice (**Figure 20**). This could be due to either the increased amount of Nef or the increased loss

of CD4, however it is difficult to speculate about a dose-dependant effect without further investigation.

Our approach to explain the AIRE loss was to investigate the possibility of a loss of the unique cellular population expressing AIRE (mTECs) however the current model depicts that AIRE promotes the differentiation program of mTECs and that the developmental process of these cells is altered with an alteration of AIRE expression (Yano et al., 2008). In mTECs, expression of AIRE is dependent upon NF-kB activation downstream of RANK activation by CD4+ thymocytes (Hamazaki et al., 2007; Kajiura et al., 2004; Rossi et al., 2007). By studying the mTEC population by single cell analysis, we reveal that these cells (CD45-, UEA-1+, Ly51lo) are actually enriched in CD4C/HIV-Nef Tg mice (**Figure 21).** These data are in coherence with proliferation studies showing that AIRE+ cells represent post-mitotic terminally differentiated cells whereas AIRE- mTECs are highly proliferative (Dooley et al., 2008; Gray et al., 2007). Initially surprising was that we observed an enrichment in our gated population which normally consists of cTECs (CD45-, UEA-1-, Ly51lo), which do not express AIRE (**Figure 21**). Recent work now shows that TEC stem from bipotent progenitors that first express hallmarks of cTECs and then differentiate into mTECs guided by RANKL stimulation (Baik et al., 2013). Therefore the same mechanisms that interfere with mTEC *maturation* may also be interfering with mTEC *differentiation* resulting in more cells developing into cTECs by not differentiating into mTECs. Moreover, while the UEA-1 lectin is consistently used to detect the mTEC population (Akiyama et al., 2008; Baik et al., 2013; Hamazaki et al., 2007; Hikosaka et al., 2008; Nishikawa et al., 2010; Williams et al., 2009), there is a minor mTEC population that does not bind the UEA-1 lectin (Lomada et al., 2007),

which may be observed as enriched in the UEA-1, Ly51lo population of **Figure 21**. It is highly likely that the enrichment that we observe in mTEC populations of CD4C/HIV-Nef mice is due to proliferation as a result of the loss of AIRE activation, this would be confirmed by performing a proliferation assay however there are technical issues due to the extremely small size of these cell populations, representing 0.005% of the thymus (Hubert et al., 2008) and the experiment was not performed. However by obtaining an AIRE/GFP reporter mouse to breed with our CD4C/HIV-Nef mice, we show a decrease in the number of mature mTECs expressing a high amount of AIRE shown in flow cytometry (**Figure 23**) supporting our hypothesis that there is an error in promotion of sufficient AIRE for maturation in Nef+ thymocytes. Our data strongly suggest that AIRE is lost in CD4C/HIV-Nef mice, which also results in interferences with the normal development of cTECs and mTECs.

AIRE loss and TEC phenotype is dependent on CD4 SP loss and can be rescued

In search for a mechanism for loss of AIRE and impaired maturation of TECs, we saw two possibilities. The first and more easily explained possibility is that AIRE was lost due to a loss of CD4+ thymocytes (already shown as a consequence of Nef infection in our model by (Chrobak et al., 2010)), which bear RANK and can activate AIRE through RANKL on mTECs. A second possibility is that Nef infection has a direct effect on TECs by interfering with pathways upstream or downstream of the transcription factor AIRE.

We pursued the second hypothesis as a reasonable explanation as there are reports of CD4 expression on epithelial cells of the colon (Jordan et al., 1999), intestine (Dwinell et al., 1999), uterus (Yeaman et al., 2003), however the existence of CD4 has never been

investigated in the TECs. We used a CD4C/GFP reporter mouse to test for CD4 activity in TECs. **Figure 24** shows CD4 activity by flow cytometry in two distinct founder transgenic mice, we find GFP in mTECs and cTECs but not in CD45-, Ly51-, UEA-1- endothelial cells suggesting that Nef could in fact infect these populations, however we were unable to detect Nef mRNA after sorting (**Figure 26**). Moreover when we bred CD4C/HIV-Nef mice with CD4C/GFP mice, we found that the GFP expression was unaltered by Nef, suggesting that it does not directly affect these cells (**Figure 25**). Consequently, we are not able to completely disprove the presence of Nef in these cells but if it is, it is not convincing that it directly affects AIRE as we subsequently find that the AIRE phenotype is clearly dependent on CD4 loss. When crossed with a constitutively active Lck Tg mouse (DLGF), CD4C/HIV-Nef X DLGF dTg rescues the loss of CD4 observed in the thymus (Chrobak et al., 2010). In this model where CD4 thymocytes are rescued, we also rescued the loss of AIRE mRNA (**Figure 27**) as well as the enrichment of TECs (**Figure 28**). These data very strongly suggest that regardless of Nef presence in TECs, their impaired differentiation/maturation and the loss of AIRE in mTECs is clearly dependent on CD4 loss in the thymus, as even in the presence of Nef, it is rescued with the rescue of CD4+ thymocytes.

CD4C/HIV-Nef induced AIRE loss impairs central tolerance and confers autoimmunity

Recent work shows that AIRE promotes the differentation of mTECs and promiscuous gene expression is accomplished by AIRE in terminally differentiated, fully matured mTECs (Yano et al., 2008). We directly correlated the loss of AIRE mRNA in the thymus to the loss of TRA expression by studying two of the most commonly reported TRAs in

the context of AIRE study: insulin and SAP1. We find a profound loss (80%) of these genes in the thymi of CD4C/HIV-Nef with respect to wildtype mice correlating the data with a clinical phenotype, as insulin loss of a similar magnitude is experimentally linked to CD4+ T cell infiltration into the islet cells of the pancreas (Fan et al., 2009; Liston et al., 2003) as well as various autoantibodies resulting in multi-organ disease (Yano et al., 2008). Moreover, the lupus-like autoimmune related pathologies observed in the context of AIDS are strikingly similar to those seen in patients with a polymorphism in the AIRE gene from lung disease and pulmonary hypertension (reviewed in (Nicolls et al., 2005) to interstitial nephritis and kidney disease (Al-Owain et al., 2010; Gardenswartz et al., 1984; Mouratoff et al., 2000; Ulinski et al., 2006). The next steps will be to identify specific TRAs realted to these diseases that could be measured in the thymus, as well as to correlate these data of central tolerance loss in the CD4C/HIV-Nef mice with other peripheral autoimmune-like pathologies seen in these mice (not published). Overall, these data depict a mechanism that may explain breakdown of central tolerance observed in HIV/AIDS due to damage in the thymus that is not reversed with current anti-retroviral therapies, and also explains why AIDS was originally though to be an autoimmune disorder (Ziegler and Stites, 1986).

9. Conclusions

Our data have shown that Nef alters the function and activation level of Lck, in the thymocytes of CD4C/HIV-Nef mice which disconnects T cell receptor engagement from activation of intraceluular mediators and production of proliferative cytokine IL-2. By studying mediators of the extremely fine regulation of Lck, we show that the delocalization of the protein has more consequences than its increased- or decreased-activation. The lack of ZAP-70 activation downstream of Lck affects many canonical pathways steming from LAT/SLP-76 microclusters. Lck may be implicated in mediating activation downstream of ZAP-70 in Nef-infected cells which could explain the recruitment of Rac, but this needs to be further studied. These data further clarify how Nef keeps the cell in limbo between quiescence and strong activation however there is still much work to be done in order to understand the biochemisty of a Nef-infected cell if we want to search for pharmaceutical targets.

The second part of the project offers a novel mechanism for the autoimmunity that is seen in HIV/AIDS patients. The model is transferable to humans as we have shown that the phenotype depends not on Nef but a loss of CD4+ thymocytes, which is part of the observed pathology in HIV^+ individuals. These data suggest that even in the presence of ART (during which we see increased autoimmunity), irreversible damage in the thymus can cause defects in central tolerance. Strategies that rely on peripheral T cell replenishment in HIV/AIDS patients rather than from the thymus (as is seen after lymphopenia) could help reduce the incidence of autoimmunity due to defects in *central* tolerance.

10. References

University Thesis:

Guertin, J., 2011, La protéine Nef du VIH-1 altère la fonction de Lck dans les thymocytes de souris transgéniques, Université de Montréal Montréal, Canada.

Publications:

Abraham, L., P. Bankhead, X. Pan, U. Engel, and O. T. Fackler, 2012, HIV-1 Nef limits communication between linker of activated T cells and SLP-76 to reduce formation of SLP-76-signaling microclusters following TCR stimulation: J Immunol, v. 189, p. 1898-910.

Abraham, L., and O. T. Fackler, 2012, HIV-1 Nef: a multifaceted modulator of T cell receptor signaling: Cell Commun Signal, v. 10, p. 39.

Aiken, C., L. Krause, Y. L. Chen, and D. Trono, 1996, Mutational analysis of HIV-1 Nef: identification of two mutants that are temperature-sensitive for CD4 downregulation: Virology, v. 217, p. 293-300.

Akiyama, T., S. Maeda, S. Yamane, K. Ogino, M. Kasai, F. Kajiura, M. Matsumoto, and J. Inoue, 2005, Dependence of self-tolerance on TRAF6-directed development of thymic stroma: Science, v. 308, p. 248-51.

Akiyama, T., Y. Shimo, H. Yanai, J. Qin, D. Ohshima, Y. Maruyama, Y. Asaumi, J. Kitazawa, H. Takayanagi, J. M. Penninger, M. Matsumoto, T. Nitta, Y. Takahama, and J. Inoue, 2008, The tumor necrosis factor family receptors RANK and CD40 cooperatively establish: Immunity, v. 29, p. 423-37.

Al-Owain, M., N. Kaya, H. Al-Zaidan, I. Bin Hussain, H. Al-Manea, H. Al-Hindi, S. Kennedy, M. A. Iqbal, H. Al-Mojalli, A. Al-Bakheet, A. Puel, J. L. Casanova, and S. Al-Muhsen, 2010, Renal failure associated with APECED and terminal 4q deletion: evidence of autoimmune nephropathy: Clin Dev Immunol, v. 2010, p. 586342.

Anderson, G., W. E. Jenkinson, T. Jones, S. M. Parnell, F. A. Kinsella, A. J. White, J. E. Pongrac'z, S. W. Rossi, and E. J. Jenkinson, 2006, Establishment and functioning of intrathymic microenvironments: Immunol Rev, v. 209, p. 10-27.

Anderson, M. S., E. S. Venanzi, L. Klein, Z. Chen, S. P. Berzins, S. J. Turley, H. von Boehmer, R. Bronson, A. Dierich, C. Benoist, and D. Mathis, 2002, Projection of an immunological self shadow within the thymus by the aire protein: Science, v. 298, p. 1395-401.

Arold, S., P. Franken, M. P. Strub, F. Hoh, S. Benichou, R. Benarous, and C. Dumas, 1997, The crystal structure of HIV-1 Nef protein bound to the Fyn kinase SH3 domain suggests a role for this complex in altered T cell receptor signaling: Structure, v. 5, p. 1361-72.

Arora, V.K., R.P. Molina, J.L. Foster, J.L Blakemore, J. Chernoff, B.L. Brenda, and J.V. Garcia, 2000, Lentivirus Nef Specifically Activates Pak2: J Virol, v. 74, p11081-11087.

Au-Yeung, B. B., S. Deindl, L. Y. Hsu, E. H. Palacios, S. E. Levin, J. Kuriyan, and A. Weiss, 2009, The structure, regulation, and function of ZAP-70: Immunol Rev, v. 228, p. 41-57.

Baik, S., E. J. Jenkinson, P. J. Lane, G. Anderson, and W. E. Jenkinson, 2013, Generation of both cortical and Aire(+) medullary thymic epithelial compartments from CD205(+) progenitors: Eur J Immunol, v. 43, p. 589-94.

Bandivdekar, A. H., S. M. Velhal, and V. P. Raghavan, 2003, Identification of CD4-independent HIV receptors on spermatozoa: Am J Reprod Immunol, v. 50, p. 322-7.

Barré-Sinoussi, F., 1996, HIV as the cause of AIDS: Lancet, v. 348, p. 31-5.

Blagoveshchenskaya, A. D., L. Thomas, S. F. Feliciangeli, C. H. Hung, and G. Thomas, 2002, HIV-1 Nef downregulates MHC-I by a PACS-1- and PI3K-regulated ARF6 endocytic pathway: Cell, v. 111, p. 853-66.

Bobardt, M. D., U. Chatterji, S. Selvarajah, B. Van der Schueren, G. David, B. Kahn, and P. A. Gallay, 2007, Cell-free human immunodeficiency virus type 1 transcytosis through primary genital epithelial cells: J Virol, v. 81, p. 395-405.

Campbell, E. M., R. Nunez, and T. J. Hope, 2004, Disruption of the actin cytoskeleton can complement the ability of Nef to enhance human immunodeficiency virus type 1 infectivity: J Virol, v. 78, p. 5745-55.

Cancelas, J. A., A. W. Lee, R. Prabhakar, K. F. Stringer, Y. Zheng, and D. A. Williams, 2005, Rac GTPases differentially integrate signals regulating hematopoietic stem cell localization: Nat Med, v. 11, p. 886-91.

Cann, A. J., and J. Karn, 1989, Molecular biology of HIV: new insights into the virus life-cycle: AIDS, v. 3 Suppl 1, p. S19-34.

Charvet, C., A. J. Canonigo, D. D. Billadeau, and A. Altman, 2005, Membrane localization and function of Vav3 in T cells depend on its association with the adapter SLP-76: J Biol Chem, v. 280, p. 15289-99.

Chrobak, P., M. C. Simard, N. Bouchard, T. M. Ndolo, J. Guertin, Z. Hanna, V. Dave, and P. Jolicoeur, 2010, HIV-1 Nef disrupts maturation of CD4+ T cells through CD4/Lck modulation: J Immunol, v. 185, p. 3948-59.

Chuck, M. I., M. Zhu, S. Shen, and W. Zhang, 2010, The role of the LAT-PLC-gamma1 interaction in T regulatory cell function: J Immunol, v. 184, p. 2476-86.

Clark, D. R., N. M. Ampel, C. A. Hallett, V. R. Yedavalli, N. Ahmad, and D. DeLuca, 1997, Peripheral blood from human immunodeficiency virus type 1-infected patients displays diminished T cell generation capacity: J Infect Dis, v. 176, p. 649-54.

Coutinho, A., I. Caramalho, E. Seixas, and J. Demengeot, 2005, Thymic commitment of regulatory T cells is a pathway of TCR-dependent selection that isolates repertoires undergoing positive or negative selection: Curr Top Microbiol Immunol, v. 293, p. 43-71.

Crespo, P., K. E. Schuebel, A. A. Ostrom, J. S. Gutkind, and X. R. Bustelo, 1997, Phosphotyrosine-dependent activation of Rac-1 GDP/GTP exchange by the vav proto-oncogene product: Nature, v. 385, p. 169-72.

Dayton, A. I., 2004, Within you, without you: HIV-1 Rev and RNA export: Retrovirology, v. 1, p. 35.

Deacon, N. J., A. Tsykin, A. Solomon, K. Smith, M. Ludford-Menting, D. J. Hooker, D. A. McPhee, A. L. Greenway, A. Ellett, C. Chatfield, V. A. Lawson, S. Crowe, A. Maerz, S. Sonza, J. Learmont, J. S. Sullivan, A. Cunningham, D. Dwyer, D. Dowton, and J. Mills, 1995, Genomic structure of an attenuated quasi species of HIV-1 from a blood transfusion donor and recipients: Science, v. 270, p. 988-91.

Demirov, D. G., A. Ono, J. M. Orenstein, and E. O. Freed, 2002, Overexpression of the N-terminal domain of TSG101 inhibits HIV-1 budding by blocking late domain function: Proc Natl Acad Sci U S A, v. 99, p. 955-60.

Dooley, J., M. Erickson, and A. G. Farr, 2008, Alterations of the medullary epithelial compartment in the Aire-deficient thymus: J Immunol, v. 181, p. 5225-32.

Dorrance, A. M., S. De Vita, M. Radu, P. N. Reddy, M. K. McGuinness, C. E. Harris, R. Mathieu, S. W. Lane, R. Kosoff, M. D. Milsom, J. Chernoff, and D. A. Williams, 2013, The Rac GTPase effector p21 activated kinase is essential for hematopoietic stem/progenitor cell migration and engraftment: Blood.

Dwinell, M. B., L. Eckmann, J. D. Leopard, N. M. Varki, and M. F. Kagnoff, 1999, Chemokine receptor expression by human intestinal epithelial cells: Gastroenterology, v. 117, p. 359-67.

Eblen, S. T., J. K. Slack, M. J. Weber, and A. D. Catling, 2002, Rac-PAK signaling stimulates extracellular signal-regulated kinase (ERK) activation by regulating formation of MEK1-ERK complexes: Mol Cell Biol, v. 22, p. 6023-33.

Engelman, A., K. Mizuuchi, and R. Craigie, 1991, HIV-1 DNA integration: mechanism of viral DNA cleavage and DNA strand transfer: Cell, v. 67, p. 1211-21.

Erpel, T., and S. A. Courtneidge, 1995, Src family protein tyrosine kinases and cellular signal transduction pathways: Curr Opin Cell Biol, v. 7, p. 176-82.

Estes, J. D., S. N. Gordon, M. Zeng, A. M. Chahroudi, R. M. Dunham, S. I. Staprans, C. S. Reilly, G. Silvestri, and A. T. Haase, 2008, Early resolution of acute immune activation and induction of PD-1 in SIV-infected sooty mangabeys distinguishes nonpathogenic from pathogenic infection in rhesus macaques: J Immunol, v. 180, p. 6798-807.

Fackler, O. T., W. Luo, M. Geyer, A. S. Alberts, and B. M. Peterlin, 1999, Activation of Vav by Nef induces cytoskeletal rearrangements and downstream effector functions: Mol Cell, v. 3, p. 729-39.

Fan, Y., W. A. Rudert, M. Grupillo, J. He, G. Sisino, and M. Trucco, 2009, Thymus-specific deletion of insulin induces autoimmune diabetes: EMBO J, v. 28, p. 2812-24.

Fife, D.J., J.M. Waller, E.W. Jeffes, and J.Y.M Koo, 2007, Unravelling the paradoxes of HIV-associated psoriasis: A review of T-cell subsets and cytokine profiles: Dermatology Online Journal, v. 13.

Foster, J. L., and J. V. Garcia, 2008, HIV-1 Nef: at the crossroads: Retrovirology, v. 5, p. 84.

Frankel, A. D., and J. A. Young, 1998, HIV-1: fifteen proteins and an RNA: Annu Rev Biochem, v. 67, p. 1-25.

Gardenswartz, M. H., C. W. Lerner, G. R. Seligson, P. M. Zabetakis, H. Rotterdam, M. L. Tapper, M. F. Michelis, and M. S. Bruno, 1984, Renal disease in patients with AIDS: a clinicopathologic study: Clin Nephrol, v. 21, p. 197-204.

Gardner, J. M., J. J. Devoss, R. S. Friedman, D. J. Wong, Y. X. Tan, X. Zhou, K. P. Johannes, M. A. Su, H. Y. Chang, M. F. Krummel, and M. S. Anderson, 2008, Deletional tolerance mediated by extrathymic Aire-expressing cells: Science, v. 321, p. 843-7.

Gavanescu, I., C. Benoist, and D. Mathis, 2008, B cells are required for Aire-deficient mice to develop multi-organ autoinflammation: A therapeutic approach for APECED patients: Proc Natl Acad Sci U S A, v. 105, p. 13009-14.

Geyer, M., O. T. Fackler, and B. M. Peterlin, 2001, Structure--function relationships in HIV-1 Nef: EMBO Rep, v. 2, p. 580-5.
Gorska, M. M., Q. Liang, Z. Karim, and R. Alam, 2009, Uncoordinated 119 protein controls trafficking of Lck via the Rab11 endosome and is critical for immunological synapse formation: J Immunol, v. 183, p. 1675-84.
Gray, D., J. Abramson, C. Benoist, and D. Mathis, 2007, Proliferative arrest and rapid turnover of thymic epithelial cells expressing: J Exp Med, v. 204, p. 2521-8.
Greenberg, M. E., A. J. Iafrate, and J. Skowronski, 1998, The SH3 domain-binding surface and an acidic motif in HIV-1 Nef regulate trafficking of class I MHC complexes: EMBO J, v. 17, p. 2777-89.
Grzesiek, S., A. Bax, J. S. Hu, J. Kaufman, I. Palmer, S. J. Stahl, N. Tjandra, and P. T. Wingfield, 1997, Refined solution structure and backbone dynamics of HIV-1 Nef: Protein Sci, v. 6, p. 1248-63.
Grzesiek, S., S. J. Stahl, P. T. Wingfield, and A. Bax, 1996, The CD4 determinant for downregulation by HIV-1 Nef directly binds to Nef. Mapping of the Nef binding surface by NMR: Biochemistry, v. 35, p. 10256-61.
Guertin, J., 2011, La protéine Nef du VIH-1 altère la fonction de Lck dans les thymocytes de souris transgéniques, Université de Montréal Montréal, Canada.
Haller, C., S. Rauch, and O. T. Fackler, 2007, HIV-1 Nef employs two distinct mechanisms to modulate Lck subcellular localization and TCR induced actin remodeling: PLoS One, v. 2, p. e1212.
Hamazaki, Y., H. Fujita, T. Kobayashi, Y. Choi, H. S. Scott, M. Matsumoto, and N. Minato, 2007, Medullary thymic epithelial cells expressing Aire represent a unique lineage derived from cells expressing claudin: Nat Immunol, v. 8, p. 304-11.
Hanna, Z., D. G. Kay, M. Cool, S. Jothy, N. Rebai, and P. Jolicoeur, 1998a, Transgenic mice expressing human immunodeficiency virus type 1 in immune cells develop a severe AIDS-like disease: J Virol, v. 72, p. 121-32.
Hanna, Z., D. G. Kay, N. Rebai, A. Guimond, S. Jothy, and P. Jolicoeur, 1998b, Nef harbors a major determinant of pathogenicity for an AIDS-like disease induced by HIV-1 in transgenic mice: Cell, v. 95, p. 163-75.
Hanna, Z., E. Priceputu, P. Chrobak, C. Hu, V. Dugas, M. Goupil, M. Marquis, L. de Repentigny, and P. Jolicoeur, 2009, Selective expression of human immunodeficiency virus Nef in specific immune cell populations of transgenic mice is associated with distinct AIDS-like phenotypes: J Virol, v. 83, p. 9743-58.
Hawash, I. Y., K. P. Kesavan, A. I. Magee, R. L. Geahlen, and M. L. Harrison, 2002, The Lck SH3 domain negatively regulates localization to lipid rafts through an interaction with c-Cbl: J Biol Chem, v. 277, p. 5683-91.
Hayes, R., and H. Weiss, 2006, Epidemiology. Understanding HIV epidemic trends in Africa: Science, v. 311, p. 620-1.
Haynes, B. F., M. L. Markert, G. D. Sempowski, D. D. Patel, and L. P. Hale, 2000, The role of the thymus in immune reconstitution in aging, bone marrow transplantation, and HIV-1 infection: Annu Rev Immunol, v. 18, p. 529-60.
Herrmann, C. H., and A. P. Rice, 1995, Lentivirus Tat proteins specifically associate with a cellular protein kinase, TAK, that hyperphosphorylates the carboxyl-terminal domain of the large subunit of RNA polymerase II: candidate for a Tat cofactor: J Virol, v. 69, p. 1612-20.

Hikosaka, Y., T. Nitta, I. Ohigashi, K. Yano, N. Ishimaru, Y. Hayashi, M. Matsumoto, K. Matsuo, J. M. Penninger, H. Takayanagi, Y. Yokota, H. Yamada, Y. Yoshikai, J. Inoue, T. Akiyama, and Y. Takahama, 2008, The cytokine RANKL produced by positively selected thymocytes fosters medullary: Immunity, v. 29, p. 438-50.

Horejsh, D., T. J. Ruckwardt, and C. David Pauza, 2002, CXCR4-dependent HIV-1 infection of differentiated epithelial cells: Virus Res, v. 90, p. 275-86.

Hough, C., M. Radu, and J. J. Doré, 2012, Tgf-beta induced Erk phosphorylation of smad linker region regulates smad signaling: PLoS One, v. 7, p. e42513.

Hubert, F. X., S. A. Kinkel, K. E. Webster, P. Cannon, P. E. Crewther, A. I. Proeitto, L. Wu, W. R. Heath, and H. S. Scott, 2008, A specific anti-Aire antibody reveals aire expression is restricted to medullary: J Immunol, v. 180, p. 3824-32.

Husain, M., and P. C. Singhal, 2011, HIV-1 entry into renal epithelia: J Am Soc Nephrol, v. 22, p. 399-402.

Huse, M., 2009, The T-cell-receptor signaling network: J Cell Sci, v. 122, p. 1269-73.

Irla, M., S. Hugues, J. Gill, T. Nitta, Y. Hikosaka, I. R. Williams, F. X. Hubert, H. S. Scott, Y. Takahama, G. A. Hollander, and W. Reith, 2008, Autoantigen-specific interactions with CD4+ thymocytes control mature medullary: Immunity, v. 29, p. 451-63.

Janardhan, A., T. Swigut, B. Hill, M. P. Myers, and J. Skowronski, 2004, HIV-1 Nef binds the DOCK2-ELMO1 complex to activate rac and inhibit lymphocyte chemotaxis: PLoS Biol, v. 2, p. E6.

Jayaraman, T., K. Ondrias, E. Ondriasová, and A. R. Marks, 1996, Regulation of the inositol 1,4,5-trisphosphate receptor by tyrosine phosphorylation: Science, v. 272, p. 1492-4.

Jiang, Y., and H. Cheng, 2007, Evidence of LAT as a dual substrate for Lck and Syk in T lymphocytes: Leuk Res, v. 31, p. 541-5.

Jordan, N. J., G. Kolios, S. E. Abbot, M. A. Sinai, D. A. Thompson, K. Petraki, and J. Westwick, 1999, Expression of functional CXCR4 chemokine receptors on human colonic epithelial cells: J Clin Invest, v. 104, p. 1061-9.

Joshi, V. V., J. M. Oleske, A. B. Minnefor, S. Saad, K. M. Klein, R. Singh, M. Zabala, C. Dadzie, M. Simpser, and R. H. Rapkin, 1985, Pathologic pulmonary findings in children with the acquired immunodeficiency syndrome: a study of ten cases: Hum Pathol, v. 16, p. 241-6.

Kabouridis, P. S., D. A. Isenberg, and E. C. Jury, 2011, A negatively charged domain of LAT mediates its interaction with the active form of Lck: Mol Membr Biol, v. 28, p. 487-94.

Kajiura, F., S. Sun, T. Nomura, K. Izumi, T. Ueno, Y. Bando, N. Kuroda, H. Han, Y. Li, A. Matsushima, Y. Takahama, S. Sakaguchi, T. Mitani, and M. Matsumoto, 2004, NF-kappa B-inducing kinase establishes self-tolerance in a thymic stroma-dependent manner: J Immunol, v. 172, p. 2067-75.

Kestler, H. W., D. J. Ringler, K. Mori, D. L. Panicali, P. K. Sehgal, M. D. Daniel, and R. C. Desrosiers, 1991, Importance of the nef gene for maintenance of high virus loads and for development of AIDS: Cell, v. 65, p. 651-62.

Kirchhoff, F., T. C. Greenough, D. B. Brettler, J. L. Sullivan, and R. C. Desrosiers, 1995, Brief report: absence of intact nef sequences in a long-term survivor with nonprogressive HIV-1 infection: N Engl J Med, v. 332, p. 228-32.

Klimas, N., A. O'Brien Koneru, and M. A. Fletcher, 2008, Overview of HIV, Psychosomatic Medicine, p. 523-530.
Kohlstaedt, L. A., and T. A. Steitz, 1992, Reverse transcriptase of human immunodeficiency virus can use either human tRNA(3Lys) or Escherichia coli tRNA(2Gln) as a primer in an in vitro primer-utilization assay: Proc Natl Acad Sci U S A, v. 89, p. 9652-6.
Koot, M., P. T. Schellekens, J. W. Mulder, J. M. Lange, M. T. Roos, R. A. Coutinho, M. Tersmette, and F. Miedema, 1993, Viral phenotype and T cell reactivity in human immunodeficiency virus type 1-infected asymptomatic men treated with zidovudine: J Infect Dis, v. 168, p. 733-6.
Kopelman, R. G., and S. Zolla-Pazner, 1988, Association of human immunodeficiency virus infection and autoimmune phenomena: Am J Med, v. 84, p. 82-8.
Koretzky, G. A., F. Abtahian, and M. A. Silverman, 2006, SLP76 and SLP65: complex regulation of signalling in lymphocytes and beyond: Nat Rev Immunol, v. 6, p. 67-78.
Kourtis, A. P., C. Ibegbu, A. J. Nahmias, F. K. Lee, W. S. Clark, M. K. Sawyer, and S. Nesheim, 1996, Early progression of disease in HIV-infected infants with thymus dysfunction: N Engl J Med, v. 335, p. 1431-6.
Krautkrämer, E., S. I. Giese, J. E. Gasteier, W. Muranyi, and O. T. Fackler, 2004, Human immunodeficiency virus type 1 Nef activates p21-activated kinase via recruitment into lipid rafts: J Virol, v. 78, p. 4085-97.
Kyewski, B., and L. Klein, 2006, A central role for central tolerance: Annu Rev Immunol, v. 24, p. 571-606.
Learmont, J. C., A. F. Geczy, J. Mills, L. J. Ashton, C. H. Raynes-Greenow, R. J. Garsia, W. B. Dyer, L. McIntyre, R. B. Oelrichs, D. I. Rhodes, N. J. Deacon, and J. S. Sullivan, 1999, Immunologic and virologic status after 14 to 18 years of infection with an attenuated strain of HIV-1. A report from the Sydney Blood Bank Cohort: N Engl J Med, v. 340, p. 1715-22.
Lee, C. H., K. Saksela, U. A. Mirza, B. T. Chait, and J. Kuriyan, 1996, Crystal structure of the conserved core of HIV-1 Nef complexed with a Src family SH3 domain: Cell, v. 85, p. 931-42.
Lenassi, M., G. Cagney, M. Liao, T. Vaupotic, K. Bartholomeeusen, Y. Cheng, N. J. Krogan, A. Plemenitas, and B. M. Peterlin, 2010, HIV Nef is secreted in exosomes and triggers apoptosis in bystander CD4+ T cells: Traffic, v. 11, p. 110-22.
Li, J. C., H. C. Yim, and A. S. Lau, 2010, Role of HIV-1 Tat in AIDS pathogenesis: its effects on cytokine dysregulation and contributions to the pathogenesis of opportunistic infection: AIDS, v. 24, p. 1609-23.
Liston, A., S. Lesage, J. Wilson, L. Peltonen, and C. C. Goodnow, 2003, Aire regulates negative selection of organ-specific T cells: Nat Immunol, v. 4, p. 350-4.
Liu, L. X., N. Heveker, O. T. Fackler, S. Arold, S. Le Gall, K. Janvier, B. M. Peterlin, C. Dumas, O. Schwartz, S. Benichou, and R. Benarous, 2000, Mutation of a conserved residue (D123) required for oligomerization of human immunodeficiency virus type 1 Nef protein abolishes interaction with human thioesterase and results in impairment of Nef biological functions: J Virol, v. 74, p. 5310-9.

Liu, S. K., N. Fang, G. A. Koretzky, and C. J. McGlade, 1999, The hematopoietic-specific adaptor protein gads functions in T-cell signaling via interactions with the SLP-76 and LAT adaptors: Curr Biol, v. 9, p. 67-75.
Lomada, D., B. Liu, L. Coghlan, Y. Hu, and E. R. Richie, 2007, Thymus medulla formation and central tolerance are restored in IKKalpha-/- mice: J Immunol, v. 178, p. 829-37.
Malatzky-Goshen, E., and Y. Shoenfeld, 1989, AIDS and autoimmunity: Autoimmunity, v. 3, p. 201-12.
Mariani, R., F. Kirchhoff, T. C. Greenough, J. L. Sullivan, R. C. Desrosiers, and J. Skowronski, 1996, High frequency of defective nef alleles in a long-term survivor with nonprogressive human immunodeficiency virus type 1 infection: J Virol, v. 70, p. 7752-64.
Massabki, P. S., C. Accetturi, I. A. Nishie, N. P. da Silva, E. I. Sato, and L. E. Andrade, 1997, Clinical implications of autoantibodies in HIV infection: AIDS, v. 11, p. 1845-50.
Matsubara, M., T. Jing, K. Kawamura, N. Shimojo, K. Titani, K. Hashimoto, and N. Hayashi, 2005, Myristoyl moiety of HIV Nef is involved in regulation of the interaction with calmodulin in vivo: Protein Sci, v. 14, p. 494-503.
Matsumoto, M., 2011, Contrasting models for the roles of Aire in the differentiation program of: Eur J Immunol, v. 41, p. 12-7.
Methi, T., T. Berge, K. M. Torgersen, and K. Taskén, 2008, Reduced Cbl phosphorylation and degradation of the zeta-chain of the T-cell receptor/CD3 complex in T cells with low Lck levels: Eur J Immunol, v. 38, p. 2557-63.
Metzger, T. C., and M. S. Anderson, 2011, Control of central and peripheral tolerance by Aire: Immunol Rev, v. 241, p. 89-103.
Mikulak, J., and P. C. Singhal, 2010, HIV-1 entry into human podocytes is mediated through lipid rafts: Kidney Int, v. 77, p. 72-3; author reply 73-4.
Mouratoff, J. G., J. Tokumoto, J. L. Olson, and G. M. Chertow, 2000, Acute renal failure with interstitial nephritis in a patient with AIDS: Am J Kidney Dis, v. 35, p. 557-61.
Muratori, C., L. E. Cavallin, K. Krätzel, A. Tinari, A. De Milito, S. Fais, P. D'Aloja, M. Federico, V. Vullo, A. Fomina, E. A. Mesri, F. Superti, and A. S. Baur, 2009, Massive secretion by T cells is caused by HIV Nef in infected cells and by Nef transfer to bystander cells: Cell Host Microbe, v. 6, p. 218-30.
Mustelin, T., and K. Taskén, 2003, Positive and negative regulation of T-cell activation through kinases and phosphatases: Biochem J, v. 371, p. 15-27.
Naramura, M., I. K. Jang, H. Kole, F. Huang, D. Haines, and H. Gu, 2002, c-Cbl and Cbl-b regulate T cell responsiveness by promoting ligand-induced TCR down-modulation: Nat Immunol, v. 3, p. 1192-9.
Neumeister, E. N., Y. Zhu, S. Richard, C. Terhorst, A. C. Chan, and A. S. Shaw, 1995, Binding of ZAP-70 to phosphorylated T-cell receptor zeta and eta enhances its autophosphorylation and generates specific binding sites for SH2 domain-containing proteins: Mol Cell Biol, v. 15, p. 3171-8.
Nicolls, M. R., L. Taraseviciene-Stewart, P. R. Rai, D. B. Badesch, and N. F. Voelkel, 2005, Autoimmunity and pulmonary hypertension: a perspective: Eur Respir J, v. 26, p. 1110-8.

Nika, K., C. Soldani, M. Salek, W. Paster, A. Gray, R. Etzensperger, L. Fugger, P. Polzella, V. Cerundolo, O. Dushek, T. Höfer, A. Viola, and O. Acuto, 2010, Constitutively active Lck kinase in T cells drives antigen receptor signal transduction: Immunity, v. 32, p. 766-77.

Nishikawa, Y., F. Hirota, M. Yano, H. Kitajima, J. Miyazaki, H. Kawamoto, Y. Mouri, and M. Matsumoto, 2010, Biphasic Aire expression in early embryos and in medullary thymic epithelial cells before end-stage terminal differentiation: J Exp Med, v. 207, p. 963-71.

Nájera, R., M. I. Herrera, and R. de Andrés, 1987, Human immunodeficiency virus and related retroviruses: West J Med, v. 147, p. 702-8.

O'Leary, J.G., K. Zachary, J. Misdraji, and R.T. Chung, 2008, De novo autoimmune hepatitis during immune reconstitution in an HIV-infected patient receiving highly active antiretroviral therapy: Clin Infect Dis, v, 46, e12-14.

Palacios, E. H., and A. Weiss, 2004, Function of the Src-family kinases, Lck and Fyn, in T-cell development and activation: Oncogene, v. 23, p. 7990-8000.

Pan, X., J. M. Rudolph, L. Abraham, A. Habermann, C. Haller, J. Krijnse-Locker, and O. T. Fackler, 2012, HIV-1 Nef compensates for disorganization of the immunological synapse by inducing trans-Golgi network-associated Lck signaling: Blood, v. 119, p. 786-97.

Pantaleo, G., C. Graziosi, and A. S. Fauci, 1993, New concepts in the immunopathogenesis of human immunodeficiency virus infection: N Engl J Med, v. 328, p. 327-35.

Peter, F., 1998, HIV nef: the mother of all evil?: Immunity, v. 9, p. 433-7.

Piguet, V., L. Wan, C. Borel, A. Mangasarian, N. Demaurex, G. Thomas, and D. Trono, 2000, HIV-1 Nef protein binds to the cellular protein PACS-1 to downregulate class I major histocompatibility complexes: Nat Cell Biol, v. 2, p. 163-7.

Pizzato, M., E. Popova, and H. G. Göttlinger, 2008, Nef can enhance the infectivity of receptor-pseudotyped human immunodeficiency virus type 1 particles: J Virol, v. 82, p. 10811-9.

Pollakis, G., and W. A. Paxton, 2012, Use of (alternative) coreceptors for HIV entry: Curr Opin HIV AIDS, v. 7, p. 440-9.

Putney, J. W., and G. S. Bird, 1993, The signal for capacitative calcium entry: Cell, v. 75, p. 199-201.

Quinn, T. C., and J. Overbaugh, 2005, HIV/AIDS in women: an expanding epidemic: Science, v. 308, p. 1582-3.

Rao, N., S. Miyake, A. L. Reddi, P. Douillard, A. K. Ghosh, I. L. Dodge, P. Zhou, N. D. Fernandes, and H. Band, 2002, Negative regulation of Lck by Cbl ubiquitin ligase: Proc Natl Acad Sci U S A, v. 99, p. 3794-9.

Resh, M. D., 1999, Fatty acylation of proteins: new insights into membrane targeting of myristoylated and palmitoylated proteins: Biochim Biophys Acta, v. 1451, p. 1-16.

Rosenzweig, M., D. P. Clark, and G. N. Gaulton, 1993, Selective thymocyte depletion in neonatal HIV-1 thymic infection: AIDS, v. 7, p. 1601-5.

Rossi, S. W., M. Y. Kim, A. Leibbrandt, S. M. Parnell, W. E. Jenkinson, S. H. Glanville, F. M. McConnell, H. S. Scott, J. M. Penninger, E. J. Jenkinson, P. J. Lane, and G. Anderson, 2007, RANK signals from CD4(+)3(-) inducer cells regulate

development of Aire-expressing epithelial cells in the thymic medulla: J Exp Med, v. 204, p. 1267-72.
Rowland-Jones, S. L., 2003, AIDS pathogenesis: what have two decades of HIV research taught us?, Nature Immunology, p. 343-348.
Sakai, H., H. Siomi, H. Shida, R. Shibata, T. Kiyomasu, and A. Adachi, 1990, Functional comparison of transactivation by human retrovirus rev and rex genes: J Virol, v. 64, p. 5833-9.
Salghetti, S., R. Mariani, and J. Skowronski, 1995, Human immunodeficiency virus type 1 Nef and p56lck protein-tyrosine kinase interact with a common element in CD4 cytoplasmic tail: Proc Natl Acad Sci U S A, v. 92, p. 349-53.
Sanzenbacher, R., D. Kabelitz, and O. Janssen, 1999, SLP-76 binding to p56lck: a role for SLP-76 in CD4-induced desensitization of the TCR/CD3 signaling complex: J Immunol, v. 163, p. 3143-52.
Schade, A. E., and A. D. Levine, 2002, Lipid raft heterogeneity in human peripheral blood T lymphoblasts: a mechanism for regulating the initiation of TCR signal transduction: J Immunol, v. 168, p. 2233-9.
Schaller, C. E., C. L. Wang, G. Beck-Engeser, L. Goss, H. S. Scott, M. S. Anderson, and M. Wabl, 2008, Expression of Aire and the early wave of apoptosis in spermatogenesis: J Immunol, v. 180, p. 1338-43.
Schoenborn, J. R., Y. X. Tan, C. Zhang, K. M. Shokat, and A. Weiss, 2011, Feedback circuits monitor and adjust basal Lck-dependent events in T cell receptor signaling: Sci Signal, v. 4, p. ra59.
Schrager, J. A., V. Der Minassian, and J. W. Marsh, 2002, HIV Nef increases T cell ERK MAP kinase activity: J Biol Chem, v. 277, p. 6137-42.
Schwartz, O., V. Maréchal, O. Danos, and J. M. Heard, 1995, Human immunodeficiency virus type 1 Nef increases the efficiency of reverse transcription in the infected cell: J Virol, v. 69, p. 4053-9.
Schwartz, O., V. Maréchal, S. Le Gall, F. Lemonnier, and J. M. Heard, 1996, Endocytosis of major histocompatibility complex class I molecules is induced by the HIV-1 Nef protein: Nat Med, v. 2, p. 338-42.
Seach, N., T. Ueno, A. L. Fletcher, T. Lowen, M. Mattesich, C. R. Engwerda, H. S. Scott, C. F. Ware, A. P. Chidgey, D. H. Gray, and R. L. Boyd, 2008, The lymphotoxin pathway regulates Aire-independent expression of ectopic genes: J Immunol, v. 180, p. 5384-92.
Shakib, S., G. E. Desanti, W. E. Jenkinson, S. M. Parnell, E. J. Jenkinson, and G. Anderson, 2009, Checkpoints in the development of thymic cortical epithelial cells: J Immunol, v. 182, p. 130-7.
Sharp, P. M., and B. H. Hahn, 2010, The evolution of HIV-1 and the origin of AIDS: Philos Trans R Soc Lond B Biol Sci, v. 365, p. 2487-94.
Silvestri, G., D. L. Sodora, R. A. Koup, M. Paiardini, S. P. O'Neil, H. M. McClure, S. I. Staprans, and M. B. Feinberg, 2003, Nonpathogenic SIV infection of sooty mangabeys is characterized by limited bystander immunopathology despite chronic high-level viremia: Immunity, v. 18, p. 441-52.
Simmons, A., V. Aluvihare, and A. McMichael, 2001, Nef triggers a transcriptional program in T cells imitating single-signal T cell activation and inducing HIV virulence mediators: Immunity, v. 14, p. 763-77.

Simon, V., D. D. Ho, and Q. Abdool Karim, 2006, HIV/AIDS epidemiology, pathogenesis, prevention, and treatment: Lancet, v. 368, p. 489-504.

Stolp, B., L. Abraham, J. M. Rudolph, and O. T. Fackler, 2010, Lentiviral Nef proteins utilize PAK2-mediated deregulation of cofilin as a general strategy to interfere with actin remodeling: J Virol, v. 84, p. 3935-48.

Stratton, R., G. Slapak, T. Mahungu, and S. Kinloch-de Loes, 2009, Autoimmunity and HIV: Curr Opin Infect Dis, v. 22, p. 49-56.

Surh, C. D., E. K. Gao, H. Kosaka, D. Lo, C. Ahn, D. B. Murphy, L. Karlsson, P. Peterson, and J. Sprent, 1992, Two subsets of epithelial cells in the thymic medulla: J Exp Med, v. 176, p. 495-505.

Takahama, Y., 2006, Journey through the thymus: stromal guides for T-cell development and selection: Nat Rev Immunol, v. 6, p. 127-35.

Takarabe D., Y. Rokukawa, Y. Takahashi, A. Goto, M. Takaichi, M. Okamoto, T. Tsujimoto, H. Noto, M. Kishimoto, Y. Kaburaqi, K. Yasuda, R. Yamamoto-Honda, K. Tsukada, M. Honda, K. Teruya, H. Kaijo, Y. Kikuchi, S. Oka, M. Noda, 2010, Autoimmune diabetes in HIV-infected patients on highly active antiretroviral therapy: J Clin Endocrinol Metab, v. 95: 4056-4060.

Tavassoli, A., 2011, Targeting the protein-protein interactions of the HIV lifecycle: Chem Soc Rev, v. 40, p. 1337-46.

Thien, C. B., and W. Y. Langdon, 2001, Cbl: many adaptations to regulate protein tyrosine kinases: Nat Rev Mol Cell Biol, v. 2, p. 294-307.

Thien, C. B., and W. Y. Langdon, 2005, c-Cbl and Cbl-b ubiquitin ligases: substrate diversity and the negative regulation of signalling responses: Biochem J, v. 391, p. 153-66.

Thien, C. B., R. M. Scaife, J. M. Papadimitriou, M. A. Murphy, D. D. Bowtell, and W. Y. Langdon, 2003, A mouse with a loss-of-function mutation in the c-Cbl TKB domain shows perturbed thymocyte signaling without enhancing the activity of the ZAP-70 tyrosine kinase: J Exp Med, v. 197, p. 503-13.

Thoulouze, M. I., N. Sol-Foulon, F. Blanchet, A. Dautry-Varsat, O. Schwartz, and A. Alcover, 2006, Human immunodeficiency virus type-1 infection impairs the formation of the immunological synapse: Immunity, v. 24, p. 547-61.

Torgersen, K. M., T. Vang, H. Abrahamsen, S. Yaqub, V. Horejsí, B. Schraven, B. Rolstad, T. Mustelin, and K. Taskén, 2001, Release from tonic inhibition of T cell activation through transient displacement of C-terminal Src kinase (Csk) from lipid rafts: J Biol Chem, v. 276, p. 29313-8.

Tsygankov, A. Y., S. Mahajan, J. E. Fincke, and J. B. Bolen, 1996, Specific association of tyrosine-phosphorylated c-Cbl with Fyn tyrosine kinase in T cells: J Biol Chem, v. 271, p. 27130-7.

Ulinski, T., L. Perrin, M. Morris, M. Houang, S. Cabrol, C. Grapin, N. Chabbert-Buffet, A. Bensman, G. Deschênes, and I. Giurgea, 2006, Autoimmune polyendocrinopathy-candidiasis-ectodermal dystrophy syndrome with renal failure: impact of posttransplant immunosuppression on disease activity: J Clin Endocrinol Metab, v. 91, p. 192-5.

Van den Broeke, C., M. Radu, J. Chernoff, and H. W. Favoreel, 2010, An emerging role for p21-activated kinases (Paks) in viral infections: Trends Cell Biol, v. 20, p. 160-9.

van Ewijk, W., E. W. Shores, and A. Singer, 1994, Crosstalk in the mouse thymus: Immunol Today, v. 15, p. 214-7.
Vincent, P., E. Priceputu, D. Kay, K. Saksela, P. Jolicoeur, and Z. Hanna, 2006, Activation of p21-activated kinase 2 and its association with Nef are conserved in murine cells but are not sufficient to induce an AIDS-like disease in CD4C/HIV transgenic mice: J Biol Chem, v. 281, p. 6940-54.
Waters, L., S. Mandalia, P. Randell, A. Wildfire, B. Gazzard, and G. Moyle, 2008, The impact of HIV tropism on decreases in CD4 cell count, clinical progression, and subsequent response to a first antiretroviral therapy regimen: Clin Infect Dis, v. 46, p. 1617-23.
Whatmore, A. M., N. Cook, G. A. Hall, S. Sharpe, E. W. Rud, and M. P. Cranage, 1995, Repair and evolution of nef in vivo modulates simian immunodeficiency virus virulence: J Virol, v. 69, p. 5117-23.
Williams, K. M., H. Mella, P. J. Lucas, J. A. Williams, W. Telford, and R. E. Gress, 2009, Single cell analysis of complex thymus stromal cell populations: rapid thymic: Clin Transl Sci, v. 2, p. 279-85.
Yang, G., Q. Li, S. Ren, X. Lu, L. Fang, W. Zhou, F. Zhang, F. Xu, Z. Zhang, R. Zeng, F. Lottspeich, and Z. Chen, 2009, Proteomic, functional and motif-based analysis of C-terminal Src kinase-interacting proteins: Proteomics, v. 9, p. 4944-61.
Yang, P., and A. J. Henderson, 2005, Nef enhances c-Cbl phosphorylation in HIV-infected CD4+ T lymphocytes: Virology, v. 336, p. 219-28.
Yang, X., and D. Gabuzda, 1999, Regulation of human immunodeficiency virus type 1 infectivity by the ERK mitogen-activated protein kinase signaling pathway: J Virol, v. 73, p. 3460-6.
Yano, M., N. Kuroda, H. Han, M. Meguro-Horike, Y. Nishikawa, H. Kiyonari, K. Maemura, Y. Yanagawa, K. Obata, S. Takahashi, T. Ikawa, R. Satoh, H. Kawamoto, Y. Mouri, and M. Matsumoto, 2008, Aire controls the differentiation program of thymic epithelial cells in the medulla for the establishment of self-tolerance: J Exp Med, v. 205, p. 2827-38.
Yaqub, S., H. Abrahamsen, B. Zimmerman, N. Kholod, K. M. Torgersen, T. Mustelin, F. W. Herberg, K. Taskén, and T. Vang, 2003, Activation of C-terminal Src kinase (Csk) by phosphorylation at serine-364 depends on the Csk-Src homology 3 domain: Biochem J, v. 372, p. 271-8.
Yasuda, K., M. Nagafuku, T. Shima, M. Okada, T. Yagi, T. Yamada, Y. Minaki, A. Kato, S. Tani-Ichi, T. Hamaoka, and A. Kosugi, 2002, Cutting edge: Fyn is essential for tyrosine phosphorylation of Csk-binding protein/phosphoprotein associated with glycolipid-enriched microdomains in lipid rafts in resting T cells: J Immunol, v. 169, p. 2813-7.
Ye, P., D. E. Kirschner, and A. P. Kourtis, 2004, The thymus during HIV disease: role in pathogenesis and in immune recovery: Curr HIV Res, v. 2, p. 177-83.
Yeaman, G. R., A. L. Howell, S. Weldon, D. J. Demian, J. E. Collins, D. M. O'Connell, S. N. Asin, C. R. Wira, and M. W. Fanger, 2003, Human immunodeficiency virus receptor and coreceptor expression on human uterine epithelial cells: regulation of expression during the menstrual cycle and implications for human immunodeficiency virus infection: Immunology, v. 109, p. 137-46.
Yokosuka, T., K. Sakata-Sogawa, W. Kobayashi, M. Hiroshima, A. Hashimoto-Tane, M. Tokunaga, M. L. Dustin, and T. Saito, 2005, Newly generated T cell receptor